SYNTHESIS AND CHARACTERIZATION OF LISICON STRUCTURED SOLID ELECTROLYTES FOR POTENTIAL APPLICATION IN SOLID STATE ELECTROCHEMICAL CELLS

SYED BAHARI RAMADZAN BIN SYED ADNAN

INSTITUTE OF GRADUATE STUDIES
UNIVERSITY OF MALAYA
KUALA LUMPUR

2014

SYNTHESIS AND CHARACTERIZATION OF LISICON STRUCTURED SOLID ELECTROLYTES FOR POTENTIAL APPLICATION IN SOLID STATE ELECTROCHEMICAL CELLS

SYED BAHARI RAMADZAN BIN SYED ADNAN

THESIS BY PUBLICATION SUBMITTED IN FULFILMENT OF THE REQUIREMENTS FOR THE DEGREE OF DOCTOR OF PHILOSOPHY

INSTITUTE OF GRADUATE STUDIES
UNIVERSITY OF MALAYA
KUALA LUMPUR

2014

UNIVERSITI MALAYA

ORIGINAL LITERARY WORK DECLARATION

Name of Candidate : **SYED BAHARI RAMADZAN BIN SYED ADNAN**

I.C/Passport No : **840618-11-5419**)

Registration/Matric No : **HHC 100007**

Name of Degree : **DOCTOR OF PHILOSOPHY**

Title of Project Paper/Research Report/Dissertation/Thesis ("this Work"):

SYNTHESIS AND CHARACTERIZATION OF LISICON STRUCTURED SOLID ELECTROLYTES FOR POTENTIAL APPLICATION IN SOLID STATE ELECTROCHEMICAL CELLS

Field of Study : **ADVANCED MATERIALS**

I do solemnly and sincerely declare that:

(1) I am the sole author/writer of this Work;
(2) This Work is original;
(3) Any use of any work in which copyright exists was done by way of fair dealing and for permitted purposes and any excerpt or extract from, or reference to or reproduction of any copyright work has been disclosed expressly and sufficiently and the title of the Work and its authorship have been acknowledged in this Work;
(4) I do not have any actual knowledge nor do I ought reasonably to know that the making of this work constitutes an infringement of any copyright work;
(5) I hereby assign all and every rights in the copyright to this Work to the University of Malaya ("UM"), who henceforth shall be owner of the copyright in this Work and that any reproduction or use in any form or by any means whatsoever is prohibited without the written consent of UM having been first had and obtained;
(6) I am fully aware that if in the course of making this Work I have infringed any copyright whether intentionally or otherwise, I may be subject to legal action or any other action as may be determined by UM.

Candidate's Signature :…… Date:

Subscribed and solemnly declared before,

Witness's Signature :…… Date:

Name:

Designation:

UNIVERSITI MALAYA

PERAKUAN KEASLIAN PENULISAN

Nama : **SYED BAHARI RAMADZAN BIN SYED ADNAN**

(No. K.P/Pasport : **840618-11-5419**)

No. Pendaftaran/Matrik : **HHC 100007**

Nama Ijazah : **DOCTOR OF PHILOSOPHY**

Tajuk Kertas Projek/Laporan Penyelidikan/Disertasi/Tesis ("Hasil Kerja ini"):

SYNTHESIS AND CHARACTERIZATION OF LISICON STRUCTURED SOLID ELECTROLYTES FOR POTENTIAL APPLICATION IN SOLID STATE ELECTROCHEMICAL CELLS

Bidang Penyelidikan : **ADVANCED MATERIALS**

Saya dengan sesungguhnya dan sebenarnya mengaku bahawa:

(1) Saya adalah satu-satunya pengarang/penulis Hasil Kerja ini;
(2) Hasil Kerja ini adalah asli;
(3) Apa-apa penggunaan mana-mana hasil kerja yang mengandungi hakcipta telah dilakukan secara urusan yang wajar dan bagi maksud yang dibenarkan dan apa-apa petikan, ekstrak, rujukan atau pengeluaran semula daripada atau kepada mana-mana hasil kerja yang mengandungi hakcipta telah dinyatakan dengan sejelasnya dan secukupnya dan satu pengiktirafan tajuk hasil kerja tersebut dan pengarang/penulisnya telah dilakukan di dalam Hasil Kerja ini;
(4) Saya tidak mempunyai apa-apa pengetahuan sebenar atau patut semunasabahnya tahu bahawa penghasilan Hasil Kerja ini melanggar suatu hakcipta hasil kerja yang lain;
(5) Saya dengan ini menyerahkan kesemua dan tiap-tiap hak yang terkandung di dalam hakcipta Hasil Kerja ini kepada Universiti Malaya ("UM") yang seterusnya mula dari sekarang adalah tuan punya kepada hakcipta di dalam Hasil Kerja ini dan apa-apa pengeluaran semula atau penggunaan dalam apa jua bentuk atau dengan apa juga cara sekalipun adalah dilarang tanpa terlebih dahulu mendapat kebenaran bertulis dari UM;
(6) Saya sedar sepenuhnya sekiranya dalam masa penghasilan Hasil Kerja ini saya telah melanggar suatu hakcipta hasil kerja yang lain sama ada dengan niat atau sebaliknya, saya boleh dikenakan tindakan undang-undang atau apa-apa tindakan lain sebagaimana yang diputuskan oleh UM.

Tandatangan Calon :…… Tarikh:

Diperbuat dan sesungguhnya diakui di hadapan,

Tandatangan Saksi :…….. Tarikh:

Nama:

Jawatan:

ABSTRACT:

The aim of this study is to obtain LISICON structured Li_4SiO_4 based solid electrolyte with adequate conductivity for application in electrochemical cells. The parent and modified Li_4SiO_4 compounds were synthesized by sol gel method. The modified compounds were prepared by partial substitution using divalent ion ($Li_{4-2x}Zn_xSiO_4$), trivalent ion ($Li_{4-3x}Cr_xSiO_4$), tetravalent ion ($Li_4Sn_xSi_{1-x}O_4$ and $Li_4Zr_xSi_{1-x}O_4$) and double partial substitution using trivalent and tetravalent ions ($Li_{4-3x}Cr_xZr_ySi_{1-y}O_4$). The prepared samples were characterized using various techniques such as X-ray diffraction, Fourier transform infrared spectroscopy, scanning electron microscope, energy dispersive X-ray, laser particle analyser, differential scanning calorimetry, impedance spectroscopic, lithium transference number, linear sweep voltammetry and charge-discharge study. The XRD results showed that the Li_4SiO_4 system can be indexed to monoclinic structure in space group $P2_{1/m}$. The highest bulk, grain boundary and total conductivity of this compound at ambient temperature were 3.36×10^{-6}, 1.58×10^{-6} and 1.51×10^{-6} S cm^{-1} respectively. The frequency dependence of conductivity followed Jonscher's universal power law, $\sigma_{ac}(\omega) = \sigma_o + A\omega^s$. The plot of pre-exponent, s versus temperature suggests that the conduction mechanism in the system can be described using correlated barrier hopping model. The increase in dielectric constant and dielectric loss and peak shift of tan δ to higher frequencies with temperature indicated that the increase in conductivity with temperature was due to the increase in number and hopping rate of charge carriers with temperature. The effects of partial substitution to this parent compound have also been investigated. The impedance spectroscopic analysis shows that the conductivity of the parent compound increases with different doping ions. The substitutions using

divalent ions Zn^{2+}, ($Li_{3.88}Zn_{0.06}SiO_4$) showed increment of conductivity at ambient temperature. The value of bulk, grain boundary and total conductivity were 3.20×10^{-5}, 2.79×10^{-5} and 1.51×10^{-5} S cm^{-1} respectively. This effect was due to increase in number of vacant sites in the crystal lattice. Meanwhile, differential scanning calorimetry analysis showed increases in phase transition and melting temperature in this compound indicating the enhancement in thermal stability of the Li_4SiO_4 compound upon substitutions of Zn^{2+} to $2Li^+$ ions. The transference number corresponding to Li^+ ion transport value was 0.82 which indicated that the majority of charge carrier in the compound was Li^+ ions. The substitutions using Cr^{3+} into Li_4SiO_4 structure was confirmed by X-ray diffraction and Fourier transform infrared studies. This partial substitution also showed enhancement of conductivity at ambient temperature. The highest bulk, grain boundary and total conductivity were 7.93×10^{-5}, 3.68×10^{-5} and 2.51×10^{-5} S cm^{-1} respectively for $Li_{3.94}Cr_{0.02}SiO_4$ compound. The scanning electron microscope and particle size analysis showed that particle size decreases with Cr^{3+} ion doping. The average grain size decreases from 11.8 μm in Li4SiO4 sample to 0.59 μm in $Li_{3.94}Cr_{0.02}SiO_4$ sample. Ionic transference number of Li^+ ion determined by means of Bruce and Vincent technique was 0.79 for Li_4SiO_4 compound is increased to 0.95 for $Li_{3.94}Cr_{0.02}SiO_4$ compound. Linear sweep voltammetry results showed that the doping by Cr^{3+} ion improved the limit of electrolyte decomposition from 2.73 V in Li_4SiO_4 to 4.51 V in $Li_{3.94}Cr_{0.02}SiO_4$ versus Li/Li^+ reference electrode. The partial substitutions on silicon ion by cation of larger size (Sn^{4+} and Zr^{4+}) also enhanced the conductivity of Li_4SiO_4 compound by one order of magnitude. The highest bulk, grain boundary and total conductivity were 1.00×10^{-4}, 4.42×10^{-5} and 3.07×10^{-5} S cm^{-1} respectively for $Li_4Sn_{0.02}Si_{0.98}O_4$ compound. Meanwhile, $Li_4Zr_{0.06}Si_{0.94}O_4$ compound showed maximum

bulk, grain boundary and total conductivity values of 1.19×10^{-4}, 4.75×10^{-5} and 3.41×10^{-5} S cm^{-1} respectively. The size of Sn^{4+} (0.069 nm) and Zr^{4+} (0.080 nm), are larger than that of Si^{4+} (0.041 nm) increased the size of Li^{+} migration channels which led to increase of ion mobility. The charge carrier concentration was found to be constant over the temperature range from 303 to 773 K while mobility of ion increased with temperature. This was due to increase in ion mobility. Linear sweep voltammetry results showed that $Li_4Sn_{0.02}Si_{0.98}O_4$ sample is electrochemically stable in the voltage range of -5.3 to 5.3 V versus Li/Li^{+} reference electrode. The average particle size for $Li_4Zr_{0.06}Si_{0.98}O_4$ was 1.198 μm, is smaller compared to the parent compound. Energy dispersive x-ray analysis also showed that the chemical compositions of the prepared $Li_4Zr_{0.06}Si_{0.94}O_4$ samples were very close to the desired compositions. The value of lithium transference number for $Li_4Zr_{0.06}Si_{0.94}O_4$ compound was 0.92. This value was higher compared to that of the parent compound. A more significant enhancement occurred on double partial substitutions on Li^{+} and Si^{4+} sites by Cr^{3+} and Zr^{4+}. The DC conductivity at ambient temperature rose to 1.88×10^{-4} S cm^{-1} in $Li_{3.94}Cr_{0.02}Zr_{0.06}Si_{0.94}O_4$ compound with a maximum value in the order of 10^{-3} S cm^{-1} at 500°C. Apart from created vacant sites by Cr^{3+} doping, the doping by Zr^{4+} was believed to enlarge the Li^{+} migration channels of the sample. The lithium transference number also increased to 0.97 in this double substituted compound. $Li_{3.94}Cr_{0.02}Zr_{0.06}Si_{0.94}O_4$ has a maximum discharge capacity of 103 mA h g^{-1} at constant current of 5 mA g^{-1} (0.05 C) between 3.0 and 4.2 V. This indicated that this ceramic electrolyte can be used in lithium cells.

ABSTRAK:

Tujuan kajian ini adalah untuk mendapatkan elektrolit pepejal berstruktur LISICON berasaskan Li_4SiO_4 dengan kekonduksian yang mencukupi untuk diaplikasikan dalam sel-sel elektrokimia. Bahan induk Li_4SiO_4 dan yang diubahsuai di sintesis menggunakan kaedah sol gel. Bahan yang diubahsuai disediakan melalui penggantian separa menggunakan ion dwivalen ($Li_{4-2x}Zn_xSiO_4$), ion trivalen ($Li_{4-3x}Cr_xSiO_4$), ion tetravalen ($Li_4Sn_xSi_{1-x}O_4$ dan $Li_4Zr_xSi_{1-x}O_4$) dan menggunakan penggantian separa berganda daripada ion trivalen dan ion tetravalen ($Li_{4-3x}Cr_xZr_ySi_{1-y}O_4$). Sampel yang disediakan dicirikan dengan menggunakan pelbagai teknik pencirian, iaitu belauan sinar-x, inframerah transformasi Fourier, mikroskopi pengimbas elektron, serakan tenaga sinar-x, analisis saiz zarah, pengimbasan kebezaan kalorimeter, spektroskopi impedans, nombor pemindahan litium, voltammetri sapuan linear dan kajian cas-discas. Dapatan belauan sinar-x menunjukkan sistem Li_4SiO_4 boleh diindeks kepada struktur monoclinik dalam ruang kumpulan $P2_{1/m}$. Nilai paling tinggi untuk kekonduksian pukal, kekonduksian sempadan butiran dan kekonduksian jumlah sebatian ini pada suhu bilik adalah masing-masing 3.36×10^{-6}, 1.58×10^{-6} dan 1.51×10^{-6} S cm^{-1}. Pergantungan kekonduksian kepada frekuensi mematuhi undang-undang sejagat Jonscher's, $\sigma_{ac}(\omega) = \sigma_o + A\omega^s$. Plot pra- pelopor *s* melawan suhu menunjukkan bahawa mekanisme pengaliran dalam sistem boleh diterangkan dengan menggunakan model korelasi halangan loncat. Peningkatan dalam dielektrik malar dan dielektrik hilang dan peralihan puncak tan δ kepada frekuensi yang lebih tinggi dengan peningkatan suhu menunjukkan bahawa peningkatan dalam kekonduksian dengan suhu adalah disebabkan oleh peningkatan bilangan dan kadar loncatan pembawa cas dengan suhu. Kesan penggantian separa dalam bahan induk, Li_4SiO_4 ini juga disiasat. Analisis spektroskopi impedans menunjukkan bahawa

kekonduksian bahan induk meningkat dengan penggantian separa ion. Penggantian menggunakan ion dwivalen, Zn^{2+} ($Li_{3.88}Zn_{0.06}SiO_4$) menunjukkan peningkatan kekonduksian pada suhu bilik. Nilai kekonduksian pukal, sempadan butiran dan jumlah adalah masing – masing 3.20×10^{-5} , 2.79×10^{-5} dan 1.51×10^{-5} S cm^{-1}. Kesan ini adalah disebabkan oleh peningkatan kekosongan dalam kekisi kristal. Sementara itu, analisis pengimbasan pembezaan kalorimetri menunjukkan peningkatan fasa peralihan dan suhu lebur yang menunjukkan peningkatan kestabilan terma sebatian Li_4SiO_4 apabila penggantian Zn^{2+} dengan $2Li^+$ ion dilakukan. Nilai nombor pemindahan bagi pengangkutan ion litium adalah 0.82, menunjukkan pembawa cas majoriti dalam sebatian ini adalah ion litium. Penggantian menggunakan ion trivalen, Cr^{3+} ke dalam struktur Li_4SiO_4 telah disahkan oleh kajian belauan sinar-x dan inframerah transformasi Fourier. Penggantian separa ini juga menunjukkan peningkatan kekonduksian pada suhu bilik. Nilai kekonduksian tertinggi untuk kekonduksian pukal, sempadan butiran dan jumlah adalah masing –masing 7.93×10^{-5}, 3.68×10^{-5} dan 2.51×10^{-5} S cm^{-1} untuk sebatian $Li_{3.94}Cr_{0.02}SiO_4$. Analisis mikroskopi pengimbas elektron dan analisis saiz zarah menunjukkan bahawa saiz zarah berkurangan apabila ion Cr^{3+} didopkan ke dalam struktur bahan induk. Saiz purata butiran berkurangan daripada 11.8 μm dalam sampel Li_4SiO_4 kepada 0.59 μm dalam sampel $Li_{3.94}Cr_{0.02}SiO_4$. Nombor pemindahan bagi ion litium ditentukan menggunakan teknik Bruce dan Vincent adalah 0.79 bagi sebatian Li_4SiO_4 dan meningkat kepada 0.95 bagi sebatian $Li_{3.94}Cr_{0.02}SiO_4$. Voltammetri sapuan linear menunjukkan bahawa penggantian ion Cr^{3+} meningkatkan had penguraian elektrolit daripada 2.73 V dalam Li_4SiO_4 kepada 4.51 V dalam $Li_{3.94}Cr_{0.02}SiO_4$ menggunakan rujukan elektrod Li/ Li^+. Penggantian separa ion silikon dengan kation yang bersaiz lebih besar (Sn^{4+} dan Zr^{4+}) juga meningkatkan kekonduksian sebatian Li_4SiO_4 sebanyak satu

magnitud. Nilai tertinggi kekonduksian pukal, sempadan butiran dan jumlah adalah masing-masing 1.00×10^{-4}, 4.42×10^{-5} dan 3.07×10^{-5} S cm^{-1} untuk sebatian $Li_4Sn_{0.02}Si_{0.98}O_4$. Sementara itu, sebatian $Li_4Zr_{0.06}Si_{0.94}O_4$ menunjukkan nilai kekonduksian maksimum pukal, sempadan butiran dan jumlah iaitu masing-masing 1.19×10^{-4} , 4.75×10^{-5} dan 3.41×10^{-5} S cm^{-1}. Saiz Sn^{4+} (0.069 nm) dan Zr^{4+} (0.080 nm), yang lebih besar daripada Si^{4+} (0.041 nm) meningkatkan saiz saluran pergerakan litium ion yang membawa kepada peningkatan pergerakan ion. Kepekatan pembawa cas didapati malar pada julat suhu dari 303 K kepada 773 K manakala peningkatan kekonduksian dengan suhu adalah disebabkan oleh peningkatan pergerakan ion. Voltammetri sapuan linear menunjukkan bahawa sampel $Li_4Sn_{0.02}Si_{0.98}O_4$ adalah stabil dari segi elektrokimia dalam julat voltan -5.3 - 5.3 V. Saiz zarah purata $Li_4Zr_{0.06}Si_{0.98}O_4$ adalah 1.198 μm iaitu lebih kecil berbanding dengan bahan induk. Analisis serakan tenaga sinar-x pula menunjukkan komposisi kimia yang disediakan adalah hampir menyamai dengan komposisi dikehendaki. Nilai nombor pemindahan ion litium untuk sebatian $Li_4Zr_{0.06}Si_{0.94}O_4$ adalah 0.92. Nilai ini adalah lebih tinggi berbanding dengan nilai bagi bahan induk. Peningkatan kekonduksian yang lebih ketara berlaku apabila penggantian separa berganda pada kedudukan Li^+ dan Si^{4+} dengan ion Cr^{3+} dan Zr^{4+}. Nilai kekonduksian arus terus pada suhu bilik meningkat kepada 1.83×10^{-4} S cm^{-1} dalam sebatian $Li_{3.94}Cr_{0.02}Zr_{0.06}Si_{0.94}O_4$ dengan kekonduksian maksimum dalam magnitud 10^{-3} S cm^{-1} pada suhu 500°C. Selain daripada mewujudkan kekosongan tapak dengan pendopan Cr^{3+}, Zr^{4+} yang didopkan dipercayai meningkatkan saluran pergerakan litium ion di dalam sampel. Nilai nombor pemindahan ion litium juga meningkat kepada 0.97 dalam sebatian ini. $Li_{3.94}Cr_{0.02}Zr_{0.06}Si_{0.94}O_4$ mempunyai kapasiti discas maksimum iaitu 103 $mAhg^{-1}$ pada arus malar 5 mAg^{-1} (0.05 C) antara 3.0 - 4.2 V. Ini menunjukkan bahawa elektrolit seramik ini boleh digunakan dalam sel litium.

ACKNOWLEDGEMENTS

I would like to express my deep gratitude to my supervisor Professor Dr. Nor Sabirin Mohamed for the invaluable guidance, advice and patience that led to the success of this project. Her constant encouragement throughout the course has inspired me to work harder for success.

I am also indebted to my laboratory colleagues, Norazlin Zainal, Helmi Jaafar, Mazdida Sulaiman, Akmaliah Dzulkarnain and Salmiah Ibrahim for their assistance and valuable experience during the course of this work. The financial aids from the University of Malaya are greatly acknowledged. My acknowledgment also goes to the staff members of Pusat Asasi Sains, University of Malaya, Mrs Saripah Ismail and Ms Hazlizaaini Basri for their care and help. Finally, I would like to express my deepest thanks to my beloved mother, Asmah Mat Amin and wife, Norwati Khairul Anuar.

In memory: My late father Syed Adnan Bin Syed Draman (1957- 1990)…….....Al Fatihah

TABLE OF CONTENTS

LISTS OF FIGURES

LIST OF TABLE

CHAPTER 1:

INTRODUCTION TO THE PRESENT WORK

1.1 Introduction

Solid electrolytes are solid materials that provide an ionic conduction pathway between anode and cathode in electrochemical devices such as lithium batteries, fuel cells, supercapacitors etc. Unlike liquid electrolytes, solid electrolytes have various advantages such as simple design, natural seal, resistance to shock and vibration, resistance to pressure, absence of leakage, longer lifetime and high degree of reliability. It also varies in form and design and has a wide range of operating temperature (Park *et al*, 2010).

Generally, the requirements for good solid electrolytes are high ionic conductivity at operating temperature (~10^{-3}S cm^{-1}), low electronic conductivity and good electrochemical stability toward electrodes. In addition, they must have compatible thermal expansion with that of electrodes and other construction materials, negligible volatilization of components, suitable mechanical properties and negligible interaction with electrode materials under operating conditions (Sariboga *et al*, 2013). Furthermore, a negligible small grain boundary resistance is also important in polycrystalline ceramic type materials. Meanwhile, for industrial development, solid electrolytes must be environmentally benign,

non-toxic, non-hygroscopic and low cost materials. Their preparation should be easy and cost effective (Knauth, 2009).

There are two groups of materials used as solid electrolytes in electrochemical devices: Inorganic solid electrolytes (ceramic, amorphous and composite) and organic solid electrolytes (polymers). Unlike other electrolytes, which have various kinds of carrier ions (cations and anions), the ceramic electrolyte has only one carrier ions (cations) because the other constituent elements are necessary used to maintain the rigid structure (Aono *et al*, 1994). Meanwhile, the application of ceramic electrolytes forms an important class of materials due to their superior incombustibility, high energy density and a wider electrochemical stability (Scrosati *et al*, 2000). Furthermore, the employment of ceramic materials in electrochemical devices can solve the problem of capacity decrease and self discharge caused by side reactions (Takada *et al*, 2004).

1.2 Research Background

Several kinds of conductors such as Li-βAl_2O_3 and Li_3N show high ionic conductivities at room temperature (~ 10^{-3} S cm^{-1}). However, because of their chemical instability, they are not widely used as solid electrolytes for lithium batteries. Crystalline oxide based inorganic solid electrolytes with higher chemical stability have been explored since late 1970s. Goodenough *et al,* 1976 designed a three dimensional network structure and named the $Na_{1+x}Zr_2Si_xP_{3-x}O_{12}$ material as a Na^+ super ionic conductor (NASICON). However, they have modified the structure with the implementation of Li^+ in that NASICON structure ($Li_{1+x}Zr_2Si_xP_{3-x}O_{12}$) owing to its small size, light weight and high electrochemical potential. Partial substitutions creating lithium vacancy and interstitial in this structure have greatly

enhanced its ionic conductivity. The maximum conductivity value observed for this NASICON materials, is 3×10^{-3} S cm^{-1} at room temperature for $Li_{1.3}Al_{0.3}Ti_{1.7}(PO_4)_3$ (LATP), (x = 0.3). However, it is extremely difficult to obtain well ceramics with these materials as the total conductivity is one or two magnitude order less than that value, due to the presence of large grain boundary resistances (Robertson *et al*, 1997).

Li^+ super ionic conductor (LISICON) with the $Li_{14}Zn(GeO_4)_4$ composition has also been designed and prepared by Hong, 1978. The conductivity value of this material at room temperature is considerably low (~ 10^{-8} S cm^{-1}). It reaches a value of 0.125 S cm^{-1} at 300^{o}C. In 1985, a solid solution of Li_4GeO_4-Li_3VO_4, which is isostructural to LISICON and related to γ-Li_3PO_4 was synthesized by Kuwano and West (1985). Partial substitution of Li_4GeO_4 by Li_3VO_4 induced vacancies in the lithium sites, resulting in easier lithium-ion hopping in the structure. The substituted $Li_{3.6}Ge_{0.6}V_{0.4}O_4$ crystal attained ionic conductivity value of 4×10^{-5} S cm^{-1} at room temperature, which was a few orders magnitude higher than those of its parent compound (Robertson *et al*, 1997).

In 2000, Kanno *et al*. modified the oxide LISICON structure by increasing the lattice size of the LISICON-type structure with the replacement of larger size and more polarized sulfur for oxygen ion with the general formula, $Li_xM_{1-y}M'_yS_4$ (M = Si, Ge and M'= P, Al, Zn, Ga, Sb) which greatly enhanced the ionic conductivity. The highest conductivity value of 10^{-3} S cm^{-1} was previously reported for the thio-LISICON structure, $Li_{3.25}Ge_{0.25}P_{0.75}S_4$ (Kanno and Murayama, 2001). However, this type of materials has many disadvantages. They are expensive, complicated to prepare and also toxic. In addition, they

show instability against electrochemical reduction at low potential (ca. 0.1 V vs. Li/Li^+). They also exhibit incompatibility with graphite anodes (Ooura *et al*, 2012).

The present works deals with the LISICON-type ceramic Li^+ ion conductors, Li_4SiO_4 which has the same structure as γ-Li_3PO_4 and thio-LISICON. The materials can be easily synthesized, less expensive to produce, safe and also stable in air. Furthermore, they do not react with lithium, they have low self-discharge and maintain their conductivity constant with time. Li_4SiO_4 type structure has a tunnel size too small for Li^+ to migrate because oxygen ions occupy the site giving close packed structure. Larger tunnel size is necessary for making Li^+ migration smoother. Suitable tunnel size for Li^+ migration is obtained by increasing the lattice size of the Li_4SiO_4 structure. Meanwhile, suitable partial substitution were also investigated in order to create more vacant sites in the Li_4SiO_4 structure to obtain high Li^+ conductivity at room temperature.

1.3 Problem statement

1- The most common method used to prepare ceramic materials reported in the literature is solid state reaction technique. However, this method commonly leads to many problems such as the use of high heating temperature (usually >1000^{o}C) for a prolonged period (1-2 days), contamination with impurities, volatilization, lack of control of microstructure and composition and suffer from obtaining good materials free of grain boundary resistance. In order to overcome this problem, the sol-gel method can be used. This method has the advantages of lowering the synthesis temperature and thus simplifies the preparation procedure and allows labile compounds

to be entrapped in the synthesized sol-gel matrix. This method may also yield homogeneous and high purity materials leading to low grain boundary resistance. Furthermore, it is suitable for both small scale and large scale production.

2- The LISICON-type materials are highly conducting at high temperature. There are various approaches that can be used to enhance the conductivity of these materials at ambient temperature such as the substitution of isovalent cation or aliovalent cation. The introduction of larger cation size in isovalent substitution can lead to an increase in the lattice size which increases the ion mobility. In addition, the substitution of aliovalent cation can enhance the conductivity of the electrolytes materials either through creation of vacancy or interstitial ions.

3- Previous study only focused on structural and d.c. conductivity of the LISICON ceramic electrolytes. However, other properties such as a.c. conductivity, type of mobile ion, electrochemical stability window, and electrochemical performance of this type of electrolytes were not studied. The study on a.c. conductivity is valuable information to elucidate the ionic conduction such as charge carrier concentration, mobile ion concentration and ion hopping rate. The type of conducting ion and electrochemical stability window are also important to be identified in order to determine proper application of the materials.

1.4 Research Objectives

The main objective of the proposed research is to develop new types of LISICON structured ceramic solid electrolytes with suitable conductivity for application in solid state electrochemical cells using a cheap, easy and low temperature method. Experimental works were carried out to:

1) Synthesize Li_4SiO_4 parent compound using sol-gel method and characterize its structural, conductivity and electrochemical properties.
2) Modify the parent compound by partial substitutions employing different types of metal ions and study the effects of the modification to its structural, conductivity and electrochemical properties.
3) Fabricate and study the performance of electrochemical cells using the LISICON structured materials with the best conductivity value.

1.5 Linkage of scientific papers

Satisfactory performance in lithium ion batteries depends mainly on the capability of ions diffusion through the electrolytes between anode and cathode. Consequently, the prime concern in the electrolyte research is to enhance its ionic conductivity, a main challenge faced by researchers. In this study, Li_4SiO_4 that is one of the promising ceramic electrolytes has been successfully synthesized via citrate sol gel method.

The characterizations of Li_4SiO_4 parent compound are described in detail through *Paper 1 and 2.* Both *Paper 1* (*Li_4SiO_4 Prepared by Sol-Gel Method as Potential Host for LISICON Structured Solid Electrolyte)* and *2* (*Citrate sol gel synthesised Li_4SiO_4 :*

Conductivity and dielectric behaviour) investigate the structure (XRD and FTIR analysis), morphology (SEM and EDX analysis) , conductivity behaviour (DC and AC) from room temperature to 100^{o}C and also the dielectric properties of the parent compound. Although these papers explain various characterizations of the parent compound, a detailed description of its thermal behaviour, particle size distribution, high temperature conductivity (AC and DC) studies (>100^{o}C), the majority of charge carrier determination and the electrochemical window were not included. Therefore, in *Paper 4* (*Structural, Thermal and Electrical Properties of* $Li_{4-2x}Zn_xSiO_4$ *Ceramic Electrolyte Prepared by Citrate Sol Gel Technique***)** and *Paper 6* (*Properties of novel* $Li_{4-3x}Cr_xSiO_4$ *ceramic electrolyte*) provide detailed discussion on these aspects. The outcomes of this study have significantly contributed new knowledge since detailed description related to these aspects for this Li_4SiO_4 compound have never been reported in the literature.

Partial substitutions which can create vacancies in the parent structure may enhance the conductivity of the parent compound. Both *Paper 3* (*Conductivity and dielectric Studies of* Li_2ZnSiO_4 *Ceramic Electrolyte Synthesized via Citrate Sol gel Method)* and *Paper 4* highlight the improvement of Li_4SiO_4 conductivity by partial substitution using divalent ion (Zn^{2+}) with formula $Li_{4-2x}Zn_xSiO_4$. The substitution of Li with Zn ($2Li^{+} \leftrightarrow Zn^{2+}$) creates vacant sites in the structure and any lithium ion in the intermediate vicinity can diffuse easily. This leaves the previous initial sites of the ion available to host other ions. This enhances ions mobility across the solid and increases the conductivity. *Paper 3* reports detailed characteristics of the non-stoichiometric compound with $x = 1$. Meanwhile, *Paper* 4 reports detailed characteristics of the non-stoichiometric compound with $0 < x < 0.2$. *Paper 3* focuses on the conductivity and dielectric studies while *Paper 4* focuses on

the structure, thermal and electrical properties. The most significant outcome from this study was the success of Zn^{2+} substitutions in the Li_4SiO_4 structure using sol gel method. Furthermore, the conductivity of Zn-doped compound increases by an order of magnitude compared to that of the parent compound.

Paper 5 (*Properties of novel $Li_{4-3x}Cr_xSiO_4$ ceramic electrolyte*) describes the partial substitution of trivalent ion, Cr^{3+} into the structure of the parent compound. This substitution also creates vacant sites in the parent structure. However, this substitution is expected to create two vacant sites. Paper 5 discusses the structure, morphology, electrical and electrochemical properties of the $Li_{3.94}Cr_{0.02}SiO_4$ compound. The outcome of this investigation was the novel compound, $Li_{3.94}Cr_{0.02}SiO_4$. It was successfully obtained with a conductivity of an order of magnitude higher than that of the parent compound. The outcomes from *Paper 4* and *Paper 5* provide scientific base that creating vacancies in the Li_4SiO_4 increases the mobility of ions that enhances its conductivity.

Paper 6 (*Effects of Sn substitution on the properties of Li_4SiO_4 ceramic electrolyte)* and *7 (Characterization of novel $Li_4Zr_{0.06}Si_{0.94}O_4$ and $Li_{3.94}Cr_{0.02}Zr_{0.06}Si_{0.94}O_4$ ceramic electrolytes for lithium cells)* discuss the partial substitutions of Si^{4+} sites of the parent compound by tetravalent ions such as Sn^{4+} and Zr^{4+}. These cations are larger in size than Si^{4+}, this increases Li_4SiO_4 lattice and improves Li^+ migration through channels. This leads to an increase in mobility of ions. *Paper 6* highlights the structure, thermal properties, impedance analysis, frequency dependence conductivity and linear sweep voltammetry studies of $Li_4Sn_{0.02}Si_{0.98}O_4$ compound. Meanwhile *Paper 7* focuses on the structure, morphology, particle size analysis, impedance measurement and measurement of lithium

ion transference number in $Li_4Zr_{0.06}Si_{0.94}O_4$ compound. The outcome from these study show that Sn^{4+} and Zr^{4+} ions were successfully inserted into the structure of Li_4SiO_4 parent compound using sol gel method which has never been reported previously.

Paper 7 also describes a study on double partial substitution of Cr^{3+} and Zr^{4+} into the structure of Li_4SiO_4 parent compound. Apart from creating vacant sites by Cr doping, the substitution by Zr^{4+} also enlarges the Li^+ migration channels of the sample. This paper discusses the structure, morphology, particle size, impedance measurement, lithium transference number measurement and electrochemical cell test of $Li_{3.94}Cr_{0.02}Zr_{0.06}Si_{0.94}O_4$ compound. The most significant outcome from this study was the novel $Li_{3.94}Cr_{0.02}Zr_{0.06}Si_{0.94}O_4$ compound which has never been reported before. The obtained compound exhibited a conductivity of two orders of magnitude higher than that of the parent compound at ambient temperature. In addition, this study shows that $Li_{3.94}Cr_{0.02}Zr_{0.06}Si_{0.94}O_4$ ceramic electrolyte can be used in the lithium cell.

In *Paper 8* (*Ac conductivity and dielectric studies of modified Li_4SiO_4 ceramic electrolyte*) the investigation of conduction mechanism, contribution of charge carrier concentration, charge carrier mobility and dielectric studies of $Li_{3.94}Cr_{0.02}SiO_4$, $Li_4Zr_{0.06}Si_{0.94}O_4$ and $Li_{3.94}Cr_{0.02}Zr_{0.06}Si_{0.94}O_4$ compounds are presented. The outcome of this study contributed new scientific knowledge on this aspect of this type of compound which has never been reported in the literature.

CHAPTER 2

LITERATURE REVIEW

2.1 Solid electrolytes

An ideal electrolyte must pass an ionic current inside the cell that equals an electronic current flowing in an external circuit between anode and cathode in electrochemical devices such as batteries, fuel cells, supercapacitors, sensors, display units and electro chromic devices. The electrolyte must be a conductor of a single working ion and an electronic insulator. The driving forces for the current flow are a chemical reaction between reactants on opposite sides of the electrolyte, reductant at the negative electrode (the anode) and an oxidant at the positive electrode (the cathode) (Goodenough, 1997).

Solid ion conductors or solid electrolytes attract great interest compared to high conductivity liquid electrolytes which have many disadvantages such as leakage and spillage, lack of mechanical integrity and narrow range of operating temperature (Ferloni, 1994). There are two types of materials used for solid electrolytes in electrochemical devices: Inorganic solid electrolytes and organic polymer solid electrolytes. Polymer electrolytes especially gel polymer has been well-developed and commercialized while the inorganic solid electrolyte has attracted a lot of people's attention recently because of its great potential.

2.2 Classification of solid electrolytes

Solid electrolytes have several types of phase based on their microstructure and physical properties. As such, they can be classified into polymer electrolytes, amorphous glassy electrolytes, composite electrolytes and crystalline electrolytes (ceramic).

2.2.1 Polymer electrolytes

There are two types of polymers which can be used as electrolyte: natural polymers (rubber, cellulose) and synthetic polymers (plastic, nylon, adhesives). Most pure polymers exhibit very small electrical conductivity. The conductivity may significantly increase by addition of salt to the polymers. Polymer electrolytes are based on the dissolution of a salt in an ion-coordinating macromolecule such as PEO, PEMA and PVC. These polymers have got atoms or group of atoms with high electron donating power and a suitable inter-atomic separation, thus enabling them to form multiple intrapolymer coordinate bonds with cations. These polymers also have low barriers to bond rotation allowing segmental motion of the polymer chain, thus providing a mechanism for ion transport. Polymer electrolytes are now materials of choice for application in electrochemical devices due to their attractive mechanical properties (ability to relax elastically upon stresses induced by volume changes related to charge/discharge of adjacent electrodes) and ease of processing (Scrosati and Vincent, 2000).

Polymer electrolytes have several advantages over ceramic electrolytes, such as good processibility and flexibility. Rather, maintaining advantages of solid electrolytes,

including dimensional stability, safety and ability to prevent lithium dendrite formation. However, this kind of electrolyte cannot be used at very high temperature. The ionic conduction of the polymer is due to mobile anionic or cationic ions that act as the conducting species. The polymer acts as an immobile solvent for the ionic salt (Fergus, 2010).

Generally, conventional polymer-salt electrolytes show low conductivities. In order to improve the conductivities various techniques have been used such as random and comb–like copolymer, mixed salt system, mixed solvent system, polymer blending as well as impregnation of additives such as plasticizers, inorganic ceramic fillers and ionic liquids.

2.2.2 Amorphous-glassy electrolytes

Li^+ ion conducting glasses have been discovered and studied due to several advantages in comparison with crystalline solid electrolytes such as a wide choice of compositions, isotropic conduction, no grain boundaries, easy production in thin film and they are non-flammable (Tatsumisago and Minami, 1987). Sulphide based glassy electrolyte system of $GeS_2 + Li_2S + LiI + Ga_2S_3 + La_2S_3$ exhibits high ionic conductivities in the order of 10^{-3}S cm^{-1} with low activation energies (0.4-0.5 V) at room temperature. However, these glasses are highly hygroscopic, which is problematic for lithium batteries (Knauth, 2009). Later, quite high conductivities were reported for Li_2S-P_2S_5 (Tatsumisago *et al*, 2008), Li_2S-B_2S_3 (Menetrier *et al*, 1992), Li_2S-SiS_2-Li_3PO_4 (Aotani *et al*, 1994) and Li_2S-SiS_2-Li_4SiO_4 (Hirai *et al*, 1995) glasses. The high conductivity in these electrolytes is due to the open

disordered structure of the glass and higher polarization ability of the large sized sulfur and lithium atoms. The Li^+ ions are less attracted to the sulfur and as a result the ion transport is facilitated through the vacant interstitial sites. Therefore, this type of glass electrolytes is among the highly potential candidates of all solid state battery systems (Tatsumisago and Hayashi, 2012).

The disadvantage of these sulfide glass materials is that they must be prepared in a glove box with great care. They are highly water-reactive even when in contact with humid air, and are highly corrosive in silica containers. As a result, they have not been used largely in commercial industries. In addition, there are not many studies on thin films of ion conducting sulfides. This is due to the difficulty in fabricating them as they are easily oxidized and there is a tendency for lithium deficiency to occur during the process (Yamashita *et al*, 1996).

2.2.3 Composite electrolytes

Composite electrolytes are mixtures of different materials. They are also known as heterogeneously doped materials, dispersed solid electrolyte systems and materials containing dispersed second phase particles (DSPP) because of the presence of multiphase solid systems (Nancy, 1989). The composite electrolyte systems can be classified into different categories. They are (i) crystal – glass composites, (ii) glass – polymer composites, (iii) crystal – polymer composites and (iv) crystal – crystal composites. The advantages of the composite electrolytes are the existence of different types of chemicals and compositions that can be synthesized and ease of fabrication. Meanwhile, the

disadvantage of composite electrolytes is that they are thermally unstable (Agrawal and Guppta, 1999).

The mechanism of ion conduction in the solid composite electrolyte systems can be explained by various theoretical models such as space charge layer, disordered phases and blocking effect. The defect chemistry of boundary regions in heterogeneous system is required when interfacial effects are considered. Interfaces between phases in composite systems may exist because of the kinetic obstacles of different structures (Maier, 1995). Phase transitions at interfaces could occur by stabilizing the highly disordered phase when pressure and temperature are applied to the composites. In addition, nanosized materials have also been shown to be responsible for ionic transport as well as storage properties (Maier, 2003). All these characteristics displayed in the heterogeneous systems are very important for the charge transport and therefore making them very promising as solid electrolytes for use in lithium batteries.

2.2.4 Ceramic electrolytes

Inorganic crystalline or ceramic electrolytes are the only solid electrolytes that have ordered structure. They basically consist of mobile ions in less or more rigid crystalline frameworks. The ionic conduction in the crystalline electrolytes is through 1D, 2D or 3D channels depending on the crystal structure. Ionic conduction in these electrolytes occurs by movement of ionic point defects which requires energy in their periodic lattice structure. These point defects produce interstitial ions or vacant sites that can enhance the mobility of ions and ionic conductivity as well. In particular, the electrolyte which shows

high Li^+ conducting properties at room temperature is a promising material (Fergus, 2006; 2010)

They are a set of guidelines which show the likely structural characteristics that are prerequisites for high ionic conduction (West, 1984 and Thangadurai and Weppner, 2006). These are as follows:

(a) A large number of the ions of one species should be mobile.

(b) There should be a large number of empty sites available for the mobile ions to jump into.

(c) The empty and occupied sites should have similar potential energies with a low activation energy barrier for jumping between neighbouring sites.

(d) The structure should have framework, preferably three dimensional, permeated by open channel through which mobile ions may migrate.

(e) The anion framework should be highly polarisable.

(f) Weak framework and 3D structure

(g) Weak covalent bonding between the metal and oxygen

(h) Host and guest metal ion should be stable with different coordination number of oxygen.

Recently the research on solid electrolyte based on the ceramic Li-ion conductor is mainly focused on four types of structure: NASICON, Garnet, Perovskite and LISICON-type.

2.2.4.1 NASICON-type

The term NASICON, which stands for Na^+ *S*uper *I*onic *Con*ductor, was given to the solid solution phase $NaZr_2(PO_4)_3$, discovered by Hong and Goodenough in 1976. The crystal structure of NASICON is based on the covalent skeleton $[M_2(PO_4)_3]^-$ constituted of MO_6 (M = Zr, Ti, Sn etc.) octahedral which share all their corners with PO_4 polyhedra forming 3-dimension network structure, space group *R3c* (Fig. 2.1). There are two types of cation sites, A_1 and A_2 exist in the structure. The conduction channels (bottlenecks) sites generated along the *c*-axis direction where conductor cations move from one site to another. The size of the channel depends on the nature of skeleton ions and on the carrier concentration in both types of sites (A_1 and A_2). The maximum conductivities observed for this type of compounds is observed for $Li_{1.3}Al_{0.3}Ti_{1.7}(PO_4)_3$ with value of 3×10^{-3} S cm^{-1} at room temperature. The substitution of Ti^{4+} with Al^{3+} cations reduces the unit cell structure of the NASICON. Consequently, enhances the ionic conductivity. However, this NASICON-type material is unstable with Li metal due to facile Ti^{4+} reduction (Robertson *et al* 1997; Knauth, 2009).

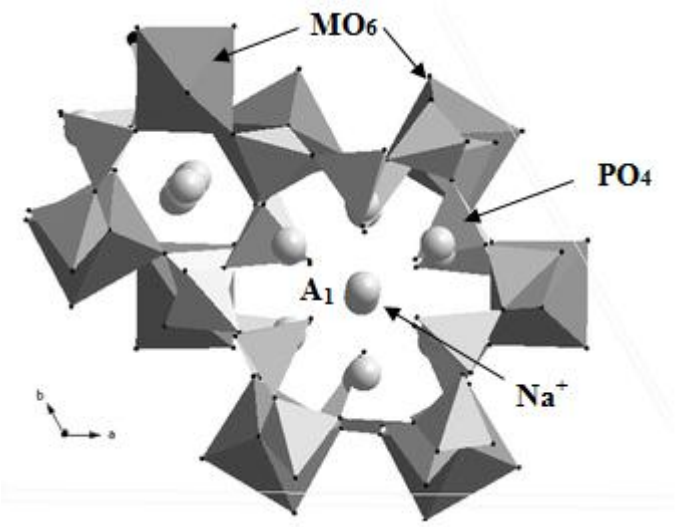

Figure 2.1: NASICON structure (Santos *et al*, 2006).

2.2.4.2 Garnet-type

Garnet-type materials with general formula $Li_5La_3M_2O_{12}$ (M = Ta, Nb, Zr) were discovered by Thangadurai and Weppner (2005). Garnet framework structure is composed of LaO_8 dodecaheldra and MO_6 octahedra. Lithium ions reside on both tetrahedral site (24*d*) and octahedral site (48*g*), but only about 80% of 24d sites and 40% of 48 *g* octahedral sites are occupied. The tetrahedral and the distorted octahedral site are linked via shared polyhedral faces (Fig. 2.2) (Awaka *et al* 2010). This type of solid electrolytes was found to exhibit pure lithium ionic conductivity and high decomposition voltage (6 V versus Li), promising for application as electrolyte in all solid state lithium secondary batteries. The parent compound of $Li_5La_3Zr_2O_{12}$ exhibits low bulk conductivity (1.63×10^{-6} S cm^{-1} at 300 K). The highest total conductivity of about 4×10^{-5} S cm^{-1} was obtained at room temperature in barium doped samples, $Li_6La_2BaTa_2O_{12}$. In indium doped samples: $Li_{5.5}La_3Nb_{1.75}In_{0.}25O12$, the lithium ionic conductivity can reach 1.8×10^{-4} S cm^{-1} at 323K (Knauth, 2009).

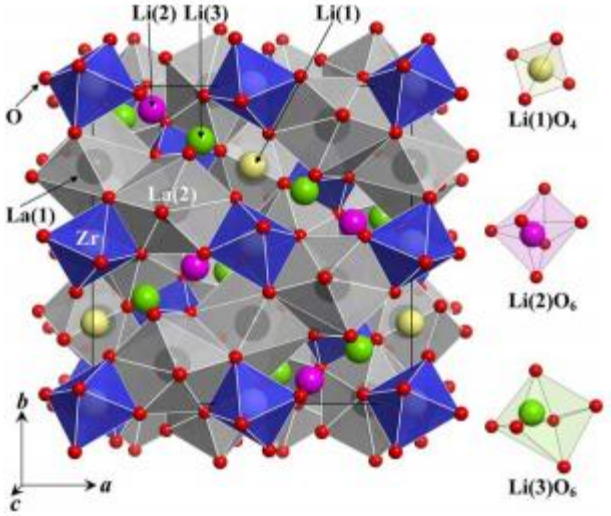

Figure 2.2: Crystal structure of $Li_5La_3Zr_2O_{12}$ garnet type (Awaka *et al*, 2010).

2.2.4.3 Perovskite-type

Perovskites (general formula ABO_3) and related structure are extremely important solid state materials and have potential uses in a variety of applications such as cathodes in solid oxide fuel cells, giant magnetoresistors and ferroelectrics (Robertson *et al*, 1997). The original compound for this Perovskites type is $CaTiO_3$. The unit cell of $CaTiO_3$ described by Ca^{2+} ions at the corner of a cube with Ti^{4+} ions at the body centre and oxygen anion at the centre of the surface (Fig. 2.3). Perovskites can host many different cations at A and B sites. Introducing lower valence ion into the ABO_3 structure of perovskites leads to an increase in ionic conductivity (Rotimi, 2010).

Perovskites and related crystal structures have been investigated more intensively with regard to the possibility of oxide ion conduction. The oxide ion conductor, well known in some non-stoichiometric perovskites, was demonstrated in $Li_{0.5-3x}La_{0.5+x}TiO_3$. The bulk ionic conductivity is high as 10^{-3} Scm^{-1} at room temperature, but the total conductivity is significantly less, 2×10^{-5} S cm^{-1} due to grain boundary resistance. The substitution of Ti^{4+} with smaller ion such as Al^{3+} in perovskites has been reported increases ionic conductivity, but the substitution of Li^+ by Na^+ leads to a decrease in conductivity. Nevertheless, electronic conductivity is strongly enhanced due to Ti^{4+} reduction at the Li interface. This means that the perovskites-type is not compatible with very reducing negative electrodes (Robertson *et al*, 1997; Knauth, 2009).

Figure 2.3: $CaTiO_3$ perovskites-type structure (Shi and Guo, 2012).

2.2.4.4 LISICON- type

LISICON is the abbreviation of Lithium Super Ionic Conductor. The first material to be given the name LISICON was $Li_{14}Zn(GeO_4)_4$ which is a compound of solid solution $Li_{2+2x}Zn_{1-x}GeO_4$ (Hong, 1978; Bruce *et al* 1980). These solid solutions may also be formed between stoichiometric low conducting end members of γ-polymorphs of Li_4XO_4 (*x* = Si, Ge, Ti) and Li_3YO_4 (Y = P, As, V), Li_2MXO_4 (M = Zn, Mg, etc), Li_2ZO_4 (Z = S, W, etc.) or $LiTO_2$ (T = Al, Ga, etc.) (Khorassani and West, 1984; Bruce, 1984; Khorassani and West, 1982; Dissanayake *et al*, 1993; Robertson and West, 1992; Sumathipala *et al*, 1996). LISICON tends to show marked reduction in ionic conductivity with time at low temperature. This is due to the trapping of the mobile lithium ions by the sublattice at lower temperature via the formation of defect complexes (Bruce *et al* 1984). Sample reannealing causes the conductivity to rise to its original value. This is an attractive feature for thermal battery application where long storage times at low temperature (when conductivity should be ignored) and a relatively high operational temperature (when ionic conductivity should be high) are envisaged (Robertson *et al*, 1997).

Lithium orthosilicate, Li_4SiO_4 is one of the promising LISICON groups. This compound has a versatile host structure and can form non-stoichiometric materials by doping aliovalent or isovalent ions. Stoichiometric Li_4SiO_4, a poor conductor ($\sigma_{100^oC} = 10^{-8}$- 10^{-10} S cm^{-1}), is not suitable for practical applications (West *et al*, 1976). The conductivity is improved by partial substitutions of Si^{4+} by Ti^{4+}. The best conductivity of around 5×10^{-4} S cm^{-1} at 300°C has been reported by West (1973) for the $Li_4Ti_xSi_{1-x}O_4$ with $x = 0.4$.

Si^{4+} in Li_4SiO_4 structure also can be partially substituted by aliovalent ion such as P^{5+} to create lithium vacancy with formula, $Li_{4-x}P_xSi_{1-x}O_4$. The maximum conductivity is observed for $x = 0.4$ has a value around 10^{-4} S cm^{-1} at 100°C. Similar effects have been observed by partial substitutions of Si^{4+} by As^{5+} and V^{5+}. Their conductivities are more than 0.1×10^{-4} S cm^{-1} at 100°C. However, As^{5+}-doped compounds can be dismissed from further consideration because of high-level of potential toxicity (Khorassani *et al*, 1982; Khorassani *et al*, 1984).

A more significant conductivity enhancement occurs on partial substitutions with both divalent and trivalent cations. These doping may create vacant sites in the crystal and any lithium ion in the immediate vicinity can jump to the vacant sites. This leaves the previous site vacant which could now host another ion (Kumar *et al*, 2006). These results in the transport of ions across the solid giving rise to conductivity. Their concentration is the main factor that determines the conductivity of this solid electrolyte. Solid solution of $Li_3Mg_{0.5}SiO_4$ show a conductivity value of 2.3×10^{-5} S cm^{-1} at 200°C which rises to 1.5×10^{-2} S cm^{-1} at 400°C (Wakihara *et al*, 1988). Trivalent cations such as B^{3+}, Al^{3+}, Ga^{3+}, In^{3+},

Cr^{3+} and Fe^{3+} can also be partially substituted into Li_4SiO_4 structure to create either Li-interstitial or two Li-vacancies with general formula, $Li_{4+x}M_xSi_{1-x}O_4$ ($Si^{4+} \leftrightarrow Li^{+} + M^{3+}$) and $Li_{4-3x}M_xSiO_4$ ($3Li^{+} \leftrightarrow M^{3+}$) respectively. Masquelier *et al* (1995) have reported interstitial solid solution for B^{3+} and Al^{3+} with conductivity values of 8.48×10^{-8} S cm^{-1} and 7.28×10^{-5} S cm^{-1} at 100 ^{o}C respectively. Chavarria *et al* (1996) have reported for the solid solution of Li_{4-3x}(Al, Ga, In)$_x SiO_4$ at 127^{o}C with the following conductivity values of 6×10^{-5} (Al system), 6×10^{-6} (Ga system) and 6×10^{-8} S cm^{-1} (In system).

Another important LISICON group member is γ-Li_3PO_4. Partial substitution of Li_4XiO_4 by Li_3YO_4 (X = Si^{4+}, Ge^{4+}, Ti^{4+} and Y = P^{5+}, As^{5+}, V^{5+}, Cr^{5+}) forming systems with general formula $Li_{3+x}Y_{1-x}X_xO_4$, created interstitial ion in octahedral site that enhances ion mobility in the structure. The conductivities of these systems are much higher than those of the end-members. These materials are good conductors at ambient temperature conductivity and thermodynamically stable and relatively insensitive to atmosphere attack. The substituted $Li_{3.6}Ge_{0.6}V_{0.4}O_4$ crystal attained highest ionic conductivity of 4×10^{-5} S cm^{-1} at room temperature (Kuwano *et al*, 1985). The silicate analogue, $Li_{3.4}Si_{0.4}V_{0.6}O_4$ has been synthesized and used in rechargeable thin film cells in 1996. It is stable in contact with lithium metal even above 180^{o}C. It also has the advantages over $Li_{3.6}Ge_{0.6}V_{0.4}O_4$ of being less expensive to produce and having a slightly lower conductivity at lower temperature (4×10^{-5} S cm^{-1} at 25^{o}C), which reduces chances of self discharge (Tao *et al*, 2008).

2.2.4.4.1 Structure of LISICON (Li_4SiO_4)

The basic structure of Li_4SiO_4 is monoclinic. It is composed of hexagonal close packed oxygen ion arrays. It is iso-structural with γ-Li_3PO_4. In the close packed structure, 74.02 % of the available space is used by the close packed atoms. This leaves 25.98 % of space available for occupation by suitably atoms or ions. In regular close packed arrays, two types of sites are found, tetrahedral and octahedral sites. There are four tetrahedral and two octahedral sites per hexaganol close packed unit cell. In Li_4SiO_4 structure, one-eighths of the tetrahedral vacancies in this packing are occupied by silicon cations and three-eighths of the vacancies occupied by the lithium, so half of the tetrahedral sites are occupied by the cations. Silicon is tetrahedrally co-ordinated to oxygen of SiO_4 but connected by sharing edges with LiO_4 (Kamphorst and Hellstrom ,1980; West 1973; Tranqui *et al*,1979; Shannon *et al* 1977).

The lithium atoms occupy different sites. There are six distinct sets of sites occupied by lithium atoms, which is in a network of linked LiO_n polyhedra where n = 4, 5, 6. The LiO_n polyhedra are often linked together by sharing common faces and edges. Four lithium atoms, labeled LiO_4 (1), LiO_4 (2), LiO_4 (3) and LiO_4 (4) are in tetrahedrally coordinated. The other two lithium atoms, LiO_5 (5) and LiO_6 (6) at the octahedral sites have 5 and 6 oxygen near-neighbors respectively due to high distortion in Li_4SiO_4. The manner and degree with which the different polyhedral share faces are shown in Table 2.1. The SiO_4 and LiO_4 tetrahedra share oxygen vertices to form three-dimensional framework which is favorable for ion transport (Kamphorst and Hellstrom, 1980; West 1973; Tranqui *et al*, 1979; Shannon *et al* 1977). The framework of the LISICON structure is shown in Figure 2.4.

Partial substitution caused a distortion of the hexagonal close packed (hcp) sublattice generating 'tetrahedral packed (tp)' array through a mechanism which allows additional cations to be accommodated on tetrahedral co-ordinated sites. During the hcp to tp conversion the former's six-fold axis is lost and a new four-fold axis is created, leading to a corrugated layer structure (see Figure 2.5) with 11-fold rather than 12-fold co-ordination. Half of the tetrahedral and octahedral sites within the hcp sublattice remain undistorted but the remainders are replaced by a large number of sites with irregular octahedrally and tetrahedrally co-ordinated environments. This is especially advantageous for Li^+, a small sized cation, that can be readily accommodated in the distorted tetrahedrally and octahedrally co-ordinated (Hull, 2004).

Table 2.1: The manner and degree with which the different polyhedral share faces (West, 1973).

Polyhedron	Fractional Occupancy	Shares common faces with the polyhedral of:
$Li(1)O_4$	$\frac{2}{3}$	Li(4), Li(5), Li(6), Li(6')
$Li(2)O_4$	$\frac{1}{2}$	Li(3)
$Li(3)O_4$	$\frac{1}{2}$	Li(2), Li(5), Li(5'), Li(6)
$Li(4)O_4$	$\frac{1}{3}$	Li(1)
$Li(5)O_5$	$\frac{1}{3}$	Li(1), Li(3), Li(5')
$Li(6)O_6$	$\frac{1}{3}$	Li(1), Li(1'), Li(3)

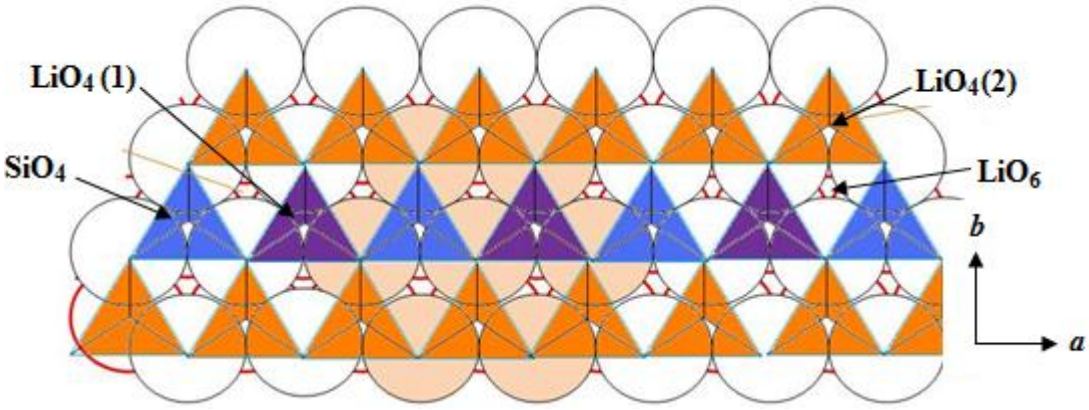

Figure 2.4: The framework of Li_4SiO_4 structure

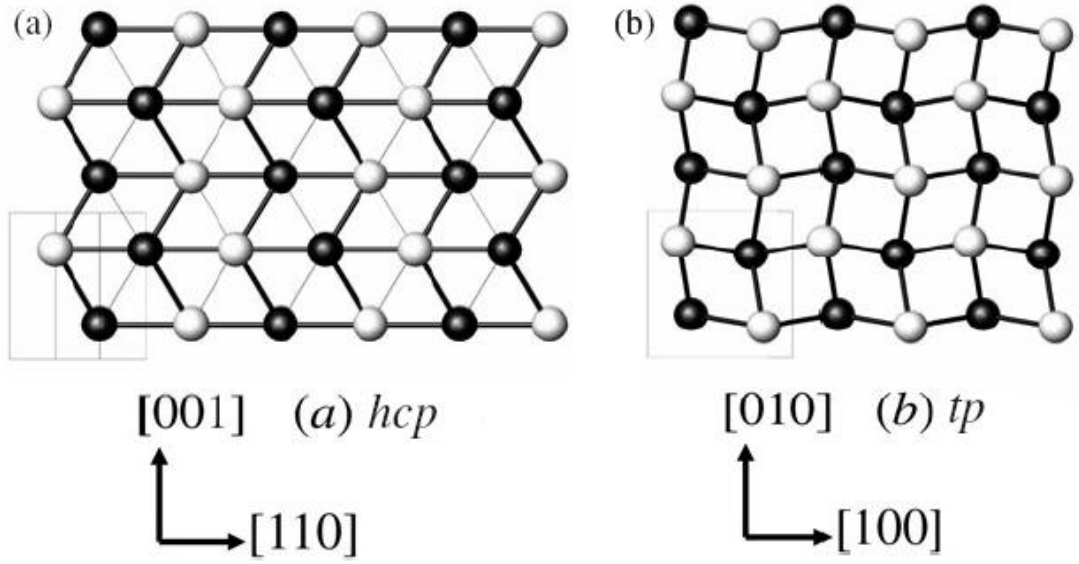

Figure 2.5 : The distortion of the hexagonal close packed (hcp) to 'tetrahedral packed (tp)' array (Hull, 2004).

The majority of fast ion crystalline conductors are derived from stoichiometric solid by making substitutions in order to create interstitial ions or vacancies. The lithium ion diffusion might be expected through the migration channel in *c*-direction which involved the tetrahedral and interstitial octahedral sites pathways in three dimensions (Fig. 2.6). Ionic conduction in LISICON structure materials is due to the mobile ions hopping among energetically favorable sites in

the surrounding potential. The motion of the surrounding ions simply provides the activation energy for mobile ions to migrate through channels in the LISICON framework. Moreover, the LISICON structure also exhibits high ionic conductivity due to its 3D channel structure that enables easy migration of the ions.

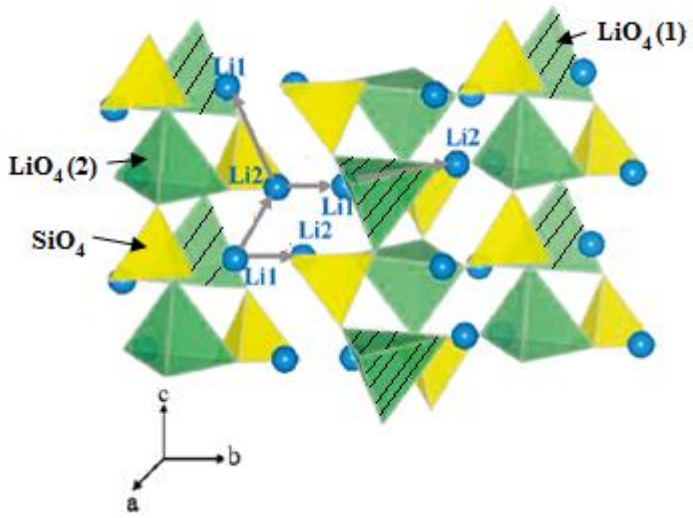

Figure 2.6: Lithium ion migration path in LISICON monoclinic structure (Islam and Kuganathan, 2009)

CHAPTER 3

LIST OF PUBLICATIONS

Published Paper 1: **S.B.R.S Adnan**, N.S Mohamed, Norwati K.A **(2011),** Li_4SiO_4 Prepared by Sol-Gel Method as Potential Host for LISICON Structured Solid Electrolyte. *World Academy of Science, Engineering and Technology, Special Issue* 74, 2011, pages 676-679.

Published Paper 2: **S.B.R.S Adnan** and N.S Mohamed **(2012).** Citrate Sol Gel Synthesised Li_4SiO_4: Conductivity and Dielectric Behaviour, *Materials Research Innovations*, 4,16, 281-285.

Published Paper 3: **S.B.R.S Adnan** and N.S Mohamed **(2012).** Conductivity and dielectric Studies of Li_2ZnSiO_4 Ceramic Electrolyte Synthesized via Citrate Sol gel Method, *International Journal of Electrochemical Science,* 7, 9844-9858.

Published Paper 4: **S.B.R.S Adnan** and N.S Mohamed (**2013).** Structural, Thermal and Electrical Properties of $Li_{4-2x}Zn_xSiO_4$ Ceramic Electrolyte Prepared by Citrate Sol Gel Technique, *International Journal of Electrochemical Science, 8, 6055-6067.*

Published Paper 5: **S.B.R.S Adnan** and N.S Mohamed **(2014).** Properties of Novel $Li_{4-3x}Cr_xSiO_4$ Ceramic Electrolyte**,** *Ceramics International,* 40, 5033-5038.

Published Paper 6: **S.B.R.S Adnan** and N.S Mohamed **(2014).** Effect of Sn Substitution on the Properties of Li_4SiO_4 Ceramic Electrolyte, *Solid State Ionics,* **D*oi.org/10.1016/j.ssi.2013.07.008.***

Published Paper 7: **S.B.R.S Adnan** and N.S Mohamed **(2014).** Characterization of Novel $Li_4Zr_{0.06}Si_{0.94}O_4$ and $Li_{3.94}Cr_{0.02}Zr_{0.06}Si_{0.94}O_4$ Ceramic Electrolytes for Lithium Cells, *Ceramics International,* 40, 6373-6379.

Published Paper 8: **S.B.R.S Adnan** and N.S Mohamed **(2014).** AC Conductivity and Dielectric Studies of Modified Li_4SiO_4 Ceramic Electrolytes**,** *Ceramics International,* **D*oi.org/10.1016/j.ceramint.2014.03.149.***

Li_4SiO_4 Prepared by Sol-gel Method as Potential Host for LISICON Structured Solid Electrolytes

Syed Bahari Ramadzan Syed Adnan, Nor Sabirin Mohamed and Norwati K.A

***Abstract*—**In this study, Li_4SiO_4 powder was successfully synthesized via sol gel method followed by drying at 150°C. Lithium oxide, Li_2O and silicon oxide, SiO_2 were used as the starting materials with citric acid as the chelating agent. The obtained powder was then sintered at various temperatures. Crystallographic phase analysis, morphology and ionic conductivity were investigated systematically employing X-ray diffraction, Fourier Transform Infrared, Scanning Electron Microscopy and AC impedance spectroscopy. XRD result showed the formation of pure monoclinic Li_4SiO_4 crystal structure with lattice parameters a = 5.140 Å, b = 6.094 Å, c = 5.293 Å, β = 90° in the sample sintered at 750°C. This observation was confirmed by FTIR analysis. The bulk conductivity of this sample at room temperature was 3.35×10^{-6} S cm^{-1} and the highest bulk conductivity of 1.16×10^{-4} S cm^{-1} was obtained at 100°C. The results indicated that, the Li_4SiO_4 compound has potential to be used as host for LISICON structured solid electrolyte for low temperature application.

***Keywords*—** Conductivity, LISICON, Li_4SiO_4, Solid electrolyte, Structure.

I. Introduction

CRYSTALLINE as well as glassy Li_4SiO_4-based compounds have been investigated with regard to their use as solid electrolytes in secondary lithium batteries. The structure of Li_4SiO_4 has moderately good Li^+ conductivity and is a versatile host structure for doping to form LISICON (Lithium Super Ionic) structure. Both Li^+ interstitials and Li^+ vacancies can be created resulting in high conductivities [1]. For example, when Si^{4+} ions are substituted by Al^{3+} ions, the Al^{3+} ions occupy Si^{4+} sites with Li^+ ion entering interstitial sites, ($Si^{4+} = Al^{3+} + Li^+$) to give a compound with a general formula, $Li_{4+x}Al_xSi_{1-x}O_4$ and when Si^{4+} ions are substituted by V^{5+} ions, Li^+ vacancies are created, ($Si^{4+} + Li^+ = V^{5+}$) to give a compound with a general formula, $Li_{4-x}V_xSi_{1-x}O_4$ [2].

LISICON structured solid electrolytes based on Li_4SiO_4 have been reported to show high conductivity at high temperatures (200°C – 500°C) [3]. These compounds are commonly synthesized by conventional solid state reaction method. This method are lead to many problems such as its use of high firing temperature, contamination with impurities, volatilization, lack of control of the microstructure and composition and suffer to obtaining good ceramics free of grain boundary resistances.

Syed Bahari Ramadzan Bin Syed Adnan is with University Of Malaya.Malaysia. e-mail:syed_bahari@yahoo.com

In order to overcome this problem, the sol gel method was used to prepare ion conductor materials. The sol gel technique has the advantages of lowering the synthesis temperature and can improving grain boundary conductivity and is a high purity process which leads to good homogeneity [4].

Recently Wu et al. reported the synthesis of Li_4SiO_4 employing sol gel technique [5-6]. In the former paper, the conductivity behavior of the compound was reported for the temperature range from 250 to 400°C. In the present study, Li_4SiO_4 compound was synthesized using a similar method. However, its conductivity behavior was studied at low temperatures ranging from 25 to 100°C in order to study the potential of this compound to be used as a host in LISICON structured solid electrolytes for low temperature electrochemical devices.

II. Experimental Procedure

A. Synthesis of Li_4SiO_4

Li_4SiO_4 powder was prepared by sol gel method. Li_2O and SiO_2 were used as the starting materials and citric acid ($C_6H_8O_7$) was used as the chelating agent. The molar ratio of Li_2O: SiO_2 was fixed at 4:1. Li_2O was dissolved in distilled water before mixing with SiO_2 and citric acid. Citric acid was used to adjust the pH value of the solution to alkali (pH = 8.5). After that, the mixture was stirred under continuous reflux process for 1 hour until a colloidal solution was obtained. The colloidal solution was vaporized at 80°C and a gel was formed ultimately. The gel was dried at 150°C for 24 hours to remove H_2O particle, resistance organic group and also to avoid ceramic cracks. The flowchart of the synthesis procedure is shown in Figure 1. The obtained powder was palletized and the pallets formed were later sintered at temperatures from 600 – 750°C for four hours.

B. Characterization Techniques.

Crystallographic phases present in the prepared samples were identified by XRD using Bruker AXS, with CuKα radiation. To confirm the formation of the phases, FTIR was done on the samples employing Perkin Elmer FTIR Spectrum RX1 Spectrometer. The FTIR spectra were recorded at a resolution of 1 cm^{-1}. The morphology of the samples was observed by the Energy Dispersive Xray (EDX) technique. The AC impedance measurements were carried out using impedance analyzer, SOLATRON 1260 with platinum as the blocking electrode in the temperature range from 25 to 300°C over a frequency range from 0.1 to 10^6 Hz.

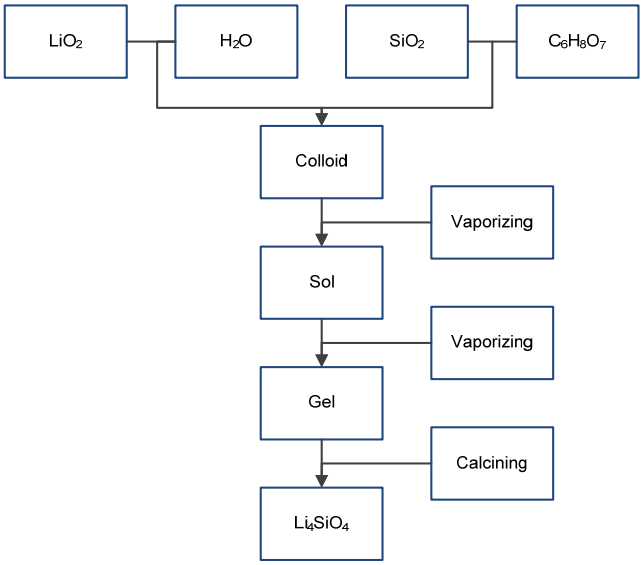

Fig. 1 Flow chart of sol gel procedure for the preparation of Li_4SiO_4 powder.

III. Result And Discussion

A. X-ray Diffraction.

Figure 2 shows XRD spectra of Li_4SiO_4 sintered at different temperatures for four hours. As can be seen in the figure, the samples sintered at 600-700°C exhibit sharp diffraction peaks attributed to Li_4SiO_4 and Li_2CO_3 indicated the presence of both Li_4SiO_4 and Li_2CO_3 in the samples. The XRD spectrum of the sample sintered at 750°C shows peaks attributed only to Li_4SiO_4 demonstrating that pure Li_4SiO_4 has been obtained. The crystal structure of Li_4SiO_4 is monoclinic with space group $P2_1/m$ and lattice parameters are a = 5.140 Å, b = 6.094 Å, c = 5.293 Å, β = 90° which are close to those of West et al.[7].

B. Fourier Transform Infrared

Figure 3 depicts the FTIR spectra of the Li_4SiO_4 sample, sintered at 700°C and 750°C. The sample sintered at 700°C show strong bands in the regions of 726-1071 cm^{-1} and 1366-1588 cm^{-1}. This may be attributed to stretching and bending vibrational modes of Si-O (800 cm^{-1}) in SiO_4 tetrahedral [8-9], stretching and bending vibrational modes of C=O (1550-1650 cm^{-1}) in CO_2 of Li_2CO_3 [10].

The Li_4SiO_4 sample sintered at 750°C does not show the bands between 1366 and 1588 cm^{-1} which is due to the disappearance of C=O from Li_2CO_3. This observation is consistent with the result of XRD study and hence, confirms the formation of pure Li_4SiO_4 phase in the sample sintered at 750°C.

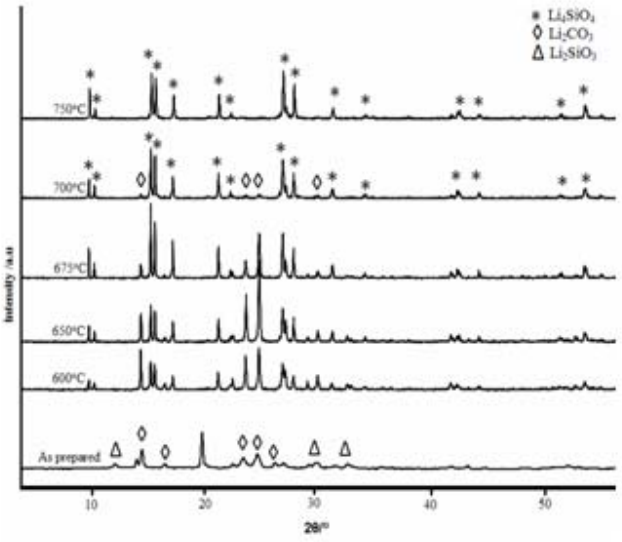

Fig. 2 XRD pattern of samples sintered at different temperatures.

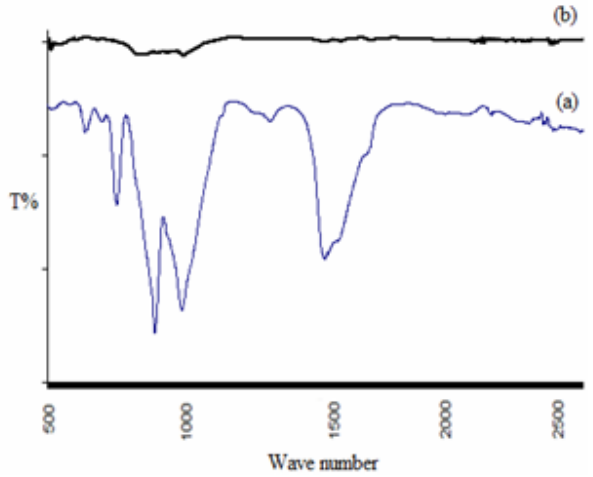

Fig. 3 FTIR spectra for Li_4SiO_4 sample sintered at (a) 700°C and (b) 750°C

C. SEM and EDX analysis

The SEM micrograph of the sample sintered at 750°C is shown in Figure 4 (a) and its EDX analysis is presented in Figure 4 (b). The atomic ratio of Si:O is determined to be 1:4. Since Li^+ ion is not detectable by EDX, the concept of charge neutrality is employed [11]. Using this concept it is found that the stoichiometry of EDX analysis is in good agreement with the designated stoichiometry. This observation is consistent with the result of XRD analysis. Carbon detected in this analysis may come from citric acid.

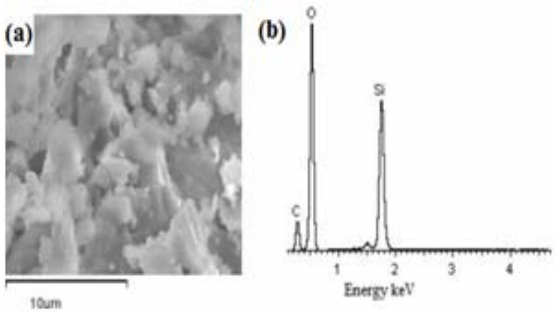

Fig. 4 a) SEM micrograph and (b) EDX analysis of Li_4SiO_4 sample sintered at 750°C

D. Ionic Conductivity

Figures 5(a) and 5(b) display impedance spectra of the sample sintered at 750°C recorded at 27°C and 100°C. The conductivity value of the bulk conductivity was calculated using (1):

$$\sigma_b = \frac{d}{AR_b} \quad (1)$$

where d is the sample thickness, A is the area of the electrode and R_b is the bulk resistance. The bulk conductivity of this sample at 27°C is found to be 3.35×10^{-6} S cm^{-1}. The conductivity is observed to increase with increase in temperature. The increase in conductivity could be attributed to the greater movement of ionic point defect and the creation of greater ions movement due to an increase in thermal of energy [12]. The conductivity of the sample is determined to be 1.16×10^{-4} S cm^{-1} at 100° C. The value is an order of magnitude higher compared to the $Li_{4-3x}Ga_xSiO_4$ (a modified Li_4SiO_4) system reported by Smith et al. measured at the same temperature [13].

The temperature dependence of the bulk conductivity is illustrated in Fig. 6 is found to be linear and well fits the Arrhenius equation (2),

$$\sigma_b T = A \exp\left(\frac{-E_\alpha}{kT}\right) \quad (2)$$

where A is the pre-exponential factor, E_α the activation energy for conduction and k the gas constant. This indicates that there are no structure and phase changes in the sample for the studied temperature range

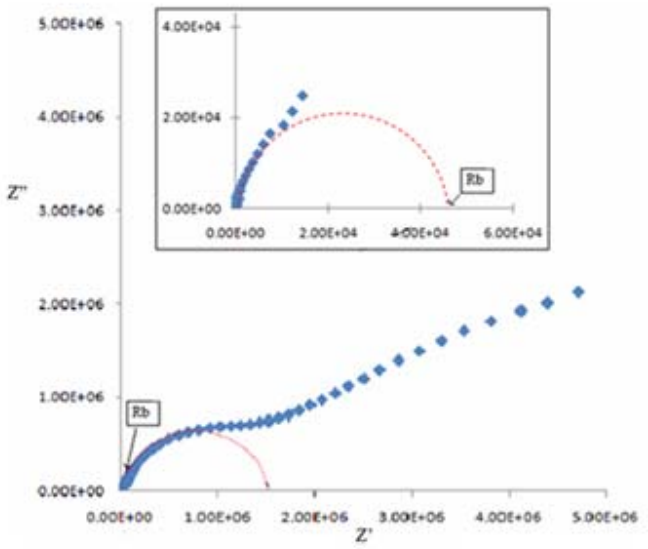

Fig. 5(a): Impedance plot of Li_4SiO_4 at room temperature (R_b = bulk resistance). The figure in insert focuses on low impedance region.

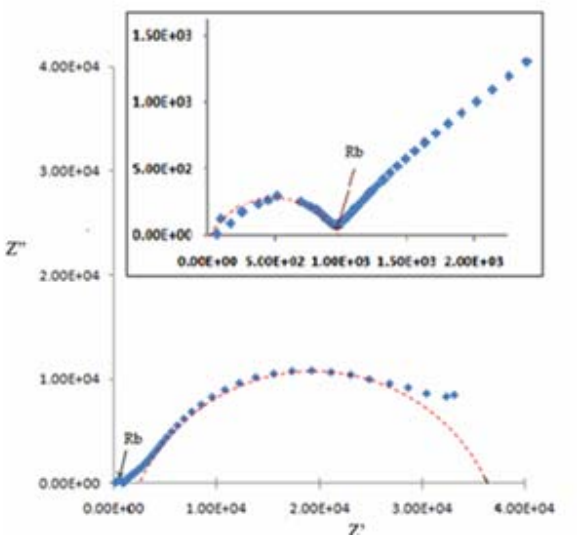

Fig. 5(b): The conductivity of Li_4SiO_4 at 100°C (R_b = bulk resistance). The figure in insert focuses on the low impedance region.

Activation energy normally includes energy for formation and migration of ions. The Li_4SiO_4 structure is in the extrinsic regime below 200°C [14]. In this extrinsic regime, the activation energy is dominated by the migration energy. In this case, the activation energy can be represented by the migration energy for the doped oxide ionic conductors [15]. The activation energy; E_α determined from Figure 6 is 0.19 eV. The low value of activation energy is evidence for high mobility of ions in the sample.

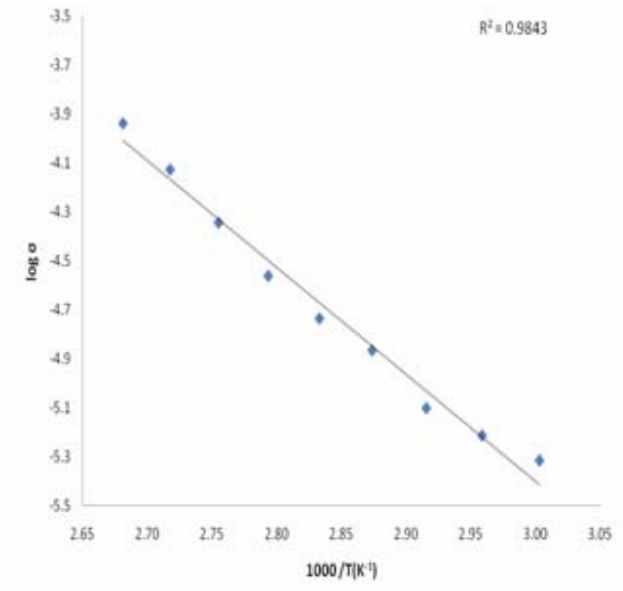

Fig. 6 Arrhenius plot of the bulk conductivity for Li_4SiO_4 sample sintered at 750°C

IV. Conclusions

A pure Li_4SiO_4 sample was successfully prepared by sol gel method followed by sintering at 750° C. The conductivity of the Li_4SiO_4 compound obtained in this study showed conductivity in the order of 10^{-4} S cm^{-1} at 100° C and is higher compared to the modified Li_4SiO_4 compound reported by other researchers. This gives an indication of its potential to be used as a host for low temperature LISICON structured solid electrolytes.

References

[1] A.R. West, "Solid State Chemistry and Its applications," John Wiley and Sons Ltd, New York, 1984, pp. 478-481.

[2] A. Khorassini and A.R. West, "Li^+ ion conductivity in the system Li_4SiO_4---Li_3VO_4 ," Solid State Chemistry, Vol. 53 , pp. 373 , July 1984.

[3] A. Khorassini and A.R. West," New Li^+ Ion Conductor in the System Li_4SiO_4-Li_3AsO_4," Solid State Ionics, Vol. 7, pp. 1, 1982.

[4] X. Song, M. Jia, R. Chen," Synthesis of Li_3VO_4 by the Citrate Sol-gel Method and its Ionic Conductivity," Journal of Materials Processing Technology, Vol. 120, pp. 21-25, 2002.

[5] X. Wu, Z. Wen, X. Xu, X. Wang, J. Lin," Fabrication of Li_4SiO_4 Pebbles by Sol Gel Technique", Journal of Nuclear Materials, Vol. 85, pp. 222, 2009.

[6] X. Wu, Z. Wen, X. Xu, X. Wang, J. Lin," Synthesis and Characterization of Li_4SiO_4 nano pawders by a water based Sol Gel process", Fusion Engineering and Design, Vol. 35, pp. 471, 2010.

[7] B.L. Dubey and A.R. West," Crystal Chemistry of Li_4XO_4 Phases X= Si,Ge,Ti," J. Inorg. nucl. Chem, Vol. 35, pp. 3714, 1973.

[8] F.J. Humphreys and M. Hatherly,"*Recrystallization and related annealing phenomena",* Elsevier, U.K 1995.

[9] B. Shokri, M. Abbasi Firouzjah, S.I. Husseini," International Symposium on Plasma Chemistry (ISPC),"conference, Bouchum, Germany, July 26-31 2009.

[10] K.S. Hwang, Y.H. Lee, S..H. Bo," Preparation of Lithium Zirconate Nano Powder Prepared by Electrostatic Spraying for CO_2 sorbent," Materials Science Poland, Vol. 25, No.4, 2007.

[11] A.Aboulaich, D.E Conte, J.Olivier-Fourcade, C.Jordy, P.Willmann, J.C. Jumas,"Influence of Alkali Ion Doping on the Electrochemical Performances on tin-based composite matrials," Journal of Power Sources, Vol. 195, pp. 3316-3322, 2010.

[12] J. W. Fergus," Ceramic and Polymeric Solid Electrolytes for Lithium Ion Batteries," Journal of Power Sources, Vol. 195, pp. 4554, 2010.

[13] R.I Smith and A.R West." Crystal Structure of the Lithium Ion Conductor , $Li_{3.4}Ga_{0.2}SiO_4$," Journal of Solid State Chemistry, Vol. 88, pp. 564-570, 1990.

[14] A.R. West," Ionic Conductivity of Oxide Based on Li_4SiO_4," Journal of Applied Electrochemistry, Vol.3, pp. 327, 1973.

[15] S. Hui, J. Roller, S. Yick, X. Zhang, Cyrille, Y. Xie, R. Maric, D. Ghose," A brief review of the ionic conductivity enhancement for selected oxide electrolytes," Journal of Power Sources,Vol.172, pp. 493, 2007.

Syed Bahari Ramadzan Bin Syed Adnan received the B.Sc. degree from University of Technology Malaysia, Skudai, Malaysia in 2006 and M.Sc. degree from University of Malaya, Kuala Lumpur, Malaysia in 2010, both in field of Science (Physics). He currently has joined the Department of Physics at Centre for Foundation Studies in Science, University of Malaya as a Ph.D. student. His research interests are Inorganic crystalline material especially in LISICON type structure as solid electrolytes.

Nor Sabirin Mohamed received the B.Sc. degree from State University of New Tork, Albany, USA in 1985, the M.Sc. degree from the same University in 1987 (both in field of Physics) and the Ph.D. degree in material field from University of Malaya, Kuala Lumpur, Malaysia, in 2004. She is currently with the Department of Physics at Centre for Foundation Studies in Science, University of Malaya. Her research interests are solid State Ionic including solid electrolyte, glass ceramic, polymer electrolyte and electrode materials.

Citrate sol–gel synthesised Li_4SiO_4: conductivity and dielectric behaviour

S. B. R. S. Adnan[1] and N. S. Mohamed*[2]

Pure Li_4SiO_4 ceramic material is obtained using citrate sol–gel method followed by sintering at 750°C. The crystallographic phase of the material is investigated by X-ray diffraction. The conductivity of the ceramic material is determined at different temperatures. Meanwhile, the dielectric properties are observed in order to obtain further information on ion dynamics in the material. The X-ray diffraction result shows the formation of a pure monoclinic Li_4SiO_4 crystal structure with lattice parameters a=5·140 Å, b=6·094 Å, c=5·293 Å and β=90°. The conductivity of the material increases linearly with the increase in temperature. The conductivity of the sample is $1{\cdot}16 \times 10^{-4}$ S cm^{-1} at 100°C. The frequency dependence of conductivity follows the universal power law variation $\sigma_{ac}(\omega)=\sigma_o+A\omega^s$. The plot of pre-exponent s versus temperature suggests that the conduction mechanism in the system can be described using correlated barrier hopping model. The increase in dielectric constant and dielectric loss and the peak shift of tan δ to higher frequencies with temperature indicate that the increase in conductivity with temperature is due to the increase in number and hopping rate of charge carriers with temperature.

Keywords: Ceramic, Conductivity, Dielectric, Solid electrolyte, Sol–gel

Introduction

In the search of electrolytes for a variety of solid state devices and batteries with Li^+ ion conductors, systems based on lithium orthosilicate, Li_4SiO_4 have been considered.[1] Li_4SiO_4 is a ceramic material with appreciable cationic conductivity.[2] This compound has a versatile host structure and can form non-stoichiometric materials by doping with different cations, such as Zn^{2+} to form lithium super ionic conductor materials.[3] The cations replace lithium ions in tetrahedral sites, while the additional lithium ions occupy interstitial octahedral sites. Their concentration is the main factor determining the conductivity of these solid electrolytes.[4,5]

The crystal structure of Li_4SiO_4, which has a tetragonal packed arrangement, is complex. Some crystals appear to contain lithium ions in partially occupied four-, five- and six-coordinate sites. Other crystals possess a large supercell in which the various four-, five- and six-coordinate sites are fully occupied. Because of the large number of lithium sites in the unit cell of the (LiO_n) polyhedral, where n=4,5,6, they are often linked together by sharing common faces. There are six distinct sets of sites occupied by lithium with occupancy factors ranging from 1/3 to 2/3.[6,7]

Li_4SiO_4 can be synthesised using conventional solid state reaction method. However, this method involves high heating temperature and yields samples with low conductivity ($\sigma_{300°C}=10^{-5}$ S cm^{-1}).[8,9] The sol–gel technique is an alternative method for preparing this compound. This technique has the advantages of lowering the synthesis temperature and improving grain boundary conductivity and is a high purity process that is expected to produce samples with higher conductivity.[10]

The work reported in this article is dedicated to obtaining Li_4SiO_4 material via the citrate sol–gel method in the hope of obtaining Li_4SiO_4 samples with higher conductivity. Dielectric studies are also performed in order to understand the ion dynamics in the samples.

Experimental

Synthesis of samples

For the preparation of Li_4SiO_4 powder, Li_2O and SiO_2 are used as starting materials, while citric acid ($C_6H_8O_7$) is used as chelating agent. The molar ratio of Li_2O/SiO_2 is fixed at 4 : 1 based on the stoichiometric formula of Li_4SiO_4. Li_2O is dissolved in distilled water before mixing with SiO_2 and citric acid, which is used to adjust the pH value of the solution to alkali (pH=8·5). The mixture is then stirred under continuous reflux process for 1 h until a colloidal solution is obtained. The colloidal solution is vapourised at 80°C, and a gel is formed ultimately. The gel is dried at 150°C for 24 h to remove H_2O and residual organic groups and also to avoid ceramic cracks. The obtained powder is pelletised, and the pellets formed are later sintered at different temperatures, from 600 to 750°C for 4 h. The sintered pellets for the ac conductivity measurements are 13 mm in diameter and 2 mm in thickness.

[1]Institute of Graduate Studies, University of Malaya, Kuala Lumpur 50603, Malaysia
[2]Centre for Foundation Studies in Science, University of Malaya, Kuala Lumpur 50603, Malaysia

*Corresponding author, email nsabirin@um.edu.my

Received 7 November 2011; accepted 16 February 2012
DOI 10.1179/1433075X12Y.0000000012

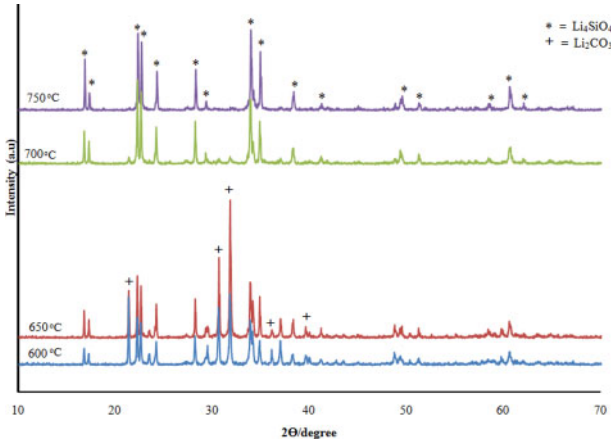

1 X-ray diffraction pattern of samples sintered at different temperatures

Characterisation of samples

Crystallographic phases present in the prepared samples are identified by X-ray diffraction (XRD) using a Bruker AXS X-Ray diffractometer with Cu K_α radiation. Complex impedance parameters (i.e. impedance and phase angle parameters) are measured with a computer controlled Solatron 1260 impedance analyser with platinum as the blocking electrode in the temperature range from 25 to 100°C over a frequency range from 0·1 to 10^6 Hz. The ac conductivity has been evaluated from dielectric data in accordance with the relation

$$\sigma_{ac} = \omega\varepsilon_o\varepsilon'' \tan\delta \quad (1)$$

where ε_o is the permittivity of free space ($8{\cdot}854 \times 10^{-14}$ F cm^{-1}), tan δ is the tangent loss factor and ε'' is the dielectric loss. The real and imaginary parts of permittivity and modulus are calculated from the relation[11]

$$\varepsilon^* = \varepsilon' - j\varepsilon'' \quad (2)$$

where

$$\varepsilon' = \frac{Z''}{\omega C_o(Z'^2 + Z''^2)}$$

and

$$\varepsilon'' = \frac{Z'}{\omega C_o(Z''^2 + Z'^2)}$$

In the above equations, Z' and Z'' are the real and imaginary impedances obtained from the impedance measurements. The ac currents (I) can be separated into charging current ($i\omega\varepsilon'$) C_oV and loss current ($\omega\varepsilon''$) C_oV as given by the following equation

$$I = (i\omega\varepsilon' + \omega\varepsilon'')C_oV \quad (3)$$

Using the relation $C_o = \varepsilon_o A/d$ (where ε_o is the permittivity in vacuum, A is the area of the electrode and d is the distance between electrode), the current density (J) can be related to the complex admittance (Y^*) as follows

$$J = (i\omega\varepsilon' + \omega\varepsilon'')E = (i\sigma'' + \sigma')E = Y^*E \quad (4)$$

Therefore

$$\sigma' = \omega\varepsilon_O\varepsilon'' \text{ and } \sigma'' = \omega\varepsilon_O\varepsilon' \quad (5)$$

where σ' is the loss current conductivity (conductance), also known as ac conductivity σ_{ac} in the present study, and σ'' is the conductivity due to charging current (susceptance). On the other hand, complex admittance (Y^*) is the inverse of Z^*.[12]

Results and discussion

Phase identification

Presented in Fig. 1 are the XRD spectra of Li_4SiO_4 sintered at different temperatures for 4 h. As can be observed in the figure, the samples sintered at 600–700°C exhibited sharp diffraction peaks attributed to Li_4SiO_4 and Li_2CO_3, indicating the presence of both compounds in the samples. The XRD spectrum of the sample sintered at 750°C shows peaks attributed only to Li_4SiO_4, demonstrating that pure Li_4SiO_4 has been obtained.[13]

The pure Li_4SiO_4 compound is found to be single phase in nature, crystallising in monoclinic structure with the space group $P2_1/m$.[6] The lattice parameters are listed in Table 1. The parameters are in good agreement with the values reported by Dubey and West.[13]

Conductivity measurement

Direct current conductivity

Illustrated in Fig. 2 are the impedance spectra of the samples sintered at 750°C (pure Li_4SiO_4 samples) recorded at room temperature (RT) and 100°C. The spectra consist of two depressed semicircles in the high frequency region followed by a spike in the low frequency region. The bulk resistance R_b is determined from the intercept at the real impedance axis of the first semicircle. The dc conductivity value of the bulk conductivity is calculated using the equation

$$\sigma_b = \frac{d}{AR_b} \quad (6)$$

where d is the sample thickness, A is the area of the electrode and R_b is the bulk resistance.

The dc ionic conductivities for the sample sintered at 750°C from complex impedance plots for different temperatures are analysed by the Arrhenius equation

$$\sigma_b T = A\exp\left(\frac{-E_\alpha}{kT}\right) \quad (7)$$

where A is the pre-exponential factor, E_α is the activation energy for conduction and k is the gas constant. Figure 3 depicts the Arrhenius plot for the sample. It is observed that the conductivity increases with the increase in temperature. The conductivity of the sample is determined to be $3{\cdot}36 \times 10^{-6}$ S cm^{-1} at RT and $1{\cdot}16 \times 10^{-4}$ S cm^{-1} at 100°C. The conductivity value at 100°C is an order of magnitude higher compared to the value reported by Smith *et al.* measured at the same temperature.[14]

Table 1

Parameter	*a*, Å	*b*, Å	*c*, Å	*V*, Å^3
Present Work	5·147	6·094	5·293	166·01
Dubey and West[13]	5·140	6·100	5·300	166·17

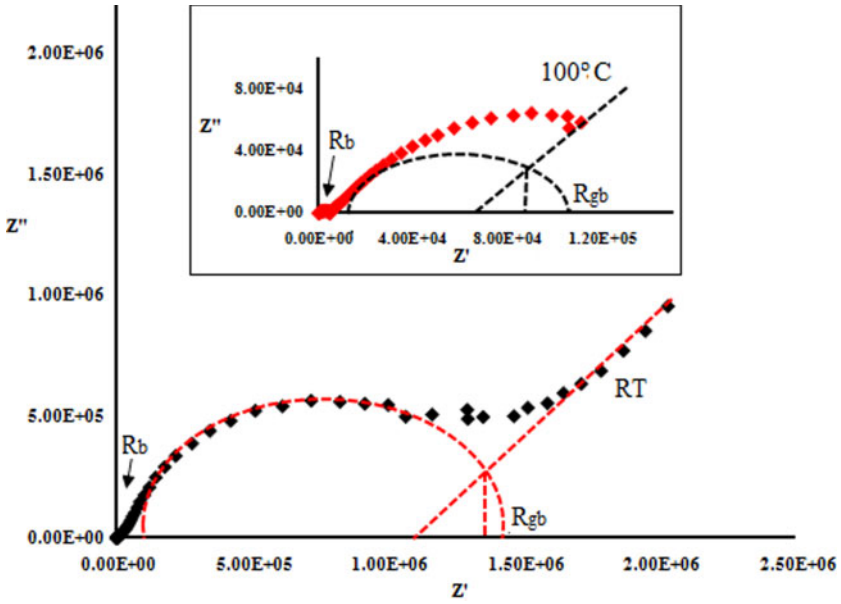

2 Impedance spectrum of Li_4SiO_4 at RT: figure in inset shows on impedance spectrum at 100°C

The linear plot in Fig. 3 suggests that there are no structure and phase changes in the sample for the studied temperature range.[15] The activation energy of the sample is determined from the gradient of the Arrhenius plot. The activation energy normally includes energy for the formation and migration of ions. According to West,[4] the Li_4SiO_4 structure is in the extrinsic regime below 200°C. In this extrinsic regime, the activation energy is dominated by the migration energy. The activation energy E_α determined from the slope of log σ_{dc} versus $1000/T$ plot is 0·19 eV. The low value of activation energy indicates high mobility of ions in the sample.

Alternating current conductivity

The log σ_{ac} versus log ω plots of the pure Li_4SiO_4 samples for different temperatures are shown in Fig. 4. The plots consist of three regions, i.e. a spike in the low frequency region, an intermediate frequency plateau and a high frequency dispersion. The dispersion in the ac conductivity at low frequencies arises from electrode polarisation. At these frequencies, the ionic conductivity is high enough to produce a significant build-up of charges at the electrodes, which reduces the effective applied field across the sample and hence the apparent conductivity.[16]

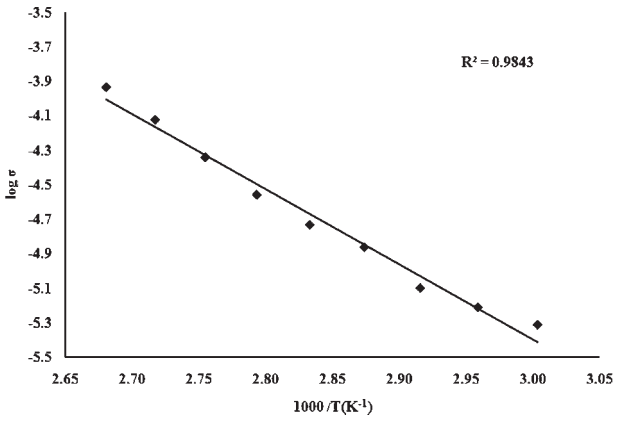

3 Arrhenius plot of dc conductivity for Li_4SiO_4

At the plateau region, the conductivity is frequency independent, and the value of conductivity at this plateau region agrees well with the dc conductivity determined from impedance plots. The switch over from the frequency independent region to the frequency dependent region signals the onset of conductivity relaxation, which shifts towards higher frequencies as the temperature increases. The observed dispersion of conductivity with frequency is in general agreement with the prediction of the jump relaxation model. According to this model, at very low frequencies ($f \rightarrow 0$), an ion can jump from one site to its neighbouring vacant site successfully contributes to dc conductivity. At high frequencies, the probability for the ion to jump back to its initial site increases due to the short time periods available. The high probability for the correlated forward backward hopping at high frequencies together with the relaxation of the dynamic cage potential is responsible for the high frequency dispersion.[17]

The conductivity behaviour obeys the universal power law $\sigma_{ac}(\omega) = \sigma_{o+} A\omega^s$, where σ_o is the dc conductivity, A is the pre-exponential factor and s is the fractional exponent. The value of s is extracted from the slope of log $\sigma_{ac}(\omega)$ versus log ω. The parameter of s obtained varies from 0·70 at RT and decreases to 0·09 at the highest temperature of 373 K. This indicates that the frequency dependence of σ_{AC} can be explained in terms of this law. The plot of variation of s with temperature is illustrated in Fig. 5. The plot can also be fitted to the equations $s = -0{\cdot}0077T + 1{\cdot}0778$. This equation suggests that $s \rightarrow 1$ when $T \rightarrow 0$.

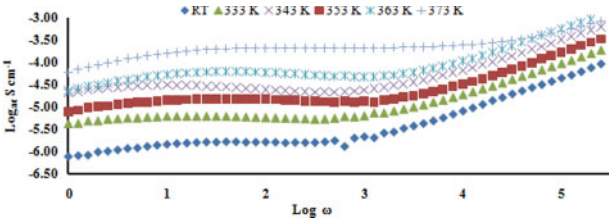

4 Alternating current conductivity (log) versus frequency (log) plot at various temperatures for Li_4SiO_4

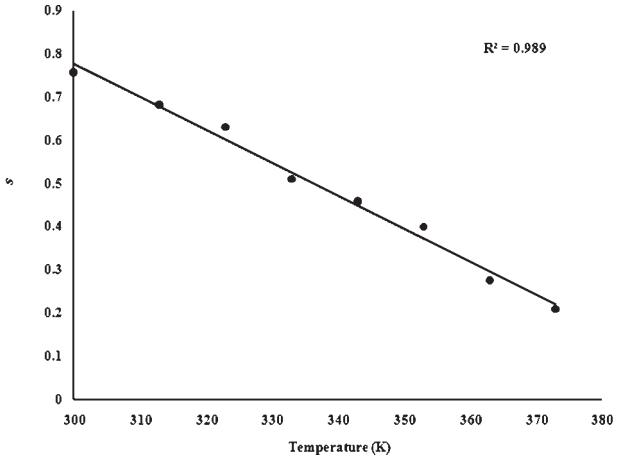

5 Value for *s* for Li_4SiO_4 material at different temperatures

The frequency exponent s in the Correlated Barrier Hoping CBH model is in the range from 0·7 to 1 at RT and decreases with increasing temperature and can be evaluated as follows[17–21]

$$s = 1 - \frac{6kT}{W_m} \tag{8}$$

where k is Boltzmann's constant, T is the temperature and W_M is the maximum barrier height.[19–21] From equation (8), it can be deduced that $s \rightarrow 1$ if $T \rightarrow 0$. This confirms that the conduction mechanism in the Li_4SiO_4 system studied in this work can be described using the CBH model.

According to the correlated barrier hopping model, it is assumed that the ions or charge carriers are surrounded by several potentials, such as the Coulombic repulsive potential between the ions and a potential well in which the ions reside. Superposition of the potentials yields a single ion potential that is actually felt by the ions. When the ion gains sufficient energy, they hop from one site to another. As the temperature increases, the number of ions that hop from one site to another increases, leading to an enhancement in conductivity with temperature, as observed in Fig. 4.[17–21]

Dielectric study

In order to obtain further information on the ion dynamic properties in the Li_4SiO_4 material, its dielectric properties are studied. Figure 6 shows the frequency dependence of dielectric constant ε' at different temperatures for the material. From the figure, it can be seen that the value of ε' decreases to a constant value with frequency but increases with temperature. The low frequency is attributed to the contribution of charge carrier accumulation at the interface of the electrode and the Li_4SiO_4 material. At high frequencies, due to the high periodic reversal of the field, the contribution of charge carriers towards dielectric constant decreases with frequency.[22] Meanwhile, the increase in ε' with temperature can be attributed to the fact that at low temperature, the charge carriers on most cases cannot orient themselves with respect to the direction of the applied field; thus, they possess a weak contribution to polarisation and ε'. When the temperature is increased, the bound charge carriers get sufficient excitation thermal energy to be able to obey the change in external field more easily. This in turn increases their contribution to polarisation, resulting in an increase in ε'.[20–24]

Figure 7 depicts the frequency dependence of dielectric loss ε'' at different temperatures for the Li_4SiO_4 material. From the figure, ε'' decreases with frequency and increases with temperature. The decrease of ε'' with frequency can be attributed to the fact that at low frequencies, the electrical energy loss is high due to the migration of ions in the material. As the ion moves, they loss some of their energy to the lattice as heat, and so ε'' has high value. Meanwhile, at moderate frequencies, ε'' is due to the mix contribution of ion jump, conduction loss of ions migration and ion polarisation loss. At high frequencies, ion vibrations may be the only source of dielectric loss, and as a consequence, ε'' has minimum value.[25] The increase in dielectric loss with temperature may be attributed to an increase of conduction processes arising from thermally generated charge carriers.[25–26]

The dielectric loss factor is the phase difference due to the loss of energy within the sample at a particular

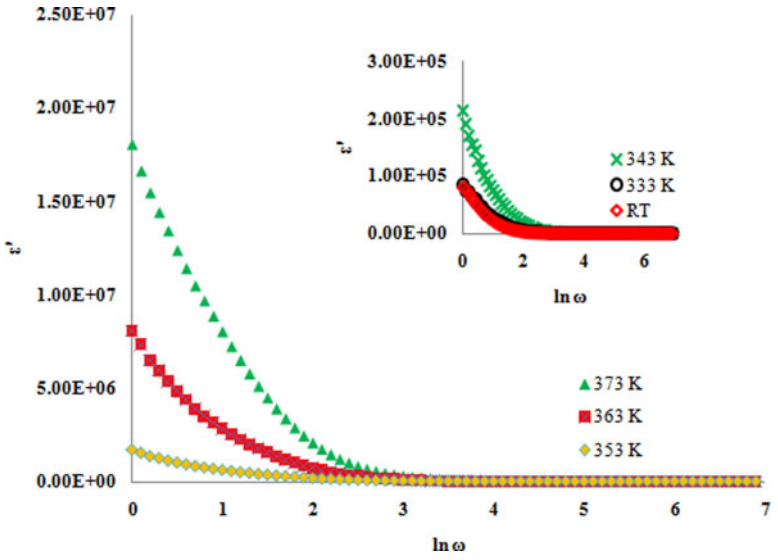

6 Plot of relative dielectric constant (ε') of Li_4SiO_4 as function of ln ω at different temperatures: figure in inset shows those at low temperature

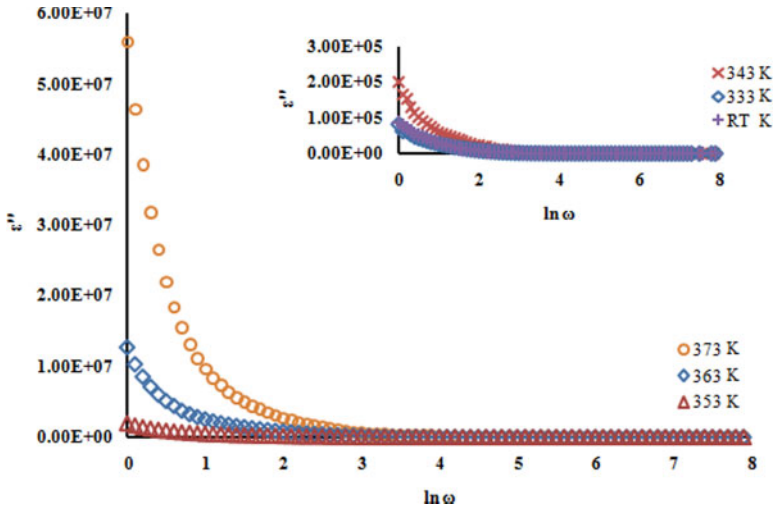

7 Value of relative dielectric loss (ε'') of Li_4SiO_4 as function of ln ω at different temperatures

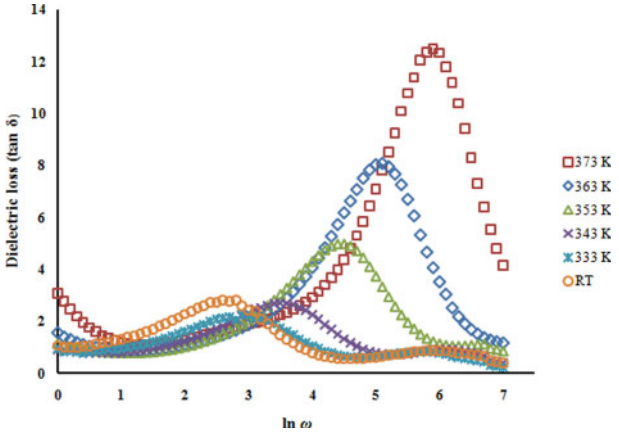

8 Frequency dependence of tan δ at various temperatures

frequency and is expressed as $\tan\delta = \varepsilon''/\varepsilon'$. Figure 8 presents the plot of frequency dependence of tan δ at various temperatures. The plot shows a peaking behaviour for all temperatures. As the temperature increases, the tan δ peak is shifted towards higher frequency. The shift of peak of tan δ towards higher frequency with the increase in temperature suggests that the ion jumping probability increases with increasing temperature.[22,26]

Conclusions

Pure Li_4SiO_4 compound has been successfully obtained via citrate sol–gel method. The dc conductivity of the Li_4SiO_4 compound increases with temperature. The conductivity is in the order of 10^{-4} S cm^{-1} at 100°C. The ac conductivity obeys the universal power law and may be described using the CBH model. The dielectric study shows that the increase in conductivity is ascribed to the increase in number as well jumping rate of charge carriers as reflected by the increase in dielectric constant and the shift of tan δ peak towards higher frequency as the temperature is increased.

References

1. C. Masquelier, M. Tabuchi and T. Takeuchi: *Solid State Ionics*, 1995, **79**, 98.
2. I. M. Hodge, M. D. Ingram and A. R. West: *J. Am. Ceram. Soc.*, 1976, **59**, 360.
3. A. R. West: 478; 'Solid State Chemistry and Its Applications', 1984, New York, John Wiley and Sons Ltd.
4. A. R. West: *J. Appl. Electrochem.*, 1973, **3**, 327.
5. E. I. Burmalin and G. S. Shekhtman: *Russ. J. Electrochem.*, 2010, **46**, 243.
6. D. Tranqui, R. D. Shannon and H.-Y. Chen: *Acta Crystallogr.*, 1979, **35**, 2479
7. R. I. Smith and A. R. West: *J. Solid State Chem.*, 1990, **88**, 564.
8. C. C. Chang, C. C. Wang and P. N. Kumta: *Mater. Des.*, 2001, **22**, 617.
9. C. Masquelier, M. Tabuchi, T. Takeuchi, W. Soizumi, H. Kageyama and O. Nakamura: *Solid State Ionics*, 1995, **79**, 98
10. 'X. Song, M. Jia and R. Chen: *J. Mater. Process. Technol.*, 2002, **120**, 21.
11. D. K. Pradhan, R. N. P. Choudhary and B. K. Samantaray: *Int. J. Electrochem. Sci.*, 2008, **3**, 597.
12. H. Yamamura, H. Nishino and K. Kakinuma: *J. Ceram. Soc. Jpn*, 2007, **115**, 23.
13. B. L. Dubey and A. R. West: *J. Inorg. Nucl. Chem.*, 1973, **35**, 3714.
14. R. I. Smith and A. R. West: *J. Solid State Chem.*, 1990, **88**, 564.
15. X. Wu, Z. Wen, X. Xu, X. Wang and J. Lin: *J. Nucl. Mater.*, 2009, **392**, 471–475.
16. M. Sugantha and U. V. Varadaraju: *Solid State Ionics*, 1997, **95**, 201.
17. M. A. Afifi, M. M. El-Nahass, A. E. Bekheet, I. T. Zedan and S. R. Elliott: *Physica B*, 2007, **400B**, 248.
18. F. Yakuphanoglu, Y. Aydogdu, U. Schatzschneider and E. Rentschler: *Solid State Commun.*, 2003, **128**, 63–67.
19. N. Mehta, D. Kumar, S. Kumar and A. Kumar: *Chalcogenide Lett.*, 2005, **2**, 103–109.
20. M. H. Buraidah, L. P. Teo, S. R. Majid and A. K. Arof: *Physica B*, 2009, **404B**, 1373.
21. A. A. Hendi: *Aust. J. Basic Appl. Sci.*, 2011, **5**, (7), 380–386.
22. A. M. Abo El Ata, S. M. Atia and T. M. Meaz: *Solid State Sci.*, 2004, **6**, 61.
23. C. R. Mariappan and G. Govindaraj: *Mater. Sci. Eng. B*, 2002, **B94**, 82.
24. E. G. El-Metwally, M. Fadel, A. M Shakra and M.A Afifi: *J. Optoelectron. Adv. Mater.*, 2008, **10**, 1320–1327
25. N. A. Hegab, A. E. Bekheet, M. A. Afifi, L. A. Wahaba and H. A. Shehata: *J. Ovonic Res.*, 2007, **3**, 71.
26. D. K. Mahato, A. Dutta and T. P. Sinha: *Physica B*, 2011, **406B**, 2703–2708.

Int. J. Electrochem. Sci., 7 **(2012)** 9844 - 9858

International Journal of
ELECTROCHEMICAL
SCIENCE
www.electrochemsci.org

Conductivity and Dielectric Studies of Li_2ZnSiO_4 Ceramic Electrolyte Synthesized via Citrate Sol Gel Method

S.B.R.S Adnan[1,*] *and N.S. Mohamed*[2]

[1]Institute of Graduate Studies, University of Malaya, 50603 Kuala Lumpur, Malaysia
[2]Centre for Foundation Studies in Science, University of Malaya, 50603 Kuala Lumpur, Malaysia
[*]E-mail: syed_bahari@yahoo.com

Received: 30 July 2012 / *Accepted:* 6 September 2012 / *Published:* 1 October 2012

Lithium zinc silicate ceramic powders have been synthesized by a sol gel method. The formation of the compound has been confirmed by X-ray diffraction and energy dispersive X-ray. The conductivity of the material increases linearly with temperature. The sample sintered at 850°C show highest dc conductivity with 5.00×10^{-6} S cm^{-1} at room temperature and increase to 5.54×10^{-4} S cm^{-1} at 500°C respectively. The frequency dependence of conductivity obeys the universal power law variation, $\sigma'(\omega) = \sigma(0) + A\omega^n$. The plot of pre-exponent *n* versus temperature suggests that the conduction mechanism in the system can be described using correlated barrier hopping model. Several important parameters such as mobile ion density and ionic mobility have been determined. The increasing trend of these parameters as well as the results of dielectric study indicates that the increase in conductivity with temperature is due to increase in mobility of mobile ions with temperature.

Keywords: Arrhenius, ceramic, dielectrics, electrolyte, Lisicon.

1. INTRODUCTION

In the search for new ion conducting crystalline materials, ceramic electrolytes form an important class of materials. This type of electrolyte materials offers advantages such as large electrochemical stability window, good thermal stability, important safety asset, absent of leakage and a high resistance to shock and vibrations [1].

Ceramics electrolytes are the only solid electrolytes that have ordered structure. They basically consist of mobile ions in less or more rigid crystalline frameworks. The ionic conduction in the crystalline electrolytes is through 1D, 2D or 3D channels depending on the crystal structure [2]. Good

ionic conductions are the key requirement for the solid electrolyte to minimize cell impedance also has little or no electronic conduction to minimize leakage currents [3].

Ionic conduction in this type of electrolytes occurs by movement of ionic point defects which requires energy in their periodic lattice structure. These point defects produce interstitial or vacancy ions. Increasing temperature will increase their ionic conductivity. Thus, crystalline solid electrolytes are well suited for high temperature application. However, ionic conduction in some compounds is reasonably high even at relatively low temperature. As such, several types of ion conducting inorganic crystalline materials have also been investigated for use in electrochemical devices operating at low and elevated temperature [4].

Li_2ZnSiO_4 one of the promising ceramic electrolytes, is categorized into LISICON (Lithium Super Ionic Conductor) type. This type is based on γ-tetrahedral structures, Li_2MXO_4, (M = Zn,Mg,Ca), (X = Ge,Si,Ti) which is isostructural with γ-Li_3PO_4 [5-8]. The LISICON structure is consisted of hexagonal close packed oxygen ion arrays where the cations occupy half of the tetrahedral site. The lithium ion diffusion is expected to occur through tetrahedral site and interstitial octahedral site pathway [9-10]. This indicates that the lithium ion distribution between tetrahedral site and interstitial octahedral site are important factors to create lithium ion conduction pathway that affects their ionic conduction [11-18].

The most common method used to prepare Li_2ZnSiO_4 ceramic materials is solid state reaction technique. However, this method commonly leads to many problems such as the use of high firing temperature (usually >1000^oC) for a prolonged period (1-2 days), contamination with impurities, volatilization, lack of control of microstructure and composition and suffer from obtaining good materials free of grain boundary resistance [19].

In recent years, considerable research has been done on the synthesis of advanced ceramic materials using the sol gel technique. Compare to the conventional methods, the most attractive features and advantages of sol-gel process include (a) molecular-level homogeneity can be easily achieved (b) the homogeneous mixture containing all the compounds in the correct stoichiometry ensures a much higher purity; and, (c) much lower heat treatment temperature to form glass or polycrystalline ceramics is usually achieved without resorting to a high temperature [20-21].

In this study, Li_2ZnSiO_4 compounds were prepared via sol gel method. Detail study on their conductivity and dielectric properties were carried out since such study on this compounds using this method has never been reported in the literature.

2. EXPERIMENTAL PROCEDURE

2.1. Synthesis of Li_2ZnSiO_4

Lithium acetate ($C_2H_3LiO_2$) zinc acetate ($C_4H_{10}O_6Zn$) and tetraethyl orthosilicate ($SiC_8H_{20}O_4$) were used as the starting materials while citric acid was used as the chelating agent. $C_2H_3LiO_2$ and $C_4H_{10}O_6Zn$ were first dissolved in distilled water before mixing with citric acid under magnetic stirring. The solution was transferred into a reflux system and continuously stirred until a

homogeneous solution was formed. Solution of $SiC_8H_{20}O_4$ was later added to this homogeneous solution and stirred for 12 hours. The solution was taken out and then vaporized for about 2 hours under magnetic stirring at 75°C. The resulting wet gel was dried in a vacuum oven at 150°C for 24 hours to remove water particles, resistance organic groups and also to avoid ceramic cracks. The obtained powder was ball milled for 1 hour using a Fritsch Pulverisette-7 which was operated at 300 rpm. The powder was pressed using a Specac pellet press to form pellet which was later sintered at different temperature for 12 hours.

2.2. Characterization techniques.

X-ray diffraction (XRD) was performed in order to elucidate structural information of the sample. The sintered ceramic powders were characterized using a Bruker AXS D8 Advance X-ray Diffraction spectrometer with Cu-K_α radiation of wavelength of 1.5406 Å in 2θ range between 10^o to 70^o . The morphology of the samples was observed by the Scanning Electron Microscopy (SEM) while Energy Dispersive Xray (EDX) technique was employed for elemental analysis.

The ceramic electrical properties were determined by ac impedance spectroscopy using Solatron 1260 impedance analyzer over a frequency range from 0.1 to 10^6 Hz. An applied voltage was fixed at 110 mV. The dc conductivity was determined using the equation:

$$\sigma_b = \frac{d}{AR_b} \qquad (1)$$

where d is the sample thickness, A is the area of the electrode and R_b is the bulk resistance.

The value of the dielectric constant (ε') and dielectric loss (ε'') of Li_2ZnSiO_4 were calculated using the formula:

$$\varepsilon' = \frac{Z''}{\omega C_o (Z'^2 + Z''^2)} \qquad (2)$$

and

$$\varepsilon'' = \frac{Z'}{\omega C_o (Z''^2 + Z'^2)} \qquad (3)$$

where Z' and Z'' are the real and imaginary impedances obtained from impedance measurements, ω is $2\pi f$ and $C_o = \varepsilon_o A/d$ (ε_o: the permittivity of the free space (8.854 x 10^{-14} F cm^{-1} and A: area of electrode).

The ac currents (I) can be separated into charging current $(i\omega\varepsilon')\ C_oV$ and loss current $(\omega\varepsilon'')\ C_oV$ as given by the following equation,

$$I = (i\omega\varepsilon' + \omega\varepsilon'')C_oV \qquad (4)$$

By using the relation $C_o = \varepsilon_o A/d$, the current density *(J)* can be related to the complex admittance (*Y**) as follows,

$$J = (i\omega\varepsilon' + \omega\varepsilon'')E = (i\sigma'' + \sigma')E = Y^*E \qquad (5)$$

Therefore,

$$\sigma' = \omega\varepsilon_o\varepsilon'' \text{ and } \sigma'' = \omega\varepsilon_o\varepsilon', \qquad (6)$$

where σ' is loss current conductivity (conductance), also known as ac conductivity σ_{ac} in the present study, and σ'' is the conductivity due to charging current (susceptance). On the other hand, complex admittance (*Y**) is the inverse of Z*.

The ac conductivity has been evaluated from dielectric data in accordance with the relation:

$$\sigma_{ac} = \omega\varepsilon_o\varepsilon'' \tan\delta$$

where ε_o is permittivity of the free space, ω is $2\pi f$ and *tan* δ is the dielectric loss factor [22].

3. RESULT AND DISCUSSION

3.1. Phase Identifications

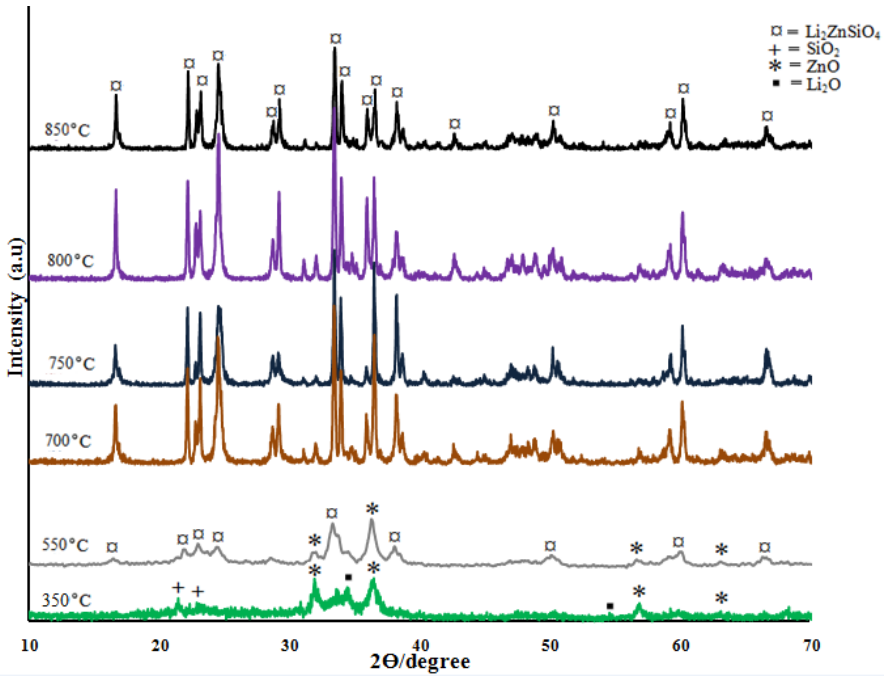

Figure . 1 : XRD pattern of samples sintered at different temperature.

Presented in Fig. 1 are the XRD spectra of Li_2ZnSiO_4 sintered at different temperatures for 12 hours. As can be seen in the figure, sintering at 350^oC did not successfully produce Li_2ZnSiO_4 compound. However the samples sintered at 550^oC exhibits diffraction peaks which is attributed to Li_2ZnSiO_4 and ZnO, indicating the presence of impurities in the sample. The XRD spectrum of the samples sintered at temperature 700 ^oC to 850 ^oC shows peak attributed only to Li_2ZnSiO_4 showing that pure Li_2ZnSiO_4 has been obtained.

The pure Li_2ZnSiO_4 compound is found to be single phase in nature, crystallizing in monoclinic structure with space group $P2_1/m$ and lattice parameters are a = 6.253Å, b = 10.685Å, c = 4.929 Å and β= 90^o [23].

3.2. SEM and EDX analysis

Fig. 2 presents SEM micrographs and EDX spectra of the Li_2ZnSiO_4 ceramic powder sintered at 700^oC, 750^oC, 800^oC and 850^oC. From these images, it is clear that the average grain size decreases with increase in sintering temperature; from 2 μm in the sample sintered at 700^oC to 0.1 μm in the sample sintered at 850^oC. In order to confirm the stoichiometric proportions, the EDX analysis was performed. This analysis was carried out at larger region (marked as A) to measure the average composition and smaller region (marked as B) to show whether the composition of A is homogeneous on a relatively small scale. The atomic ratios of Zn and Si was calculated and listed in Table 1. The result shows that the atomic ratios in both region A and region B for Zn: Si are homogeneous.

The EDX of the sample could not display the presence of lithium because of its light weight [24]. As such, the concept of charge neutrality was employed [25]. It is found that, the ratio of Li : Zn : Si = 2.0 : 1.0 : 1.0 confirming the formation of Li_2ZnSiO_4 compound.

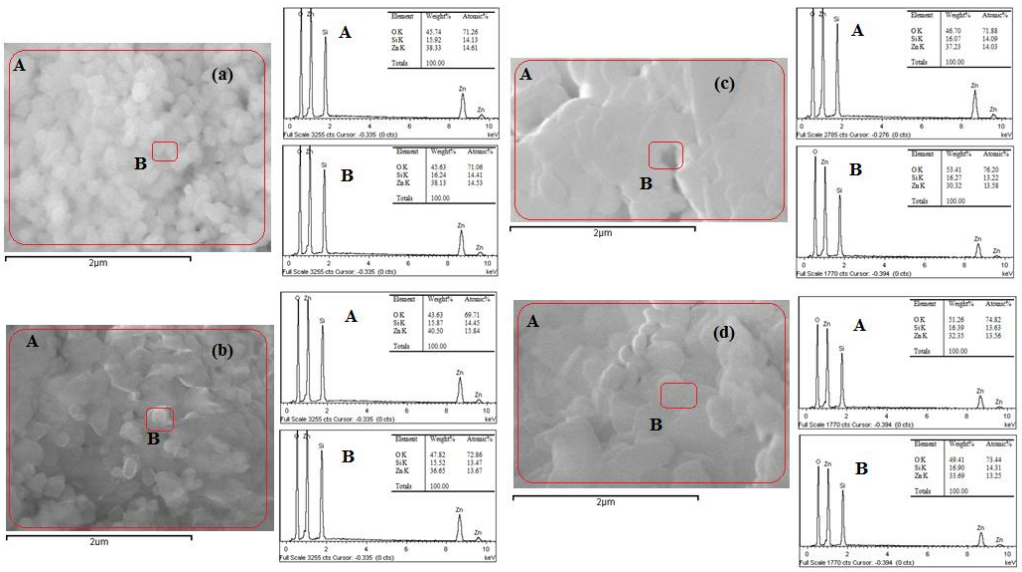

Figure 2. SEM micrographs (left) and EDX analysis (right) of the Li_2ZnSiO_4 ceramics powder sintered at (a) 850^oC (b) 800^oC (c) 750^oC and (d) 700^oC

Table 1. The atomic ratios of Zn and Si for the sample sintered at different temperature

Sample	Atomic Ratio			
	Region A		Region B	
	Zn	*Si*	*Zn*	*Si*
850^{o}C	1	0.9671	1	0.9917
800^{o}C	1	0.9122	1	0.9833
750^{o}C	0.9957	1	1	0.9734
700^{o}C	0.9949	1	0.9259	1

3.4. Conductivity Measurement

3.4.1. Direct current conductivity

The dc conductivity of Li_2ZnSiO_4 ceramic solid electrolyte has been determined from the bulk resistance, R_b using equation (1). The dc conductivity for samples sintered at 700^{o}C , 750^{o}C , 800^{o}C and 850^{o}C at 500^{o}C and RT are listed in Table 2.

Table 2. Conductivity data for Li_2ZnSiO_4 at RT and 500^{o}C for all samples

Samples	σ_{500} (S cm^{-1})	σ_{RT} (S cm^{-1})
700^{o}C	4.74 x 10^{-5}	1.81 x 10^{-7}
750^{o}C	1.08 x 10^{-4}	5.82 x 10^{-7}
800^{o}C	3.03 x 10^{-4}	1.13 x 10^{-6}
850^{o}C	5.54 x 10^{-4}	5.80 x 10^{-6}

In order to confirm the conductivity obtained from the impedance plots, conductivity spectra (imaginary part of conductivity, σ'' versus real part of conductivity, σ') are plotted and typical spectra recorded at RT are shown in Figure 3. The conductivity plots consists of a semicircle and two dispersion curves at low σ' and high σ' regions, respectively. The intercept of the dispersion curves with x-axis at high gives the value of bulk conductivity, σ_b. This method has been used by a few groups of researchers [26-31]. Table 3 lists the dc conductivity values obtained from the conductivity spectra. It is observed that the values of dc conductivity obtained from both conductivity spectra and impedance at RT are close to each other hence confirming the value of dc conductivity obtained from the impedance plots.

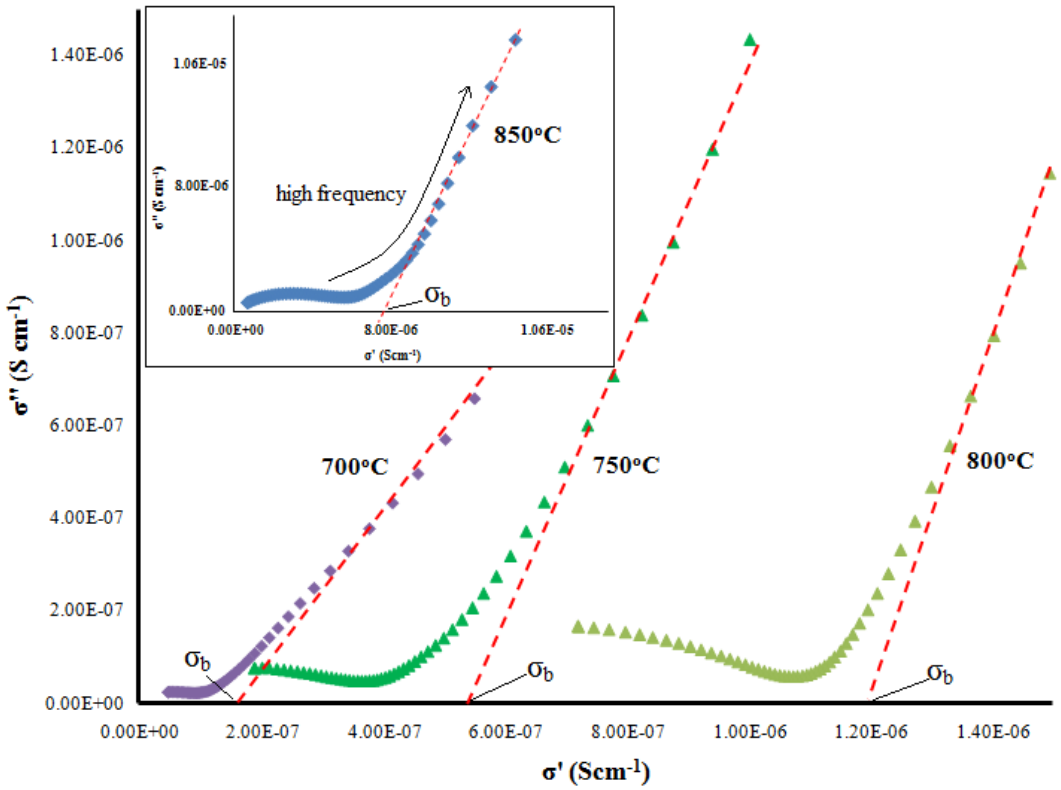

Figure 3. Conductivity plot of Li_2ZnSiO_4 sintered at various temperatures.

Table 3. Comparison of conductivity values determined from impedance and conductivity plots for all samples

Samples	Z plot (S cm^{-1})	σ plot (S cm^{-1})
	σ_{bulk}	σ_{bulk}
700°C	1.81 x 10^{-7}	1.85 x 10^{-7}
750°C	5.82 x 10^{-7}	5.86 x 10^{-7}
800°C	1.13 x 10^{-6}	1.15 x 10^{-6}
850°C	5.80 x 10^{-6}	5.82 x 10^{-6}

The increase in dc conductivity with temperature is influenced by thermally activated drift mobility of ions. The activation energy for the thermally activated hopping process was obtained by fitting the dc conductivity data with Arrhenius equation:

$$\sigma_b T = A \exp\left(\frac{-E_\alpha}{kT}\right) \qquad (8)$$

where A is the pre-exponential factor, E_α is the activation energy for conduction and k is the gas constant. Figure 4 depicts the Arrhenius plot for the samples sintered at 700°C, 750°C, 800°C and 850°C. The sample sintered at 700°C, 750°C and 800°C shows linear plot suggesting that there are no

structure and phase changes in the sample for the studied temperature range [32] . However, for the sample sintered at 850°C, two linear regions are seen with sudden change in slope at 300°C (1000/T = 1.75 K^{-1}). The change in slope could be due to phase transition occurring in the sample upon heating [33]. The activation energy for all samples were extracted from the Arrhenius plots and are shown in Fig. 4. The low value of activation energy indicates high mobility of ions in the sample.

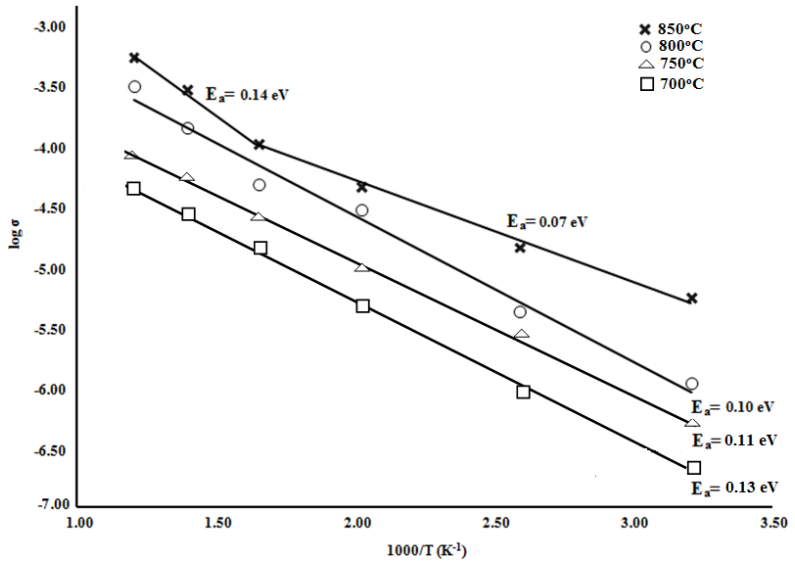

Figure 4. Arrhenius plot of the dc conductivity for Li_2ZnSiO_4 sample sintered at 700°C , 750°C, 800°C and 850°C.

3.4.2. Alternating current conductivity

Fig. 5 depicts the graph of log $\sigma(\omega)$ versus log ω for Li_2ZnSiO_4 sample sintered at 850°C. From the figure, it is clear that there is a plateau at low frequency region and extrapolating it to the y-axis gives the value of d.c conductivity. At the plateau region, the conductivity is frequency independent and the σ_{dc} values are found to be in good agreement with the value listed in Table 2.

The transition from the d.c plateau to a.c conductivity dispersion region shifts towards higher frequency range when temperature increases. The high frequency dispersion is due to the high probability for the correlated forward backward hopping at high frequencies together with the relaxation of the dynamic cage potential. Therefore we can say that the a.c conductivity is dominant in high frequency region [34].

The conductivity behavior obeys the universal power law :

$$\sigma'(\omega) = \sigma(0) + A\omega^n \qquad (9)$$

where $\sigma(0)$ is the d.c conductivity of the sample, A is a temperature dependant parameter and n is the power law exponent which represents the degree of interaction between the mobile ion and is less than 1. The value of n is extracted from the slope log $\sigma(\omega)$ versus log ω. The parameter of n

obtained varies from 0.68 at RT and decreases to 0.10 at the highest temperature of 773K. The plot of variation of *n* with temperature is illustrated in Fig. 6. The plot can also be fitted to equations $n = -0.0012x + 1.0644$. This equation suggests that $n \rightarrow 1$ when $T \rightarrow 0$.

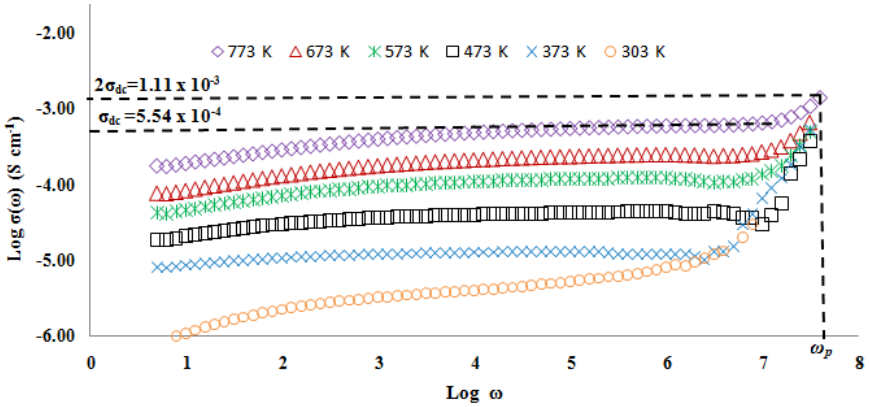

Figure 5: Log σ(ω) total versus log ω for Li_2ZnSiO_4 sample sintered at 850°C at various temperatures.

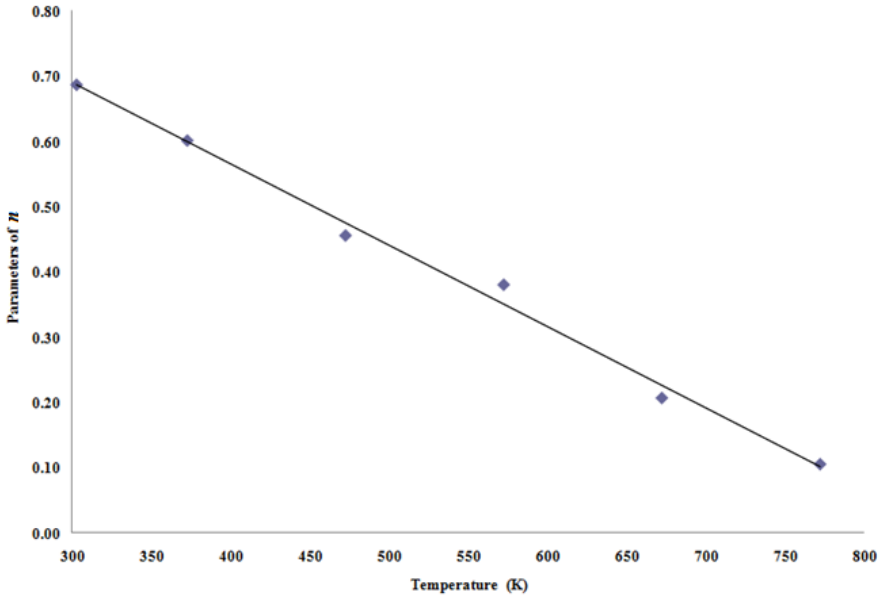

Figure 6: Value of *n* for Li_2ZnSiO_4 material at different temperature.

According to the correlated barrier hopping (CBH) model, values of *n* decrease with increasing temperatures and can be evaluated as follows

$$1 - n = \frac{6kT}{Wm} \qquad (10)$$

where k is Boltzmann's constant, T is the temperature and W_M is the maximum barrier height. From equation (8), it can be deduced that $n \rightarrow 1$ if $T \rightarrow 0$. This confirms that the conduction mechanism in the Li_2ZnSiO_4 system studied can be described using the CBH model.

In this model it is assumed that the ions or charge carriers are surrounded by several potentials, such as the Coulombic repulsive potential between the ions and a potential well in which the ions reside. Superposition of the potentials yields a single ion potential that is actually felt by the ions. When the ion gains sufficient energy, they hop from one site to another. As the temperature increases, the number of ions that hop from one site to another increases, leading to an enhancement in conductivity with temperature, as observed in Fig .5 [35-36]

According to Almond and co-researchers the a.c conductivity data can also be used to estimate the ionic hopping rate, ω_p. The hopping rate of ion in a material is a valuable information to elucidate the ionic conduction. The ω_p can be obtained from the graph log $\sigma(\omega)$ versus log ω by extrapolating at twice the value of d.c. conductivity from the vertical axis horizontally towards the graph and then extrapolating downwards vertically to the horizontal axis as shown in Fig. 5. The magnitude of the charge carrier concentration can be obtained using the equation [34,37-39]:

$$K = \frac{\sigma T}{\omega_p} \tag{11}$$

where

$$K = ne^2a^2\gamma k^{-1} \tag{12}$$

Here e is electron charge, γ is correlation factor which is set equal to 1, and a is the jump distance between two adjacent sites for the ions to hope which is assumed to be 3Å for al materials [34, 38]. n is the density of mobile ions (charge carrier) which can be calculated using eq. 10 and k is Boltzmann constant. The ionic mobility, μ can be calculated using equation:

$$\mu = \frac{\sigma_{dc}}{ne} \tag{13}$$

The value of σ, ω_p, K, n,and μ, at all temperatures studied for Li_2ZnSiO_4 sample sintered at 850^{o}C are tabulated in Table 4. From the table, the mobile ion concentration, K and density of mobile ion, n are found to be constant over the temperature range studied. This reveals that all the ions which are responsible for the conductivity are in a mobile state, thus can be best represented by the strong electrolyte model [34,37]. Hence, the conduction mechanism in the investigated Li_2ZnSiO_4 is attributed to the hopping of charge carriers. Meanwhile, from the table the mobility of ions, μ increases with increasing temperature. This means that the increase in conductivity in the samples can be attributed to the increase in ionic mobility since the density of mobile ions is constant over temperature range studied [34,37].

Table 4. Parameters of σ, ω_p, K , n and μ at various temperature for Li_2ZnSiO_4 sample sintered at 850°C

T (k)	σ (S cm^{-1})	ω_p (kHz)	K (S cm^{-1} K Hz^{-1})	n x 10^{25} (cm^{-3})	μ (cm^2 V^{-1} s^{-1})
303	5.80 x 10^{-6}	212	8.28 x 10^{-9}	5.12	7.04 x 10^{-13}
373	1.50 x 10^{-5}	680	8.22 x 10^{-9}	4.91	1.90 x 10^{-12}
473	4.74 x 10^{-5}	2709	8.28 x 10^{-9}	4.95	5.96 x 10^{-12}
573	1.08 x 10^{-4}	7508	8.24 x 10^{-9}	4.93	1.36 x 10^{-11}
673	3.03 x 10^{-4}	24,818	8.22 x 10^{-9}	4.92	3.82 x 10^{-11}
773	5.54 x 10^{-4}	51,622	8.29 x 10^{-9}	4.96	6.95 x 10^{-11}

3.5. Dielectric behavior

The plots of frequency dependence of the dielectric constant, ε' and dielectric loss, ε'' of Li_2ZnSiO_4 ceramic powder sintered at different temperatures were plotted (Fig. 7 and Fig. 8) in order to obtain further information on the ion dynamic properties in this material.

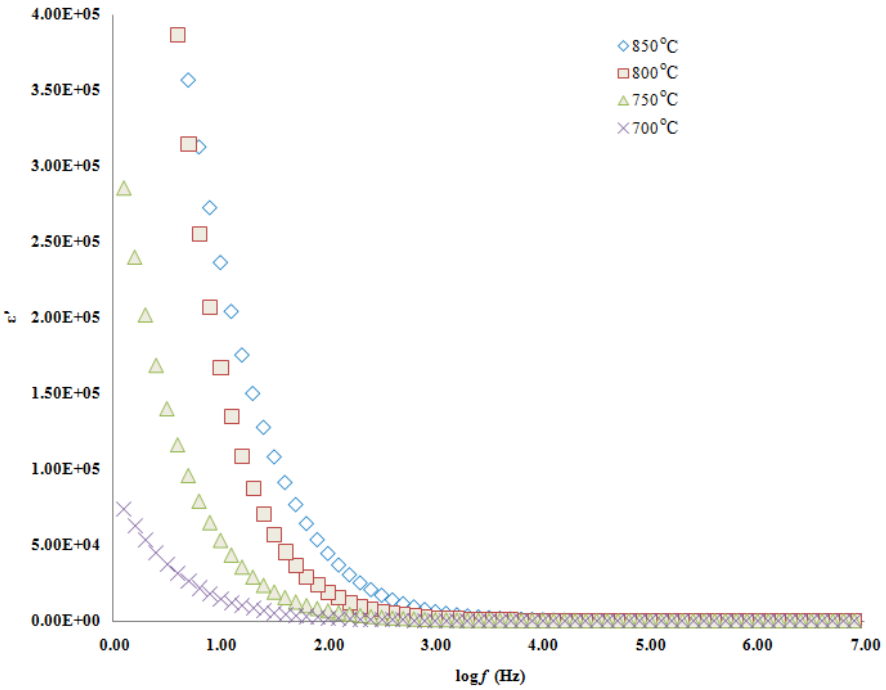

Figure 7. Plot of relative dielectric constant (ε·) of Li_2ZnSiO_4 as a function of log f at different temperatures

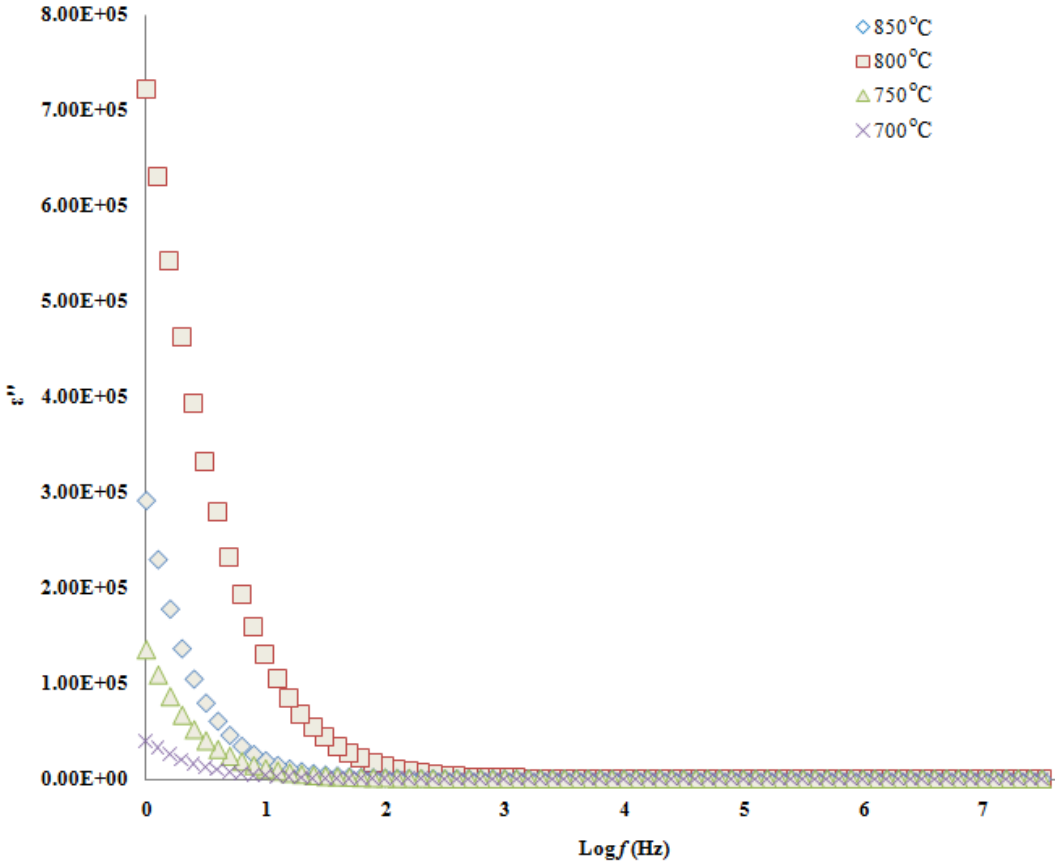

Figure 8. Plot of relative dielectric constant (ε") of Li_2ZnSiO_4 as a function of log f at different temperatures

From both figures we can see that the dielectric constant, *ε'* and dielectric loss, *ε"* decrease to a constant value at high frequency. At low frequencies, the high value of dielectric constant, *ε'* is attributed to the contribution of charge carrier accumulation at the interface of electrode and Li_2ZnSiO_4 material. Meanwhile the high value of dielectric loss, *ε"* at these frequencies is attributed to the fact that, at low frequencies the electrical energy loss is high due to the migration of ions in the material. As the ion moves, they loss some of their energy to the lattice as heat [40-41].

However, at high frequencies, the dielectric constant, *ε'* and dielectric loss, *ε"* value is low. This is due to high periodic reversal of the field and due to the limitation of dielectric loss sources (ion vibration only) respectively [42]. The *ε'* and *ε"* increase with temperature indicating the fact that when the temperature is increased, the bound charge carriers get sufficient excitation thermal energy to be able to obey the charge in external field more easily. This in turn increases their contribution to the polarization resulting in increase in *ε'* and *ε"* [40-44].

Fig. 9 presents the plot of frequency dependence of tan δ at various temperatures. The plot shows a peaking behavior for all temperatures. As the temperature increases, the tan δ peaks are shifted towards higher frequency. This peak is expected when the hopping frequency of ions is approximately equal to the external applied electric field. In this case

$$\omega\tau = 1 \qquad (14)$$

where τ is the relaxation time of the hopping process and ω is the angular frequency of the external field ($\omega = 2\pi f_{\max}$). The relaxation time τ is inversely proportional to the jumping probability per unit time, *P*, according to the relation [38-39]

$$\tau = \frac{1}{2}P \qquad (15)$$

so, from Eqs. (14) and (15), it is expected that f_{max} is proportional to *P*. The shift of the peak of the $\tan\delta$ towards high frequency with increasing temperature, indicates that the jumping probability per unit time increases with temperature [40-41]. This result is consistent with the result discussed earlier.

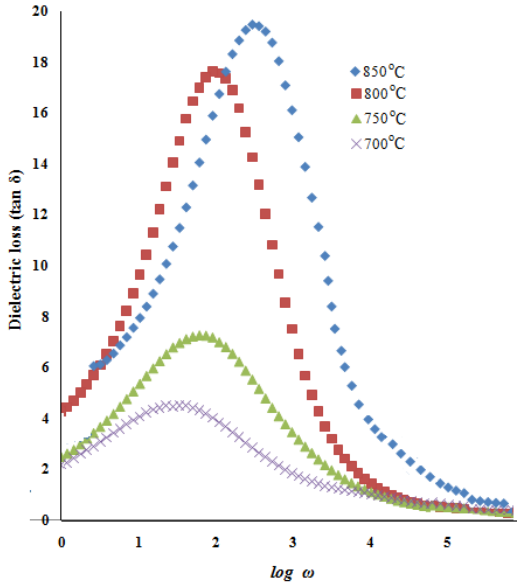

Figure 9: Frequency dependence of tan δ at various temperatures

4. CONCLUSIONS

Li_2ZnSiO_4 samples have been successfully synthesized using a simple sol gel method. The XRD and EDAX analysis confirm the formation of the compound. The conductivity–temperature study shows that the compound obeys the Arrhenius law. Conductivity and dielectric studies show that the increase in conductivity with temperature is due to increase in ion mobility.

ACKNOWLEDGMENTS
Financial support by University of Malaya (PV-027/2012A) is gratefully acknowledged.

References

1. S. Tamura, A. Mori, and N. Imanaka, *Solid State Ionics*, 175 (2004) 467
2. J. W. Fergus, *J. Power Sources*, 160 (2006) 30

3. C. J Leo, Chowdari, Rao and Souquet, *Mater. Res. Bull.*, 37 (2002) 1419
4. J. W. Fergus, *J. Power Sources*, 195 (2010) 4554
5. M.A.K.L Dissanayake, H.H Sumathipala, A.R West, *Solid State Ionics*, 86 (1996) 719
6. M.A.K.L Dissanayake, P.R Gunawardane, A.R West, *Solid State Ionics*, 62 (1993) 217
7. P.G Bruce, I. Abraham, *Solid state Ionics*, 40/41 (1990) 293
8. A.D Robertson, A.R West, *Solid State Ionics*, 58 (1992) 351
9. M. Saiful Islam, (2010) *Phil. Trans. R. Soc. A*, 368 (2010) 3255
10. N.A.W Holzwarth, Yaujun A. Du, *J. Electrochem. Soc.*, 154 (2007) A999
11. M. Murayama, R. Kanno, Y. Kawamoto, T. Kamiyama, *Solid State Ionics*, 154-155 (2002) 789
12. P.G. Bruce, I. Abraham, *J. Solid State Chem.* 95 (1991) 74
13. K. Ryoji, M. Murayama, M. Irie,W. Shinya Ito, T. Hata,N. Sonoyama, Y. Kawamotow, *J. Solid State Chem.*, 168 (2002) 140
14. K. Ryoji ,K. Homma, M. Yonemura , T. Kobayashi , M. Nagao , M. Hirayama (2001) Solid *State Ionics*, 182 (2001) 53.
15. A.R West, P.F. Glasser, *Solid State Chemistry*, 4 (1972) 20
16. S. Zhang, C.Deng, B.L Fu, S.Y Yang, L, Ma, *J. Electroanal. Chem.*, 644 (2010) 150.
17. C. Deng, S. Zhang, B.L Fu, S.Y. Yang, L. Ma, *Electrochimica Acta*, 55 (2010) 8482.
18. A.D Robertson, A.R. West, A.G. Ritchi, *Solid State Ionics*, 104 (1997) 1.
19. S.B.R.S Adnan, N.S Mohamed, K.A Norwati, *World Academy of Science, Engineering and Technology*, 74 (2011) 676.
20. X. Song, M. Jia, R. Chen, *J. Mater.Processing Technol.*, 120 (2002) 21.
21. R. Adnan, N.A Razana, I.A Rahman and M. Akhyar Farrukh, (2010) *J. Chinese Chem. Soc.* 57 (2010) 222.
22. H. Yamamura, S. Takeda, K. Kakinuma, *J. Chem. Soc. Jpn*. 115 (2007) 264.
23. H. Yamaguchi, K. Akatsuka and M.Setoguchi, *Acta Crystallographica Section B,* B35 (1979) 2678.
24. B.J Hwang, R Santhanam, D.G Liv, *J. Power Sources*, 97-98 (2001) 443.
25. R. Ramaraghavulu, S. Buddhudu, *Ceramics International*, 37 (2011) 3651.
26. A. Aboulaich, D.E Conte, J. Olivier-Fourcade, C. Jordy, P.Willmann, J.C. Jumas, *J. Power Sources*, 195 (2010) 3316.
27. A.F Orliukas, A. Dindune and Z. Kanape, *Electrochem. Acta*, 51 (2006) 6194.
28. R. Sobiestianskas, A. Dindune and Z. Kanape , *Mater. Sci. Engin. B*, 76 (2000)184.
29. M. Cretin and P. Fabry, *J. European Ceramic Soc.*, 19 (1999) 2931
30. M . Godichemier, B Micheal and Orliukas, *J. Mater. Res.* 9 (1994) 1228.
31. R. Norhaniza, R H Y Subban and N S Mohamed, *J. Mater Sci.* 46 (2011) 7815.
32. X. Wu, Z. Wen, X. Xu, X. Wang, and J. Lin, *J. Nucl. Mater,* 39 (2009) 471.
33. K.R Koteswara, G. Rambabu,M. Raghavender, G. Prasad, G.S Kumar and M. Vithal, *Solid State Ionics*, 176 (2005) 2701.
34. L. P. Teo & M. H. Buraidah & A. F. M. Nor & S. R. Majid, *Ionics* DOI 10.1007/s11581-012-0667-2.
35. M.H. Buraidah,L.P.Teo,S.R.Majid, A.K.Arof , *Physica B* 404 (2009) 1373.
36. A.A Hendi, *Australian J. Basic and Applied Sci.*, 5 (2009) 380.
37. D.P Almond, A.R West, *Solid State Ionics*, 9&10 (1983) 277.

38. M. Vijayakumar, G. Hirankumar, M.S. Bhuvaneswari, S. Selvasekarapandian, *J. Power Sources* 117 (2003) 143.
39. T. Savitha a, S. Selvasekarapandian, C.S. Ramya, M.S. Bhuvaneswari ,G. Hirankumar, R. Baskaran, P.C. Angelo, *J. Power Sources*157 (2006) 533.
40. A.M Abo El Ata, S.M Atia and T.M Meaz, *Solid State Sciences*, 6 (2004) 61.
41. Dev K. Mahato , Alo Dutta , T.P. Sinha, *Physica B*, 406 (2011) 2703.
42. N. A Hegab, A .E Bekheet, M .A Afifi, L. A Wahaba and H A Shehata, *J. Ovonic Res.*, 3 (2007) 71.
43. C.R Mariappan and G .Govindaraj, *Mater. Sci. Engin. B*, 94 (2002) 82.
44. E. G. El-Metwally, M. Fadel, A.M Shakra and M.A Afifi , *J. Optoelectronics and Advanced Mater.*, 10 (2008) 1320.

Int. J. Electrochem. Sci., 8 **(2013)** 6055 - 6067

International Journal of
ELECTROCHEMICAL
SCIENCE
www.electrochemsci.org

Structural, Thermal and Electrical Properties of $Li_{4-2x}Zn_xSiO_4$ Ceramic Electrolyte Prepared by Citrate Sol Gel Technique

S.B.R.S Adnan[1,*] *and N.S. Mohamed*[2]

[1]Institute of Graduate Studies, University of Malaya, 50603 Kuala Lumpur, Malaysia
[2]Centre for Foundation Studies in Science, University of Malaya, 50603 Kuala Lumpur, Malaysia
[*]E-mail: syed_bahari@yahoo.com; nsabirin@um.edu.my

Received: 17 November 2012 / *Accepted:* 5 April 2013 / *Published:* 1 May 2013

The aim of this work is to investigate the structural, thermal and electrical properties of Zn doped Li_4SiO_4 synthesized by a sol gel method. The formation of the compound is confirmed by X-ray diffraction study. Thermal properties of the compounds are measured using DSC analysis while the electrical characteristics are investigated by impedance spectroscopy. The introduction of zinc ions considerably raises the conductivity and improves thermal stability of the parent compound Li_4SiO_4. The compound of $Li_{3.88}Zn_{0.06}SiO_4$ gives a maximum value of 3.2 x 10^{-5} S cm^{-1} at room temperature and 1.08 x 10^{-3} S cm^{-1} at 500 ^oC. The charge carrier concentration, mobile ion concentration and ion hopping rate are calculated by fitting the conductance spectra to power law variation, $\sigma_{ac}(\omega) = \sigma_o + A\omega^{\alpha}$. The charge carrier concentration and mobile ion concentration are found to be constant over the temperature range from 303 K to 773 K while mobility of ion increases with temperature implying that the increase in conductivity with temperature is due to increase in ion mobility. The transference number corresponding to Li^+ ion transport determined by means of Bruce and Vincent technique shows that majority charge carriers in the compound are Li^+ ions.

Keywords: Arrhenius, ceramic, electrolyte, Li_4SiO_4, sol gel, transference number

1. INTRODUCTION

Interest in ceramic solid-state electrolytes has led to a widespread search for ionically conducting materials. However, the solid-state electrolytes composition must be tuned to readily admit ions, while simultaneously forming safe, impenetrable and electronically insulating barriers [1]. The role of the electrolyte is to provide an ionic conduction path between anode and the cathode in electrochemical devices such as fuel cell, super capacitors, secondary batteries etc. As such, the prime

concern in electrolyte research is to enhance ionic conductivity which is the main challenge faced by researchers in this field.

In the search for a variety of batteries and solid state electrolyte with Li^+ ion conductors, considerable interest has been shown in systems based on lithium orthosilicate (Li_4SiO_4) which is chemically stable [2-16]. Li_4SiO_4 exist in two polymorphic forms which are separated by a broad transition region between 600 ^oC and 725 ^oC [2]. The crystal structure of this compound consists of lithium-oxygen polyhedral which represent the lithium sites, are connected together by multiple sharing of faces to form three dimension network of cages linked by triangular windows. On average, the lithium sites are less than half full and so there are also plenty of other sites which are unoccupied but could be occupied transiently and afford extra conduction pathways [2,5,10].

Li_4SiO_4, itself is a poor conductor (σ_{RT} = 10^{-8}-10^{-6} S cm^{-1}) [2,5,17]. However, its conductivity can be greatly enhanced by aliovalent doping such as $Li_{4-2x}D_xSiO_4$ (D = Co^{2+}, Ni^{2+}, Mg^{2+})[5,8], $Li_{4-3x}T_xSiO_4$ (T = Al^{3+}, Ga^{3+}, B^{3+}, In^{3+})[4,6-9,15-16] and $Li_{4-x}M_xSi_{1-x}O_4$ (M = V^{5+}, As^{5+}, P^{5+}) [11-14]. These doping may create vacant sites in the crystal and any lithium ion in the immediate vicinity can jump to the vacant sites. This leaves the previous site of the ion vacant which could now host another ion. This results the transport of ions across the solid giving rise to conductivity. Their concentration is the main factor determining the conductivity of this solid electrolyte [18].

West [10] has reported previously the conductivity data for the $Li_{3.4}Zn_{0.3}SiO_4$ compound at temperature 450 ^oC to 700 ^oC with conductivity value 3.4 x 10^{-4} S cm^{-1} and 2.3 x 10^{-2} S cm^{-1} respectively using conventional solid state reaction. However, the works reported in the literature only focused for high temperature application (>450 ^oC). No works on this type material for low and medium temperature devices application has been reported. Such study is interesting one as development of the electrolytes with high conductivity at low and medium temperatures can broaden their use to low and medium temperature solid state devices such as in energy and transportation sector, communication electronics, display devices, medicine and metallurgy.

Meanwhile, the synthesis using citrate sol gel technique has been reported can enhance the conductivity compared to the conventional solid state reaction [19]. Furthermore, this technique has other advantages such as lowering the synthesis temperature, effective in improving the linkage between grain boundary, molecular-level homogeneity can be easily achieved and the homogeneous mixture containing all the compounds in the correct stoichiometry ensures a much higher purity of the sample. This method is also simple and therefore suitable for both small scale and large scale production. [2-3,19-20].

In the author's previous work, Li_4SiO_4 compound has been successfully prepared using this method. The compound exhibited conductivity of 1.16 x 10^{-4} S cm^{-1} at 100^oC [2]. This conductivity is an order of magnitude higher compared to the value of compound prepared by solid state reaction method reported by Smith and West, 1990 [21]. In this work, $Li_{4-2x}Zn_xSiO_4$ (x = 0, 0.06, 0.12, 0.20) compound were prepared by the same sol gel method. The structural, thermal and electrical properties using x-ray diffraction (XRD), different scanning calorimetry (DSC) and impedance spectroscopy were studied.

2. EXPERIMENTAL PROCEDURE

2.1 Synthesis of $Li_{4-2x}Zn_xSiO_4$

In this study, four compounds with x = 0, 0.06, 0.12, 0.20 were prepared via sol gel technique. For sample preparation, lithium acetate ($C_2H_3LiO_2$) zinc acetate ($C_4H_{10}O_6Zn$) and tetraethyl orthosilicate ($SiC_8H_{20}O_4$) were used as the starting materials. Meanwhile citric acid was used as the chelating agent. Lithium acetate and zinc acetate were dissolved in distilled water and later mixed with citric acid under magnetic stirring. The solution was transferred into a reflux system and continuously stirred until a homogeneous solution was formed. Solution of tetraethyl orthosilicate was then added to the homogeneous solution. After stirring for 12 hours, the solution was taken out and then vaporized for about two hours under magnetic stirring at 75 ^oC. The resulting wet gel was dried in an oven at 150^oC for 24 hours to remove water particles, resistance organic groups as well as to avoid ceramic cracks. The powder was pressed using a Specac pellet hydraulic press to form pellet with diameter and thickness of 13 mm and 2 mm respectively. The pellets were later sintered at 850 ^oC for 12 hours.

2.2. Characterization techniques.

Bruker AXS D8 X-ray diffractometer employing Cu-K_α radiation was used to perform X-ray diffraction in order to identify the crystalline phase of the material. Thermal behavior of the sintered sample was analyzed by differential scanning calorimetry (DSC) (EVO Lab^{sys} thermal analyzer) in N_2 atmosphere at a constant heating rate of 10^oC/min in the temperature range between room temperature and 1300 ^oC. The compounds electrical properties were determined by ac impedance spectroscopy using Solatron 1260 impedance analyzer over a frequency range from 0.1 to 10^6 Hz. An applied voltage was fixed at 110 mV.

The dc conductivity was determined using the equation:

$$\sigma_b = \frac{d}{AR_b} \tag{1}$$

where d is the sample thickness, A is the area of the electrode and R_b is the bulk resistance which is determined from impedance plot.

The ac conductivity has been evaluated from dielectric data in accordance with the relation:

$$\sigma_{ac} = \omega\varepsilon_o\varepsilon'' \tan\delta \tag{2}$$

where ε_o is permittivity of the free space (8.854 x 10^{-14} F cm^{-1}), ω is $2\pi f$, ε'' is dielectric loss and tan δ is the dielectric loss factor. Lithium transference number measurement was done using Bruce and Vincent method [22-24] in order to determine the actual type of charge carriers. This method requires characterization of cell before and after polarization (after reaching the steady state) by using combination of EIS and DC polarization technique. For this measurement the samples were

sandwiched between lithium metal electrodes which are used as non-blocking electrodes that only allow Li^+ ions to transfer. The lithium transference number (τ_{Li^+}) was calculated using the equation:

$$\tau_{Li^+} = \frac{I_{ss}(\Delta V - I_o R_o)}{I_o(\Delta V - I_{ss} R_{ss})} = \frac{R_e}{\left(\frac{\Delta V}{I_{ss}} - R_{ss}\right)} \quad (3)$$

In this equation, I_o is initial current (t = 0), I_{ss} is steady state current, R_o and R_{ss} are initial resistance of the passive layer (before polarization) and resistance of the passive layer (after polarization) respectively and ΔV is applied voltage bias (ΔV = 500 mV). R_e is resistance of the electrolyte which is calculated using Ohm's law:

$$R_e = \frac{\Delta V}{I_o} - R_o \quad (4)$$

3. RESULT AND DISCUSSION

3.1. Structural properties

Fig. 1(a) presents the XRD spectra of all the $Li_{4-2x}Zn_xSiO_4$ samples. The XRD spectra of all samples can be indexed to monoclinic structure in space group $P2_{1/m}$ [25].

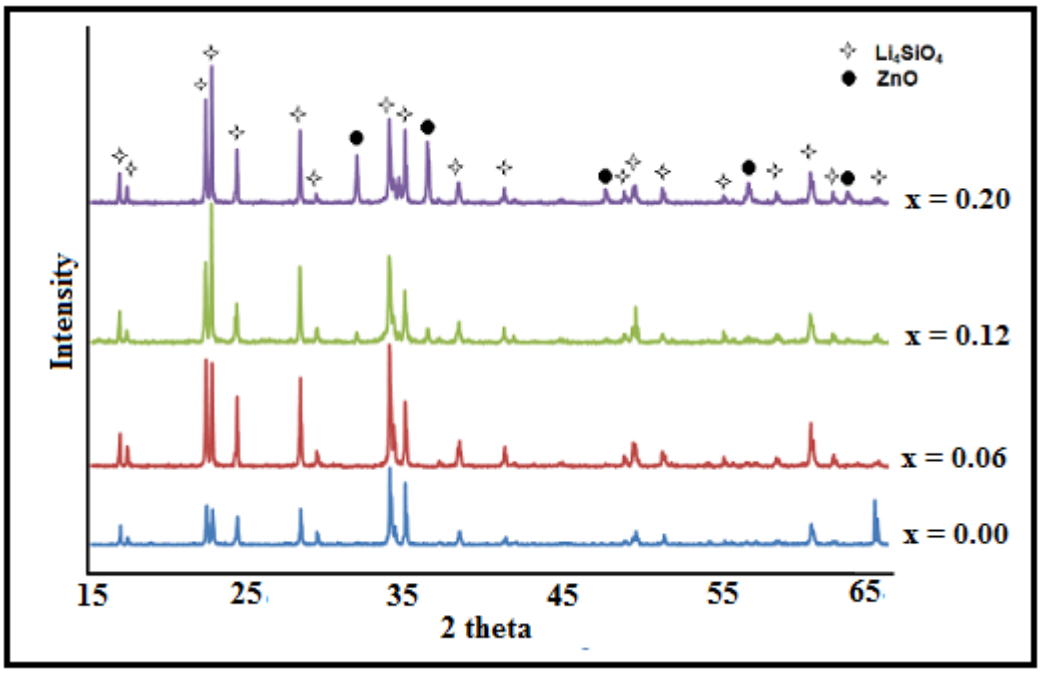

Figure 1. XRD pattern of $Li_{4-2x}Zn_xSiO_4$ samples

Table 1. Lattice parameters of the $Li_{4-2x}Zn_xSiO_4$ samples

Samples	*a* (Å)	*b* (Å)	*c* (Å)	*β* (°)	*V* (Å^3)
x = 0.00	5.147	6.094	5.293	90.33	166.01
x = 0.06	5.295	6.098	5.149	90.32	166.20
x = 0.12	5.296	6.099	5.147	90.31	166.25
x = 0.20	5.297	6.102	5.150	90.25	166.46

Compared with the XRD spectra of the Li_4SiO_4 sample, single phase solid electrolyte only appear in the sample with x=0.06 which shows no extra peaks in its XRD spectrum. The peaks shift to higher diffraction angle indicating that Zn^{2+} ion is in the Li_4SiO_4 structure rather than forming impurities. The diffraction peaks are also broadened by Zn doping, which implies that the crystal size decreases with increasing Zn content. The peak at diffraction angle 65^o tends to disappear with increasing Zn amount. Meanwhile, small peaks attributed to ZnO arise in XRD patterns appear in the sample doped with x=0.12 and x=0.20.

The lattice parameters of the $Li_{4-2x}Zn_xSiO_4$ samples are listed in Table 1. The parameters of Li_4SiO_4 are in good agreement with the values reported by Dubey and West [26]. The value of *a*, *b* and *V* (unit cell volume) increase with increasing *x* and the value of *c* is first decreases and then increases with increasing *x*. Among all of the lattice parameters, monoclinic angle β decreases slightly with increasing *x*. The increase in the unit cell volume is mostly related to the Zn^{2+} insertion into Li_4SiO_4 structure which can be attributed to the larger atomic size of Zn^{2+}(0.74 Å) than that of Li^+ (0.68 Å) [7,27].

3.2. Thermal properties

The DSC curves for $Li_{4-2x}Zn_xSiO_4$ samples are shown in Fig. 2. There are three endothermic peaks in the curve of the sample with x = 0. The first peak is located in temperature range from 60 ^{o}C to 120 ^{o}C due to evaporation of water process. The intensity of the peak decreases with the increase of x and disappears in the sample with x = 0.12 and 0.20. The second peak which is observed in temperature range from 550 ^{o}C to 610 ^{o}C is recognized as second order phase transition of Li_4SiO_4. A similar observation has been reported by other researchers [10,28-30]. The third peak which has maximum peak at temperature of 1027 ^{o}C represents the melting temperature of the sample. Increasing x value results in an increase in phase transition and melting temperature which is in contrast to the result of West [10] who reported the substitution of zinc in Li_4SiO_4 lowers the temperature of phase transition. The increases in x as well as increase in phase transition and melting temperature indicate enhancement in thermal stability of the ceramic upon substitution of Zn^{2+} ions for Li^+ ions. The broad endothermic peak observed in the DSC curve of the samples with x = 0.12 and x = 0.20 at temperature range 600 ^{o}C -1000 ^{o}C may be due to the presence of ZnO impurities in the samples.

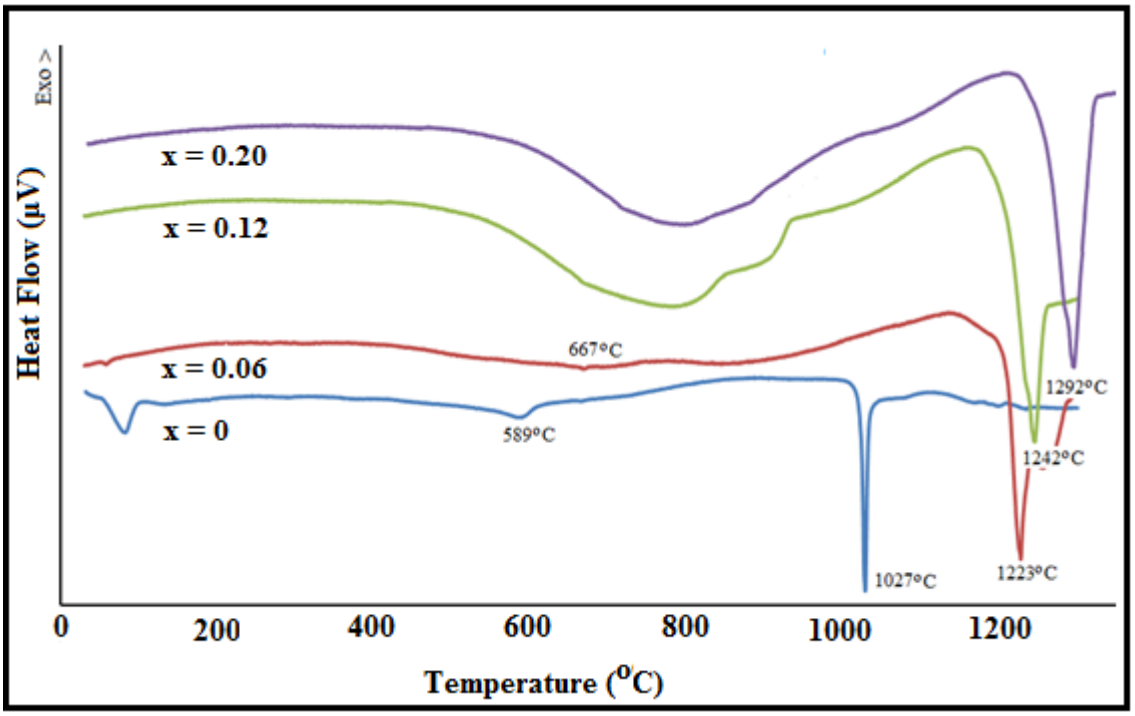

Figure 2. DSC curves of $Li_{4-2x}Zn_xSiO_4$ samples.

3.3. Electrical properties

3.3.1 Dc conductivity

The dc conductivity of $Li_{4-2x}Zn_xSiO_4$ was determined from the bulk resistance, R_b using equation (1). The dc conductivity for all samples at 500 ^oC and RT are listed in Table 2. The maximum conductivity is observed at $x = 0.06$ with conductivity value of 3.20×10^{-5} S cm^{-1} at RT and increases to 1.08×10^{-3} S cm^{-1} at 500^oC. The conductivity increases by an order of magnitude compared to the Li_4SiO_4 with replacement of Li^+ to Zn^{2+}. Even though the solubility of zinc in this electrolyte is low, small addition of Zn^{2+} significantly raises the conductivity. The conductivity decreases with further increase in x due to the presence of the impurities, ZnO which may block the migration of Li^+ ion between grains. However, the conductivity of the samples with $x = 0.12$ and $x = 0.20$ is still higher than that of Li_4SiO_4. This effect is due to the increase of cation vacancies in the monoclinic structure [5].

Table 2. Conductivity data for $Li_{4-2x}Zn_xSiO_4$ samples at ambient temperature and 500 ^oC

Samples	σ_{500} (S cm^{-1})	σ_{RT} (S cm^{-1})
x = 0.00	1.00×10^{-4}	9.36×10^{-6}
x = 0.06	1.08×10^{-3}	3.20×10^{-5}
x = 0.12	3.00×10^{-4}	2.60×10^{-5}
x = 0.20	5.54×10^{-4}	2.70×10^{-5}

The temperature dependence of the d.c conductivity of $Li_{4-2x}Zn_xSiO_4$ samples is shown in Fig.3. The activation energy, E_α of the dc conductivity is calculated according to the Arrhenius equation:

$$\sigma_b T = A \exp\left(\frac{-E_a}{kT}\right) \quad (5)$$

where A is the pre-exponential factor, E_α is the activation energy for conduction and k is the Boltzman constant. The conductivity of all samples increases with temperature. However, all the σ-1000/T plots show a discontinuity at ~ 300 ^oC (1000/T = 1.75 K^{-1}) which is in agreement with the results reported by Wakihara et al [5] but in contrast to the result of West [10] who reported a discontinuity at 180 ^oC for Li_4SiO_4. The change in slope of σ-1000/T plots could be due to an order-disorder transition of Li^+ and Zn^{2+} ions since there is no experimental evidence for a phase transition occurring in the sample upon heating at room temperature until 500 ^oC as shown in Fig. 2. In the other words, the conductivity may be influenced at even slightest change in structure arrangement [5].

The activation energy for all samples which was extracted from the Arrhenius plots is shown in Fig. 4. The low value of activation energy indicates high mobility of ions in the sample. However, the presence of impurities in the samples of x = 0.12 and x = 0.20 lowers the ionic mobility and decreases the conductivity [31].

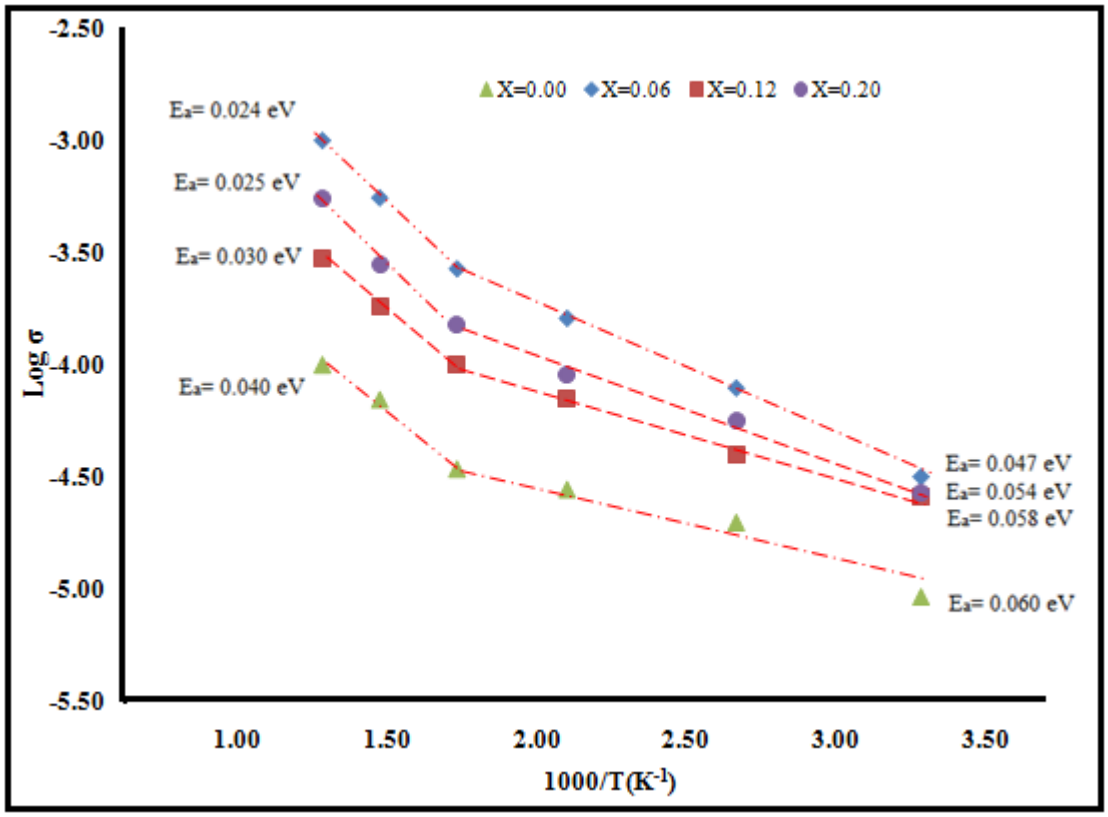

Figure 3. Arrhenius plot of the dc conductivity for sample $Li_{4-2x}Zn_xSiO_4$ (x = 0, 0.06, 0.12, 0.20)

3.3.2 Conductivity spectra

Conductivity spectra for $Li_{4-2x}Zn_xSiO_4$ samples at various temperatures are presented in Figure 4. At low frequencies, a plateau characterizes the dc conductivity. At high frequencies, conductivity increases according to universal power law. The conductivity can thus be represented by the expression as follows:

$$\sigma'(\omega) = \sigma(0) + A\omega^{\alpha} \tag{6}$$

where $\sigma(0)$ is the d.c conductivity of the sample, A is a temperature dependant parameter and α is the power law exponent which represents the degree of interaction between the mobile ion and is less than 1. When temperature increases, the transition from the d.c plateau to a.c conductivity dispersion region shifts towards higher frequency range. At high frequencies, the conductance spectra at different temperatures converge. This indicates that a.c conductivity is independent of temperature at high frequencies [2,32-36].

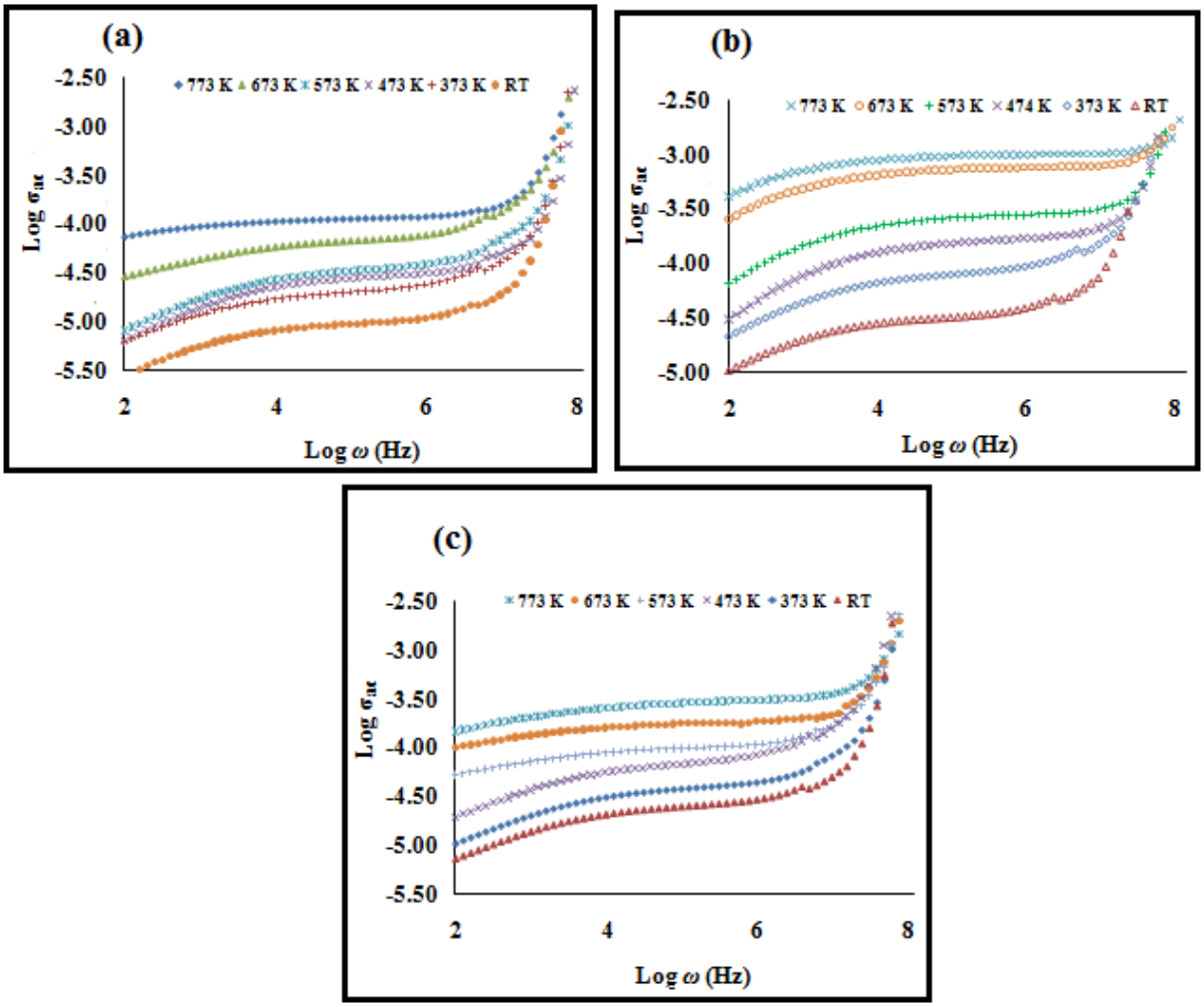

Figure 4. Conductivity spectra for (a) Li_4SiO_4 (b) $Li_{3.88}Zn_{0.06}SiO_4$ and (c) $Li_{3.76}Zn_{0.12}SiO_4$

According to the jump relaxation model, which takes account of the coulomb interaction between mobile ions, the exponent of the power law in Eq. (6) relates to ratio of [2,34,37-38]:

$$\alpha = \frac{backhop\ rate}{site\ relaxation\ rate} \tag{7}$$

The backhop is the backward motion of a hopping ion to its initial site, which is caused by the coulomb repulsive interaction between mobile ions. The site relaxation is the shift of a site potential minimum to the position of the hopping ion, which is caused by a rearrangement of neighboring ions. The decrease in α with zinc doping (Table 4) may be due to the formation of vacant sites for Li ion migration, which in turn reduces the backhop rate and hence decreases α.

According to Almond and West [32-35,39-40], the hopping rate of ion in a material is valuable information to elucidate the ionic conduction. The ionic hopping rate, ω_p can be obtained directly from a.c conductivity data since it corresponds to $\sigma(\omega) = 2\sigma(0)$ [32-33, 38]. The charge carrier concentration, C can be calculated from the definition for the dc conductivity of the ion conducting material which is given by [32-35, 39-40]:

$$C = \frac{\sigma_{dc} T}{\omega_p} \tag{8}$$

where

$$C = n(1-n)N(e^2 a^2 \gamma k^{-1}) \tag{9}$$

Here e is electron charge, γ is correlation factor which is set equal to 1, N is equivalent site per unit volume and a is the jump distance between two adjacent sites for the ions to hope which is assumed to be 3Å for all materials [33-34]. n is concentration of mobile ions which can be calculated using Eq. 9 and k is Boltzmann constant. The ionic mobility, μ can be calculated using equation:

$$\mu = \frac{\sigma_{dc}}{ne} \tag{10}$$

The values of ω_p, C, n, μ and α for sample $Li_{4-2x}Zn_xSiO_4$ samples at various temperatures are tabulated in Table 4. From the table, the charge carrier concentration, C and mobile ion concentration, n are constant over temperature range studied for all samples. This implies that all the lithium ions which are responsible for the conductivity are in mobile state thus can be best represented by the strong electrolyte model [32, 34-35, 40]. As such, the higher conductivity observed for $Li_{3.88}Zn_{0.06}SiO_4$ is due to high mobile ion concentration (~10^{26}) compared with that (~10^{25}) observed for both Li_4SiO_4 ($x = 0$) and $Li_{3.76}Zn_{0.12}SiO_4$ ($x = 0.16$).

Meanwhile, the mobility of ions, μ increases with increasing temperature in all samples. This means that the increase in conductivity with increasing temperature in all samples can be attributed to

the increase in ionic mobility since the density of mobile ions is constant over the temperature range studied [32-33,38]. The ion mobility value is higher in $Li_{3.88}Zn_{0.06}SiO_4$ sample compared to $Li_{3.76}Zn_{0.12}SiO_4$ sample. This may be attributed to the existence of ZnO impurities which distorted the crystal lattice in the sample and decreases the mobility of ions as well as the mobile ion concentration.

Table 4. Values of ω_p, C , n, μ and α at various temperatures for sample $Li_{4-2x}Zn_xSiO_4$ (x = 0, 0.06 and 0.12)

Samples	T (K)	ω_p (kHz)	C (S cm^{-1} K Hz^{-1})	n (cm^{-3})	μ (cm^{2}V^{-1} s^{-1})	α
x = 0	303	818	3.46 x 10^{-9}	5.72 x 10^{25}	1.02 x 10^{-12}	0.91
	373	2150	3.46 x 10^{-9}	5.72 x 10^{25}	2.17 x 10^{-12}	0.85
	473	3850	3.44 x 10^{-9}	5.68 x 10^{25}	3.06 x 10^{-12}	0.84
	573	5750	3.44 x 10^{-9}	5.68 x 10^{25}	3.77 x 10^{-12}	0.81
	673	13520	3.48 x 10^{-9}	5.75 x 10^{25}	7.57 x 10^{-12}	0.71
	773	22387	3.45 x 10^{-9}	5.70 x 10^{25}	1.09 x 10^{-11}	0.62
x = 0.06	303	1470	6.69 x 10^{-9}	1.11 x 10^{26}	1.95 x 10^{-12}	0.74
	373	4435	6.67 x 10^{-9}	1.10 x 10^{26}	4.48 x 10^{-12}	0.64
	473	11519	6.65 x 10^{-9}	1.10 x 10^{26}	9.15 x 10^{-12}	0.54
	573	22710	6.78 x 10^{-9}	1.12 x 10^{26}	1.33 x 10^{-11}	0.45
	673	56182	6.66 x 10^{-9}	1.10 x 10^{26}	3.14 x 10^{-11}	0.35
	773	125892	6.63 x 10^{-9}	1.10 x 10^{26}	5.65 x 10^{-11}	0.20
x = 0.12	303	1950	4.04 x 10^{-9}	2.41 x 10^{25}	6.69 x 10^{-12}	0.90
	373	3650	4.09 x 10^{-9}	2.44 x 10^{25}	1.02 x 10^{-11}	0.84
	473	8110	4.08 x 10^{-9}	2.43 x 10^{25}	1.78 x 10^{-11}	0.80
	573	14125	4.06 x 10^{-9}	2.42 x 10^{25}	2.56 x 10^{-11}	0.71
	673	29900	4.05 x 10^{-9}	2.42 x 10^{25}	4.62 x 10^{-11}	0.64
	773	57900	4.00 x 10^{-9}	2.39 x 10^{25}	7.79 x 10^{-11}	0.51

3.3.3 Lithium Transference Number

Figure 5(a) presents the plot of current versus time for the Li/ $Li_{3.88}Zn_{0.06}SiO_4$/Li cell. The impedance plot for the cell before and after polarization is shown in Figure 5(b). The value of R_e, R_{ss}, I_{ss} and τ_{Li}^+ obtained from this measurement are listed in Table 5. Calculation of Li^+ transference number was done using Eq. 3. The lithium transference number value is found to be 0.82. This value shows that the majority charge carrier in the sample are Li^+ ions and is reasonable value for lithium battery application [41].

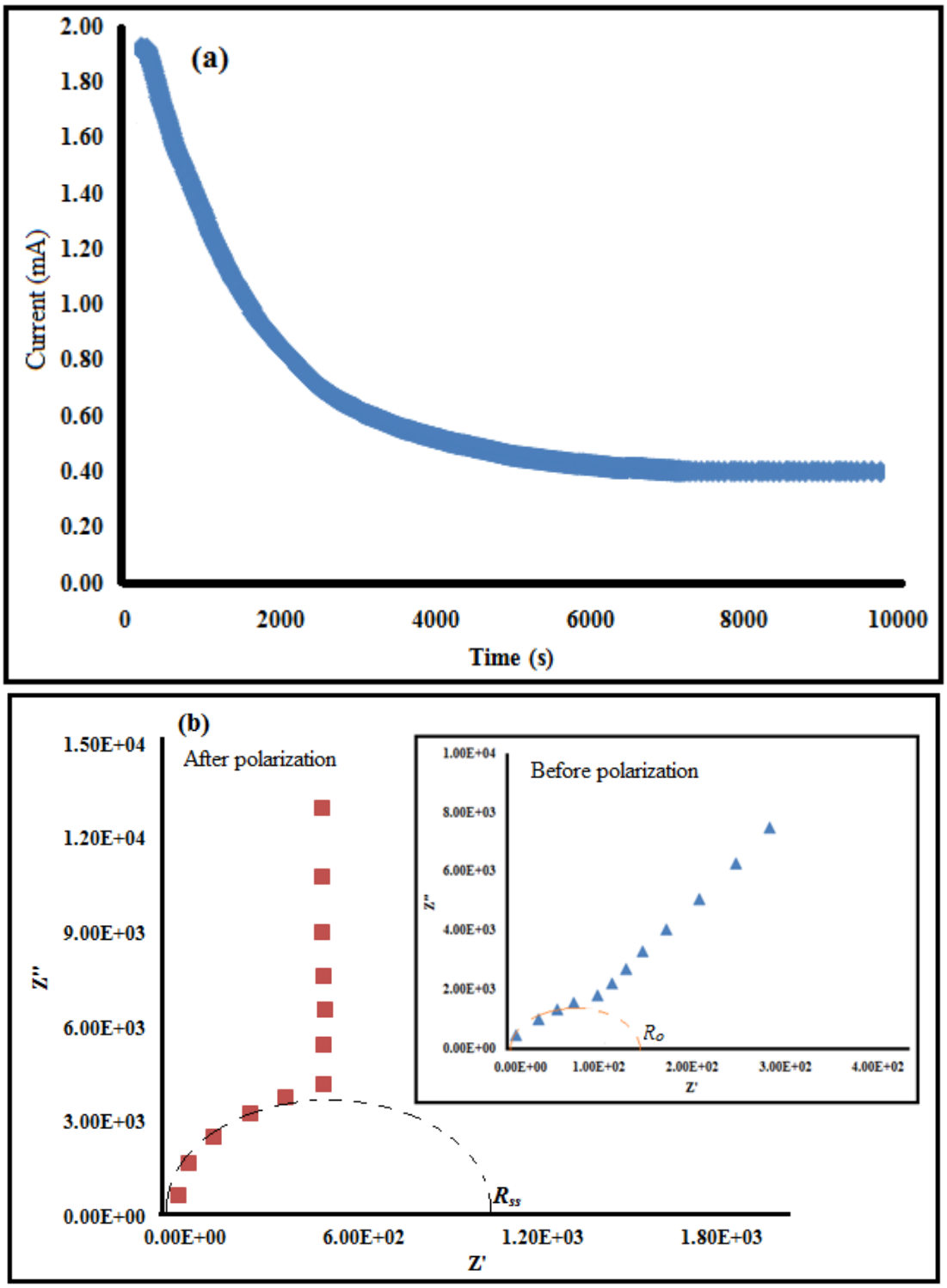

Figure 5. (a) Current verses time plot for $Li_{3.88}Zn_{0.06}SiO_4$ sample and (b) Impedance response of the sample before and after dc polarization.

Table 5. Data obtained from lithium transference number measurement of the $Li_{3.88}Zn_{0.06}SiO_4$ sample

Sample	ΔV(mV)	I_{ss}(mA)	$R_{ss}(\Omega)$	$R_e(\Omega)$	τ_{Li^+}
$Li_{3.88}Zn_{0.06}SiO_4$	500	0.384	1.13×10^3	1.41×10^2	0.82

4. CONCLUSIONS

The effect of Zn doping on Li_4SiO_4 was studied by XRD, DSC and EIS. The XRD result shows that Zn is successfully inserted into the Li_4SiO_4 structure. Meanwhile the DSC result reveals that doping with Zn increases thermal stability of the compound. The RT conductivity of the Zn doped compound is an order of magnitude higher compared to the undoped Li_4SiO_4. The conductivity–temperature study shows that the entire compound obeys the Arrhenius law. The conductivity parameters such as hopping frequencies, charge carrier concentration and mobile ion concentration have been calculated by fitting the conductance spectra to power law variation. The data of these parameters prove that increase in conductivity with temperature is due to increase in ion mobility. The value of lithium transference number in the sample with $x = 0.06$ is 0.82 and reasonable value for application in lithium batteries.

ACKNOWLEDGMENTS
Financial support by University of Malaya research grant (PV027/2012A) is gratefully acknowledged.

References

1. M. Parka, X. Zhanga, M. Chunga, G. B. Lessa, A. M. Sastrya, *J. Power Sources,* 195 (2010) 7904.
2. S.B.R.S Adnan, N.S Mohamed, *Mater. Res. Innovations*, 16 (2012) 281.
3. S.B.R.S Adnan, N.S Mohamed, K.A Norwati, *World academy of science, engineering and technologys*, 50 (2011) 670.
4. J.B Chavarria, P. Quintana, A. Huanosta, *Solid state Ionics*, 83 (2006) 24.
5. M. Wakihara, T. uchida, T. Gohara, *Solid state Ionics*, 31 (1988) 17.
6. Y. Saito, K. Ado, T. Asai, H. Kageyama, O. Nakamura, *Solid State Ionics*, 47 (1991) 149.
7. C. Masquelier, M. tabuchi, T. Takeuchi, W. Soizumi, H. Kageyama, O. Nakamura, *Solid State Ionics*, 79 (1995) 98.
8. Y. Saito, T. Asai, K. Ado, H. Kagayema, O. Nakamura, *Solid state Ionics*, 40/41 (1990) 34.
9. E.I Burmakin, *Solid State Ionics*, 36 (1988) 155.
10. A.R West, *Appl. Electrochem.*, 3 (1973) 327.
11. A. Khorassani, A. R West, *Solid State Chem.*, 53 (1984) 369.
12. A. Khorassani, A. R West, *Solid State Ionics*, 7 (1982) 1.
13. A. R Rodger, J. Kuwano, A.R West, *Solid State Ionics*, 15 (1985) 185.
14. Y. Tao, D. Yi, J. Li, *Solid State Ionics*, 179 (2008) 2396.
15. R.I Smith, A. R West , *Solid State Chem.*, 93 (1991) 436.
16. R.I Smith, A. R West, *Solid State Chem.*, 88 (1990) 564.
17. I. Hodge, M.D Ingram, A.R West, *American Ceramic Soc.*, 59 (1976) 360.
18. P.P Kumar, S. Yashonath, *Chem. Sci.*, 118 (2006) 135.
19. X. Song, M. Jia, R. Chen, *J. Mater. Processing Technol.*, 120 (2002) 21.
20. R. Adnan, N. A Razana, I. A Rahman and M. Akhyar Farrukh, *J. Chinese Chem. Soc.*, 57(2010) 222.
21. R.I Smith, A.R West, *Solid State Chem.*, 88 (1990) 564.
22. P. G. Bruce, J. Evans, C. A. Vincent, *Solid State Ionics* 28–30 (1988) 918.
23. M. Riley, S. Peter, Fedkiw, S. A. Khan, *Electrochem. Soc.*, 149 (2002) A667.
24. A.M.M. Ali , M.Z.A Yahya , H. Nahron, R. H. Y. Subban, *Ionics*, 12 (2006) 303.
25. D. Tranqui, R.D Shannon, H.Y Chen, *Acta Crystallogr*., 35 (1979) 2479.

26. B.L Dubey, A.R West, *J. Inorg. Nuclear Chem.*, 35 (1973) 3713.
27. S. Zhang, C. Deng, B.L Fu, S.Y Yang, L. Ma, *Electrochim. Acta*, 55 (2010) 8482.
28. H. Kleykamp, *Thermochim. Acta*, 287 (1996) 191.
29. G.W Hollenberg, *J. Nuclear Mater.*, 103 (1981) 591.
30. D. Vollath,H. Wedemeyer, H. Zimmermann,H. Werle, *J. Nuclear Mater.*, 174 (1990) 86.
31. M. Dudek, *Int. J. Electrochem. Sci.*, 7 (2012) 2874.
32. S.B.R.S Adnan, N.S. Mohamed, *Int. J. Electrochem. Sci.*, 7 (2012) 9844.
33. L. P. Teo & M. H. Buraidah & A. F. M. Nor & S. R. Majid, *Ionics* 18 (2012) 655.
34. M. Vijayakumar, G. Hirankumar, M.S. Bhuvaneswari, S. Selvasekarapandian, *J. Power Sources*, 117 (2003) 143.
35. T. Savitha, G. Hirankumar, M.S. Bhuvaneswari, S. Selvasekarapandian, C.S. Ramya, R. Baskaran, P.C Angelo, *J. Power Sources*,157 (2006) 553.
36. A.M. Abo El Ata, S.M. Attia, T.M Meaz, *Solid State Sci.*, 6 (2004) 61.
37. K. Funke, *Solid State Ionics*, 94 (1997) 27.
38. M.A Afifi, M.EL-Nahass, A.E Bekheet, I.T Zedan, S.R Elliot, *Physica B* : *Physics of Condensed Matter*, 400 (2007) 248.
39. D.P Almond, A.R West, *Solid State Ionics*, 9&10 (1983) 277.
40. D.P Almond, A.R West, *Solid State Ionics*, 23 (1987) 27.
41. Yongxin An, Pengjian Zuo, Xinqun Cheng, Lixia Liao, Geping Yin, *Int. J. Electrochem. Sci.*, 6 (2011) 2398 .

Available online at www.sciencedirect.com

ScienceDirect

Ceramics International 40 (2014) 5033–5038

CERAMICS INTERNATIONAL

www.elsevier.com/locate/ceramint

Short communication

Properties of novel $Li_{4-3x}Cr_xSiO_4$ ceramic electrolyte

S.B.R.S Adnan[a], N.S. Mohamed[b,*]

[a]Institute of Graduate Studies, University of Malaya, 50603 Kuala Lumpur, Malaysia
[b]Centre for Foundation Studies in Science, University of Malaya, 50603 Kuala Lumpur, Malaysia

Received 11 July 2013; received in revised form 29 August 2013; accepted 29 August 2013
Available online 8 September 2013

Abstract

Cr-doped Li_4SiO_4 compounds were prepared by a sol–gel method. The effects of Cr^{3+} doping on the characteristics of Li_4SiO_4 were carefully investigated. Compared with the XRD pattern of the Li_4SiO_4 sample, the XRD patterns of the Cr-doped Li_4SiO_4 shift to higher diffraction angle. This indicated that Cr^{3+} entered the structure of Li_4SiO_4 rather than forming impurities. The formation of the compound was confirmed by Fourier transform infrared study. The introduction of Cr^{3+} ions considerably raised the conductivity of the Li_4SiO_4 compound. The compound of $Li_{3.94}Cr_{0.02}SiO_4$ exhibited total conductivity value of 2.51×10^{-5} S cm^{-1} at ambient temperature and 5.69×10^{-4} S cm^{-1} at 500 °C. Ionic transference number corresponding to Li^+ ion transport determined by means of Bruce and Vincent technique was 0.95. Linear sweep voltammetry result showed that the doping of Cr^{3+} ion improved the limit of electrolyte decomposition to 4.51 V versus a Li/Li^+ reference electrode.

Keywords: C. Ionic conductivity; Lithium orthosilicate; Linear sweep voltammetry; Solid electrolyte

1. Introduction

Lithium super ionic conductor (LISICON) is one of promising groups of crystalline materials that is very important for future application as solid electrolyte in lithium batteries. This type of electrolytes is considered to be effective in improving the safety of lithium ion batteries compared to the traditional liquid electrolyte. Among solid electrolytes, the application of ceramic electrolytes form an important class of materials due to their large electrochemical stability window, good thermal stability, absence of leakage and a high resistance to shock and vibrations. Meanwhile, the use of ceramic materials in electrochemical devices can also solve the problem of capacity fading and self discharge cause by side reactions [1]. Many attempts to synthesize new ceramic lithium superionic conductors have been made. The highest conductivity of 10^{-3} S cm^{-1} was previously reported for the thio-LISICON structure, $Li_{3.25}Ge_{0.25}P_{0.75}S_4$ [2]. However this type of materials has disadvantages such as complicated to prepare, toxic, show instability against electrochemical reduction at low potential (ca. 0.1 V versus Li/Li^+), and also exhibits incompatibility with graphite anode [3].

In the search of fast lithium conducting solid electrolyte, the authors found recently new solid solution systems based on the lithium orthosilicate, Li_4SiO_4. These compounds with the general formula, $Li_{4-3x}Cr_xSiO_4$, are isostructural with γ-Li_3PO_4 and have the same framework structure with the thio-LISICON. However, the thio-LISICON structure have sulfur instead of oxygen in this structure. The substitution of Li with Cr ($3Li^+ \leftrightarrow Cr^{3+}$) will create two vacant sites in the structure and any lithium ion in the intermediate vicinity can jump to the vacant sites. This leaves the previous two sites of the ion vacant available to host other ions. This results in the mobility of ions across the solid giving rise the conductivity. Their concentration is the main factor determining the conductivity of this solid electrolyte [4].

Chavarria et al. [5] have previously reported conductivity data for the $Li_{4-3x}(Al,Ga,In)_xSiO_4$ at 127 °C with conductivity value 6×10^{-5} S cm^{-1} (Al system), 6×10^{-6} S cm^{-1} (Ga system) and 6×10^{-8} S cm^{-1} (In system). However, study on lithium orthosilicate doped with Cr^{3+} ions has never been reported in the literature. This doping is expected to be successful since the ion radius difference between Cr^{3+} (0.64 Å) and Li^+ (0.69 Å) is just 7.5% and does not exceed the solubility limit for atomic radii differences in solid solution which is 15% [6].

*Corresponding author. Tel.: +60 379675800.
E-mail addresses: syed_bahari@yahoo.com (S.B.R. Adnan), nsabirin@um.edu.my (N.S. Mohamed).

0272-8842/$ - see front matter © 2013 Elsevier Ltd and Techna Group S.r.l. All rights reserved.
http://dx.doi.org/10.1016/j.ceramint.2013.08.136

In this study, $Li_{4-3x}Cr_xSiO_4$ (x=0, 0.01, 0.02 and 0.03) compounds were synthesized and characterized. The effects of Cr^{3+} substitution on the properties of Li_4SiO_4 were investigated using x-ray diffraction (XRD), Fourier transform infrared (FTIR), Scanning electron microscope (SEM), Particle size analysis, impedance spectroscopy (IS), lithium transference number measurement and linear sweep voltammetry (LSV).

2. Experimental procedure

2.1. Synthesis of $Li_{4-3x}Cr_xSiO_4$

For this study, four compounds with x=0, 0.01, 0.02 and 0.03 were prepared via sol–gel technique. For sample preparation, lithium acetate, chromium (III) acetate hydroxide and tetraethyl orthosilicate were used as the starting materials. Meanwhile citric acid was used as the chelating agent. The molar ratio of Li:Cr:Si was fixed according to formula $Li_{4-3x}Cr_xSiO_4$ with x=0, 0.01, 0.02 and 0.03. Lithium acetate and chromium (III) acetate hydroxide were first dissolved in distilled water and then mixed with citric acid under magnetic stirring. The solution was transferred into a reflux system and continuously stirred until a homogeneous solution was formed. Solution of tetraethyl orthosilicate was later added to this homogeneous solution. After stirring for 12 h, the solution was taken out and then vaporized for about 2 h under magnetic stirring at 75 °C. The resulting sticky wet gel was dried in an oven at 150 °C for 24 h. The obtained powder was ball milled for 24 h using a Fritsch Pulverisette-7 ball mill operated at 500 rpm. The powder was sintered at temperature 800 °C for 12 h and later pressed using a Specac pellet press to form pellet with diameter and thickness of 13 mm and 2.0 mm respectively.

2.2. Characterization techniques

XRD patterns of the powder samples were obtained using X-ray Diffraction spectrometer (Bruker AXS D8 Advance) with Cu-K_α radiation of wavelength of 1.5406 Å in 2θ range between 10° and 70° at the rate of 0.016° in step width. FTIR was carried out to confirm the structure of the studied ceramic samples. Infrared spectra were recorded at room temperature using a Perkin-Elmer Frontier Spectrometer with resolution 1 cm^{-1}. The absorption spectra in FIR region were measured using polyethylene technique. The morphology of the sample powders were analyzed by SEM which were carried out using Scanning electron microscope spectrometer (Zeiss-Evo MA10). The particle size information was obtained using FRITSCH-Analysette 22 NanoTec laser particle sizer. The ceramic electrical properties were determined by ac impedance spectroscopy using Solatron 1260 impedance analyzer over a frequency range from 1 to 10^6 Hz. An applied voltage was fixed at 200 mV.

Lithium transference number measurement was done using Bruce and Vincent method [7–9] in order to determine the actual type of charge carriers. The lithium transference number (τ_{Li}^{+}) was calculated using the equation:

$$\tau_{Li^+} = \frac{I_{ss}(\Delta V - I_o R_o)}{I_o(\Delta V - I_{ss} R_{ss})} \quad (1)$$

In this equation, I_o is initial current (t=0), I_{ss} is steady state current, R_o and R_{ss} are initial resistance of the passive layer (before polarization) and resistance of the passive layer (after polarization) respectively and ΔV is applied voltage bias (ΔV=0.5 V). The electrochemical stability was evaluated by linear sweep voltammetry using Wonatech ZIVE MP2 multichannel electrochemical workstation.

3. Result and discussion

3.1. Phase identification

Fig. 1(a) shows XRD spectra of the monoclinic $Li_{4-3x}Cr_xSiO_4$ (x=0, 0.01, 0.02 and 0.03) samples. Cr^{3+} could be doped on the Li sites ($3Li^+ \leftrightarrow Cr^{3+}$) with up to x=0.020 without the presence of impurities. As such, further analysis was only done on the samples with $0 < x < 0.02$. To confirm the Cr^{3+} ion is in the Li_4SiO_4 structure, the peaks in 2θ range 16.50°–17.10° were carefully analyzed. Fig. 1(b) shows the magnified XRD patterns in this 2θ range. As seen in this figure, the peak shifts to higher diffraction angle when Cr^{3+} ion is doped into the parent structure indicating that Cr^{3+} ion is in the Li_4SiO_4 structure rather than forming impurities. The diffraction peak is also broadened by

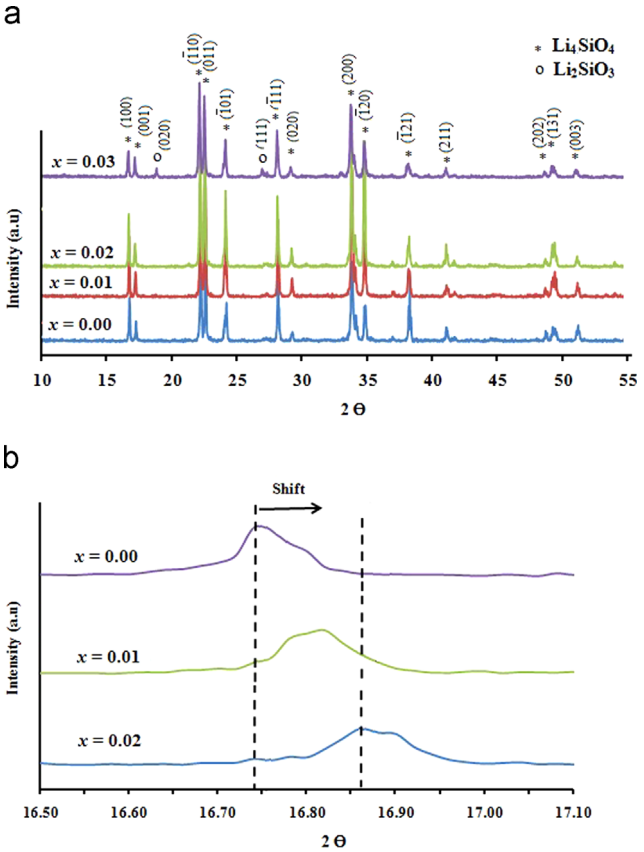

Fig. 1. (a) XRD patterns of $Li_{4-3x}Cr_xSiO_4$ samples and (b) XRD patterns of $Li_{4-3x}Cr_xSiO_4$ samples in 2θ range from 16.50° to 17.10°.

Cr^{3+} doping, which implies that the crystal size decreases with increasing Cr^{3+} content.

Meanwhile, the variation of the lattice parameters of the monoclinic γ-solid solution with different Cr^{3+} contents are shown in Table 1. Based on the table, the value of *a* increases and then decreases while the values of *b*, *c*, β and unit cell volume (*V*) decrease with increase of Cr^{3+} ion content. The decrease in the lattice constants is attributable to the substitutions of smaller volume of Cr^{3+} ion compared to three volumes of Li^{+} ions. The substitution of lithium by Cr^{3+} which results in shrinkage of unit cell volume increases the stability of the compound's structure [10].

3.2. FTIR analysis

Fig. 2 presents the FTIR spectra for $Li_{4-3x}Cr_xSiO_4$ samples in the spectral region from 460 cm^{-1} and 500 cm^{-1} which corresponds to absorption peaks originated from Li–O and Li–O–Si groups [11–13]. The increasing of Cr^{3+} concentration results in a decrease in intensity of the peaks. This effect is due to the coordination of the cation of Cr^{3+} with the oxygen, which results in the weakening of the Li–O and Li–O–Si and change in the lattice parameters as mentioned earlier.

3.3. SEM and particle size distribution

The SEM micrographs and particle size distribution of $Li_{4-3x}Cr_xSiO_4$ ceramic powders are displayed in Fig. 3. From these images, it is clear that the particle size decreases with increasing Cr^{3+} content. The average grain size decreases from 11.8 μm in the Li_4SiO_4 sample to 0.59 μm in the $Li_{3.94}Cr_{0.02}SiO_4$ sample. The smaller particles in $Li_{3.940}Cr_{0.020}SiO_4$ is favorable as this may improve contact with electrode materials when it is used for device fabrication.

3.4. Impedance measurement

Impedance spectra for $Li_{4-3x}Cr_xSiO_4$ with $x=0$, 0.01 and 0.02 at ambient temperature are presented in Fig. 4. The figure shows a high and low frequency semicircle for all samples. The total conductivity, (σ_t) (bulk conductivity, σ_b+grain boundary conductivity, σ_{gb}) which represent the direct current (d.c) conductivity in the ceramic sample can be calculated from equation [14]:

$$\frac{1}{\sigma_t} = \frac{1}{\sigma_b} + \frac{1}{\sigma_{gb}} \tag{2}$$

where $\sigma_b = d/AR_b$ and $\sigma_{gb} = d/AR_{gb}$. In these equation, *d* is the sample thickness, *A* is the cross-sectional area of sample, R_b is the bulk resistance and R_{gb} is the grain boundary resistance. As the Cr^{3+} concentration increases, the total resistance, $R_t = (R_b + R_{gb})$ value shifts towards lower values indicating increase in conductivity.

Fig. 5 depicts the plots of temperature dependence of total conductivity for all samples. The conductivity plots of the three samples are linear and fit the Arrhenius equation as expressed by:

$$\sigma_b T = A \exp\left(\frac{-E_\alpha}{kT}\right) \tag{3}$$

where *A* is the pre-exponential factor, E_α is the activation energy for conduction and *k* is the Boltzman constant. The conductivity of the samples increases with temperature and with Cr^{3+} ion concentration as well. The $Li_{3.94}Cr_{0.02}SiO_4$ compound gives the highest conductivity value of 2.51×10^{-5} S cm^{-1} at ambient temperature and 5.69×10^{-4} S cm^{-1} at 500 °C. The conductivity value at ambient temperature for $Li_{3.94}Cr_{0.02}SiO_4$ is an order of magnitude higher compared to the Li_4SiO_4. The σ-1000/T plots show a discontinuity at 300 °C (1000/T = 1.75 K^{-1}) which is in agreement with the results reported by Wakihara et al. [15] and those obtained by the author earlier [16]. The change in slope of the σ-1000/T plots could be due to an order-disorder transition of Li^{+} and Cr^{3+} ions (change in structure arrangement). This is support by the authors' previous work in which no phase transition was observed in the sample upon heating from room temperature until 500 °C [16].

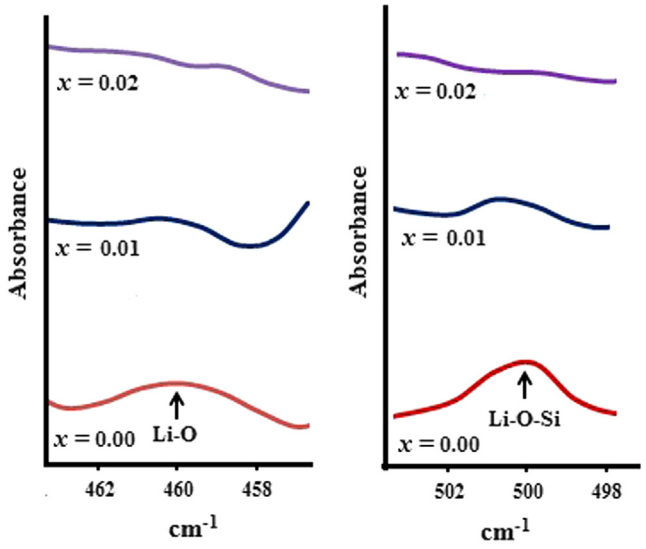

Fig. 2. FTIR spectra of $Li_{4-3x}Cr_xSiO_4$ samples in the spectral region from 458 to 462 cm^{-1} and 498 to 502 cm^{-1}.

Table 1
Lattice parameters and unit cell volume for different *x* value.

Samples	$a \pm 0.066$ (Å)	$b \pm 0.008$ (Å)	$c \pm 0.105$ (Å)	$\beta \pm 0.04$ (°)	*V* (Å^3)
$x=0.00$	5.147	6.094	5.293	90.33	166.01
$x=0.01$	5.271	6.089	5.124	90.32	164.44
$x=0.02$	5.249	6.079	5.100	90.25	162.74

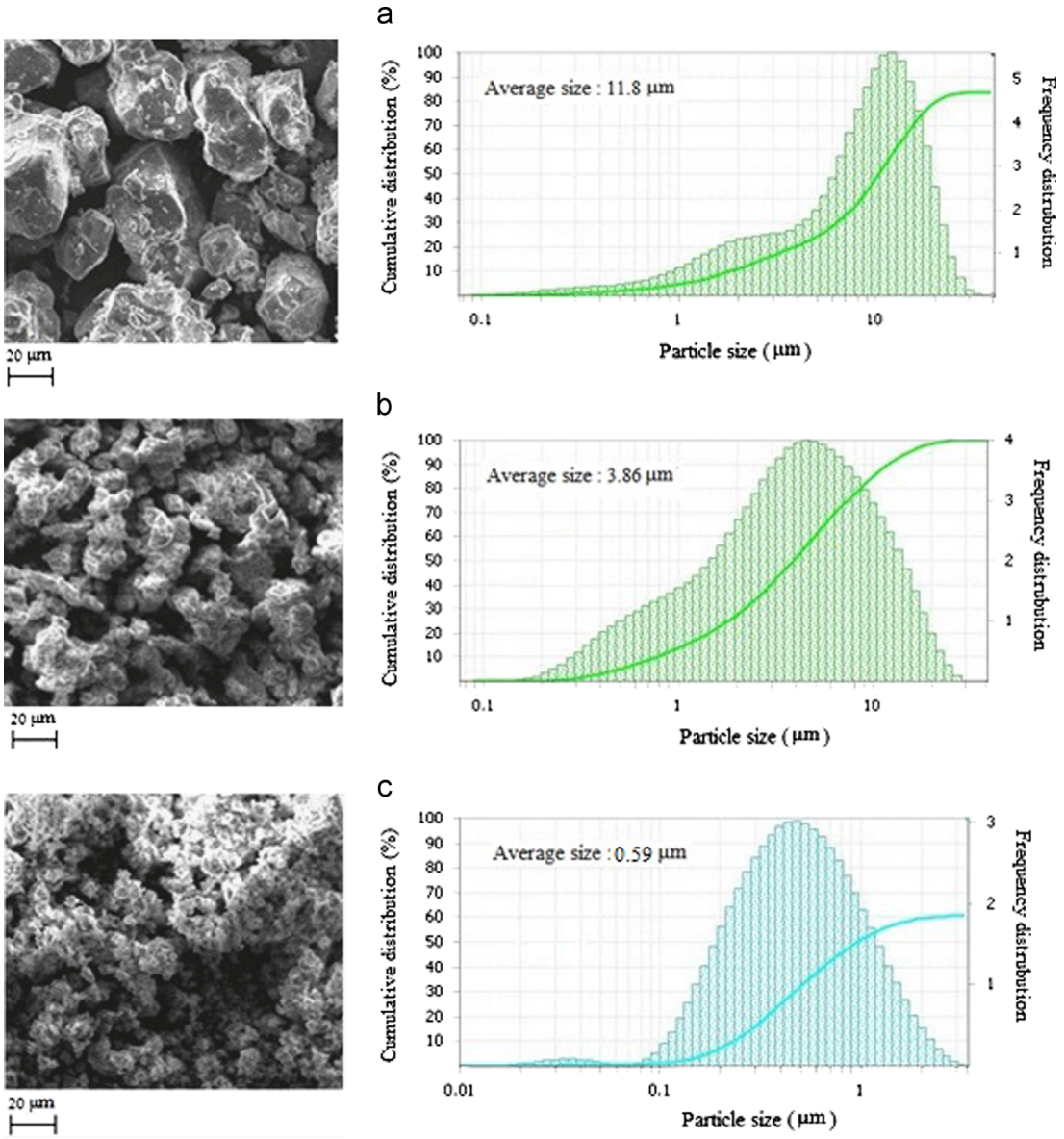

Fig. 3. SEM micrograph and particle size distribution of the (a) Li_4SiO_4 (b) $Li_{3.97}Cr_{0.01}SiO_4$ and (c) $Li_{3.940}Cr_{0.02}SiO_4$ sample.

3.5. Lithium transference number

Fig. 6(a) and (b) present plots of current versus time for the Li/$Li_{3.94}Cr_{0.02}SiO_4$/Li and Li/Li_4SiO_4/Li cells used for the lithium transference number determination of the solid electrolyte. Under a dc polarization of 0.5 V, the current in the both cells exhibit only a small decay with time. The initial and final steady current in Li/$Li_{3.94}Cr_{0.02}SiO_4$/Li cell are $I_o = 0.92$ μA and $I_{ss} = 0.87$ μA respectively. Meanwhile, the initial and final steady currents in Li/Li_4SiO_4/Li cell are $I_o = 1.67$ μA and $I_{ss} = 1.34$ μA respectively. The impedance responses of the cells prior and after polarization for Li/$Li_{3.94}Cr_{0.02}SiO_4$/Li cell are $R_o = 15{,}180$ Ω and $R_{ss} = 15{,}923$ Ω respectively. Meanwhile in Li/Li_4SiO_4/Li cell, the impedance responses prior and after polarization are $R_o = 36{,}307$ Ω and $R_{ss} = 42{,}405$ Ω respectively.

Calculation of Li^+ transference number was done using Eq. (1). The lithium transference number value is 0.95 for the $Li_{3.94}Cr_{0.02}SiO_4$ electrolyte sample and 0.79 for the Li_4SiO_4 electrolyte sample. These values show that the Cr^{3+} doping into the Li sites ($Cr^{3+} \leftrightarrow 3Li^+$) increases the Li^+ ions transport number.

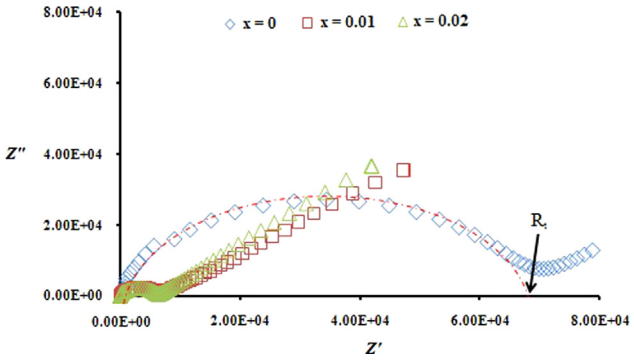

Fig. 4. The impedance spectra of $Li_{4-3x}Cr_xSiO_4$ sample.

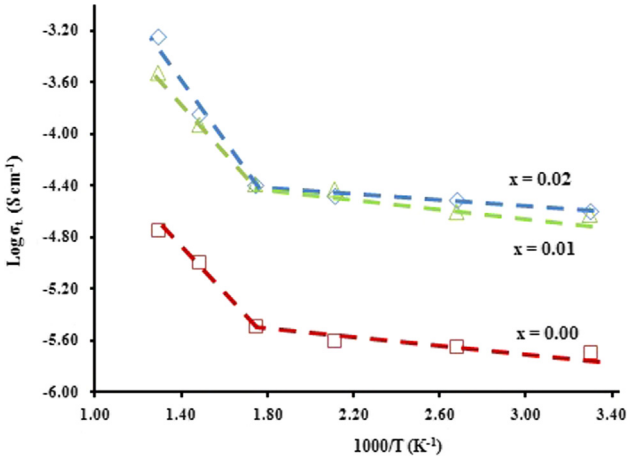

Fig. 5. Temperature dependence of total conductivity for $Li_{3.940}Cr_{0.020}SiO_4$ sample.

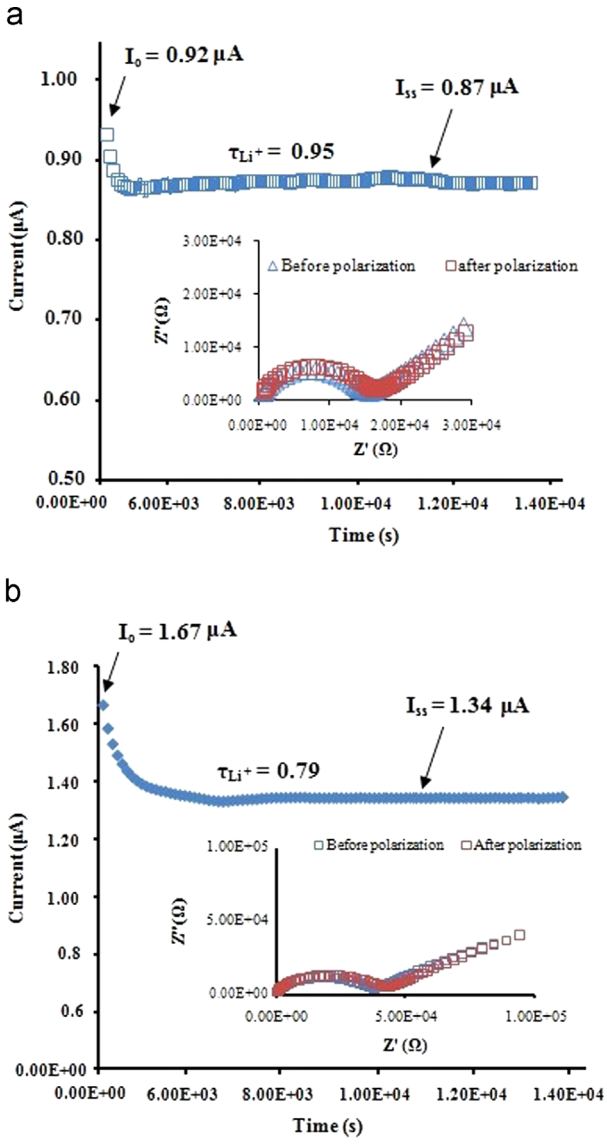

Fig. 6. (a) Current versus time plot for $Li_{3.940}Cr_{0.020}SiO_4$ sample and impedance responses of the sample before and after polarization. (b) Current versus time plot for Li_4SiO_4 sample and its impedance spectra performed before and after cell polarization are shown in inset.

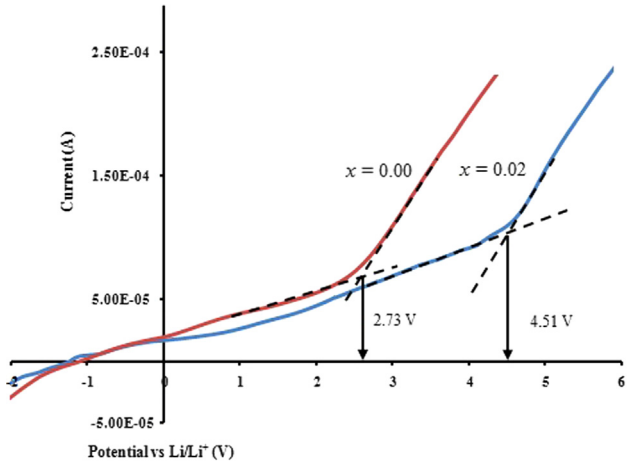

Fig. 7. Linear sweep voltammogram of Li_4SiO_4 and $Li_{3.940}Cr_{0.020}SiO_4$ at a sweep rate of 1 mV s^{-1}.

3.6. Linear sweep voltammetry

The electrochemical stability window is another important parameter of the ceramic electrolyte. The stability was evaluated by linear sweep voltammetry. Fig. 7 illustrates linear sweep voltammograms of the $Li_4Sn_{0.02}Si_{0.98}O_4$ and Li_4SiO_4 ceramic electrolyte. From the figure, the magnitude of current is fairly low below 2.73 V for Li_4SiO_4 and is 4.51 V for $Li_{3.94}Cr_{0.02}SiO_4$ respectively and the current starts increasing at potentials beyond this limit due to decomposition of the electrolyte. This suggests that the doping of Cr^{3+} ion increases the limit of electrolyte decomposition.

4. Conclusions

The effects of Cr^{3+} doping on Li_4SiO_4 were studied by XRD, FTIR, SEM, Particle size analysis, EIS, transference number and LSV. The XRD and FTIR results showed that Cr^{3+} is successfully inserted into the Li_4SiO_4 structure. The SEM showed that the grain size decreases with increase of Cr^{3+} concentration. The conductivity –temperature study illustrated that the conductivity of the compound obeys the Arrhenius law and increase with temperature. The value of lithium transference number increases upon Cr^{3+} doping. The $Li_{3.94}Cr_{0.02}SiO_4$ sample showed an increased of stable voltage window up to 4.51 V versus Li/Li^+ respectively.

Acknowledgments

Financial support from the University of Malaya (research grant PV027/2012) is gratefully acknowledged.

References

[1] B. Scrosati, Recent advances in lithium ion battery materials, Electrochimica Acta 45 (2000) 2461–2466.
[2] Masahiro Murayama, Noriyuki Sonoyama, Atsuo Yamada, Ryoji Kanno, Material design of new lithium ionic conductor, thio-LISICON, in the Li_2S–P_2S_5 system, Solid State Ionics 170 (2004) 173–180.

[3] Yuji Ooura, Nobuya Machida, Muneyuki Naito, Toshihiko Shigematsu, Electrochemical properties of the amorphous solid electrolytes in the system Li_2S–Al_2S_3–P_2S_5, Solid State Ionics 225 (2012) 350–353.
[4] P. Padma Kumar, S. Yashonathl, Ionic conduction in the solid state, Journal of Chemical Sciences 118 (2006) 135–154.
[5] J.B. Chavarria, P. Quintana, A. Huanosta, Electrical properties of the solid solution $Li_{4-3x}In_xSiO_4$, Solid State Ionics 83 (1996) 245–248.
[6] Zhanqiang Liu, Fuqiang Huang, Jianhua Yang, Baofeng Wang, Junkang Sun, New lithium ion conductor, thio-LISICON lithium zirconium sulfide system, Solid State Ionics 179 (2008) 1714–1716.
[7] P.G. Bruce, J. Evans, C.A. Vincent, Conductivity and transference number measurements on polymer electrolytes, Solid State Ionics 28-30 (1998) 918–922.
[8] M. Riley, S.Peter Fedkiw, S.A. Khan, Transport Properties of Lithium Hectorite-Based Composite Electrolytes, Electrochemical Society 149 (2002) A667–A674.
[9] A.M.M. Ali, M.Z.A Yahya, H. Nahron, R.H.Y. Subban, Electrochemical studies on polymer electrolytes based on poly(methyl methacrylate)-grafted natural rubber for lithium polymer battery, Ionics 12 (2006) 303–307.
[10] Li Fang Jiao, Ming Zhang, Hua Tang Yuan, Ming Zhao, Jian Guo, Wei Wang, Xing Di Zhou, Yong Mei Wang, Effect of Cr doping on the structural, electrochemical properties of $Li[Li_{0.2}Ni_{0.2-x/2}Mn_{0.6-x/2}Cr_x]O_2$ ($x=0$, 0.02, 0.04, 0.06, 0.08) as cathode materials for lithium secondary batteries, Journal of Power Sources 167 (2007) 178–184.
[11] Marek Nocun, Miroslaw Handke, Identification of Li–O absorption bands based on lithium isotope substitutions, Journal of Molecular Structure 596 (2001) 145–149.
[12] J. Ortiz-Landerosa, L. Martínez-dlCruz, C. Gómez-Yáñez, H. Pfeiffer, Towards understanding the thermoanalysis of water sorption on lithium orthosilicate (Li_4SiO_4), Thermochimica Acta 515 (2011) 73–78.
[13] Bo Zhang, Michel Nieuwoudt, allan J. Easteal, Sol–gel route to nanocrystalline lithium metasilicate particles, Journal of the American Ceramic Society 91 (2008) 1927–1932.
[14] Shiqiang (Rob) Hui, Justin Roller, Sing Yick, Xinge Zhang, Cyrille Decès-Petit, Yongsong Xie, Radenka Maric, Dave Ghosh, A brief review of the ionic conductivity enhancement for selected oxide electrolytes, Journal of Power Sources 172 (2007) 493–502.
[15] M. Wakihara, T. Uchida, T. Gohara, Ionic conductivity of $Li_{4-2x}Mg_{x}$-SiO_4, Solid state Ionics 31 (1988) 17–20.
[16] S.B.R.S Adnan, N.S. Mohamed, Structural, thermal and electrical properties of Li_{4-2x} Zn_xSiO_4 ceramic electrolyte prepared by citrate sol–gel technique, International Journal of Electrochemical Science 8 (2013) 6055–6067.

Solid State Ionics xxx (2013) xxx–xxx

Contents lists available at SciVerse ScienceDirect

Solid State Ionics

journal homepage: www.elsevier.com/locate/ssi

Effects of Sn substitution on the properties of Li_4SiO_4 ceramic electrolyte

S.B.R.S. Adnan [a,*], N.S. Mohamed [b]

[a] Institute of Graduate Studies, University of Malaya, 50603 Kuala Lumpur, Malaysia
[b] Centre for Foundation Studies in Science, University of Malaya, 50603 Kuala Lumpur, Malaysia

ARTICLE INFO

Article history:
Received 17 April 2013
Received in revised form 9 July 2013
Accepted 10 July 2013
Available online xxxx

Keywords:
Arrhenius
Ceramic
Conductivity
Lithium orthosilicate
Linear sweep voltammetry
Solid electrolyte

ABSTRACT

The aim of this work is to investigate the effects of Sn doping on the structural, thermal, electrical and electrochemical properties of Li_4SiO_4 synthesized by a sol gel method. The formation of the compound is confirmed by XRD study. Thermal properties of the compounds are measured using DSC analysis while the electrical characteristics are investigated by impedance spectroscopy. The introduction of Sn ions considerably raises the conductivity and improves thermal stability of the Li_4SiO_4 compound. The compound of $Li_4Sn_{0.02}Si_{0.98}O_4$ gives a maximum conductivity value of 3.07×10^{-5} S cm^{-1} at ambient temperature and 1.30×10^{-4} S cm^{-1} at 500 °C. The charge carrier concentration and mobile ion concentration are found to be constant over the temperature range from 303 K to 773 K, while the mobility of ion increases with temperature, implying that the increase in conductivity with temperature is due to increase in ion mobility. Linear sweep voltammetry result show that the $Li_4Sn_{0.02}Si_{0.98}O_4$ sample is electrochemically stable in the voltage range of −5.3 V to 5.3 V versus a Li/Li^+ reference electrode.

1. Introduction

Lithium ion batteries that have excellent characteristics such as high energy density and high voltage are widely used in small and portable information terminal devices. In the future, large-scale lithium batteries will be broadly used such as in energy and transportation sector, communication electronics, display devices, medicine and metallurgy necessitating further safety. Solid electrolytes are considered to be effective in improving the safety of lithium ion batteries. Among solid electrolytes, the application of ceramic electrolytes forms an important class of materials due to their superior incombustibility, high density and long-term stability [1].

Lithium orthosilicate, Li_4SiO_4, which have LISICON structure, is one of the promising ceramic electrolytes. It has a monoclinic unit cell and is a rather complex structure [2–4]. The oxygen form buckled layers but they do not approximate to a close packed arrangement. Silicon is tetrahedrally coordinated to oxygen and the structure is a typical orthosilicate with isolated $(SiO_4)^{4-}$ groups. Meanwhile, lithium is disordered over a number of four-, five- and six-coordination position in Li_4SiO_4 including a number of face sharing tetrahedral sites that are separated by distances as short as 0.92 Å [3,4].

Li_4SiO_4, which is a poor conductor ($\sigma_{RT} = 10^{-6}$ S cm^{-1}), is not sufficiently high for practical applications. West [4] reported the partial substitution of Ge^{4+} and Ti^{4+} for Si^{4+} improves the conductivity of Li_4SiO_4 to ~10^{-5} S cm^{-1} and ~10^{-4} S cm^{-1}, respectively, at temperature 450 °C. However, study on lithium orthosilicate doped with Sn^{4+} ions has never been reported in the literature. The size of Sn^{4+} (0.69 Å) cations, which is larger than Ge^{4+} (0.54 Å) and Ti^{4+} (0.67 Å) as expected, can enhance the conductivity of this compound [5,6]. The introduction of larger cation may increase the lattice size of the Li_4SiO_4-type structure and increase in the size of migration channels of Li^+ ion leading to increase in mobility of mobile ions [7]. As such, in this study, $Li_4Sn_xSi_{1-x}O_4$ ($x = 0$ to 0.04) were synthesized and characterized. The compound was prepared by sol-gel method. The effect of Sn substitution on the structure, thermal, electrical and electrochemical properties of Li_4SiO_4 were investigated using x-ray diffraction (XRD), different scanning calorimetry (DSC), impedance spectroscopy (EIS) and linear sweep voltammetry (LSV).

2. Experimental procedure

2.1. Synthesis of $Li_4Sn_{0.02}Si_{0.98}O_4$

Lithium acetate ($C_2H_3LiO_2$), Tin (IV) chloride pentahydrate ($SnCl_4.5H_2O$) and tetraethyl orthosilicate ($SiC_8H_{20}O_4$) were used as the starting materials while citric acid was used as the chelating agent. Lithium acetate and tin (IV) chloride were first dissolved in distilled water and then mixed with citric acid under magnetic stirring. The solution was transferred into a reflux system and continuously stirred until a homogeneous solution was formed. Solution of tetraethyl orthosilicate was later added to this homogeneous solution. The solution was taken out and then vaporized about 2 h under magnetic stirring at 75 °C. The resulting wet gel was dried in an oven at 150 °C for 24 h to remove water particles

* Corresponding author. Tel.: +60 136248737; fax: +60 379675800.
E-mail addresses: syed_bahari@yahoo.com (S.B.R.S. Adnan), nsabirin@um.edu.my (N.S. Mohamed).

0167-2738/$ – see front matter © 2013 Elsevier B.V. All rights reserved.
http://dx.doi.org/10.1016/j.ssi.2013.07.008

and resistance organic groups and also to avoid ceramic cracks. The obtained powder was ball milled for 24 h using a Fritsch Pulverisettle-7, which was operated at 500 rpm. The powder was sintered at 800 °C for 12 h and later pressed using a Specac pellet press to form pellet with diameter and thickness of 13 mm and 2.0 mm, respectively.

2.2. Characterization techniques.

X-ray diffraction (XRD) was done in order to elucidate structural information of the sample. The sintered ceramic powders were characterized using a Bruker AXS D8 Advance X-ray Diffraction spectrometer with Cu-K_α radiation of wavelength of 1.5406 Å in 2θ range between 10° and 70° at the rate of 0.016° in step width. The Fourier transfer infrared was carried out in order to determine the vibrational spectra of the sample. Thermal behavior of the sintered sample was analyzed by differential scanning calorimetry Setaram EVO Lab^{sys} thermal analyzer in argon atmosphere at a constant heating rate of 10 °C min^{-1} in the temperature range between room temperature and 1200 °C. The ceramic electrical properties were determined by AC impedance spectroscopy using Solatron 1260 impedance analyzer over a frequency range from 1 to 10^6 Hz. An applied voltage was fixed at 200 mV.

The AC conductivity has been evaluated from dielectric data in accordance with the relation:

$$\sigma_{AC} = \omega\varepsilon_o\varepsilon'' \tan\delta \quad (1)$$

where ε_o is the permittivity of the free space, ω is $2\pi f$ and tan δ is the dielectric loss factor [8]. The electrochemical stability was evaluated by linear sweep voltammetry.

3. Results and discussion

3.1. Phase identifications

Fig. 1(a) shows XRD spectra of the Sn doped and undoped Li_4SiO_4 samples. The XRD spectra of both samples can be indexed to monoclinic structure in space group $P2_{1/m}$. Sn^{4+} could be doped on the Si site ($Sn^{4+} \leftrightarrow Si^{4+}$) with up to $x = 0.02$ without the presence of a second phase, Li_2SnO_3. The sample with $x \geq 0.04$ contain impurities. As such, further analysis was only done on the sample with $x = 0.02$. To confirm the Sn^{4+} ion is in the Li_4SiO_4 structure, the peaks in the 2θ range 22.00°–23.00° were carefully analyzed. Fig. 1(b) shows the magnified XRD patterns in this 2θ range. As seen, the peaks become larger and shift to higher diffraction angle when Sn^{4+} is added, suggesting that there are more ions sitting on the tetrahedral sites. Meanwhile, the values of *a*, *b* and *V* (unit cell volume) increase and the value of *c* and β decrease with insertion of Sn^{4+} ions (Table 1). The increase in the unit cell volume is mostly related to the Sn^{4+} insertion into Li_4SiO_4 structure, which can be attributed to the larger atomic size of Sn^{4+} than that of Si^{4+}.

3.2. Thermal properties

The DSC curves for $Li_4Sn_xSi_{1-x}O_4$ samples are shown in Fig. 2. There are three endothermic peaks in the curve of the sample with $x = 0$. The first and second peaks observed in temperature range from 656 °C to 700 °C, which is recognized as second order phase transition of Li_4SiO_4. A similar observation has been reported by other researchers [4,9,10]. The last peak at temperature of 1036 °C represents eutectic temperature according to reaction liquid of Li_4SiO_4 and Li_2SiO_3 [11], which is may due to presence of small amount of Li_2SiO_3 in the samples. However, this sample is stable at least at ~ 1000 °C. The addition of stannum ions results in an increase in phase transition of the ceramic upon substitution of Sn^{4+} ions for Si^{4+} ions.

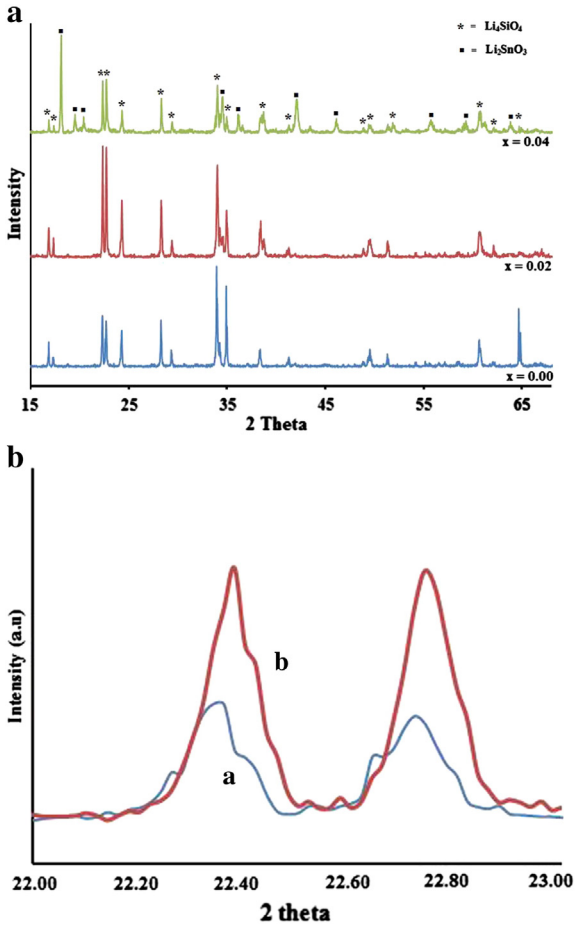

Fig. 1. (a) XRD pattern of $Li_4Sn_xSi_{1-x}O_4$ samples. (b) XRD pattern of the samples with (a) $x = 0.00$ and (b) $x = 0.02$ in 2θ range from 22.00° to 23.00°.

3.3. Impedance measurement

Impedance spectra for $Li_4Sn_{0.02}Si_{0.98}O_4$ at 303 K, 673 K and 773 K are presented in Fig. 3. The data show a high-frequency semicircle at all temperatures. The bulk resistance, R_b, can be determined using the equation:

$$\sigma_b = \frac{d}{AR_b} \quad (2)$$

where *d* is the sample thickness, *A* is the cross-sectional area of the sample and R_b is the bulk resistance determined from impedance plot. As the temperature increases, the R_b value shifts towards a lower impedance value indicating increase in conductivity. The temperature dependence of the DC conductivity of $Li_4Sn_{0.02}Si_{0.98}O_4$ is shown in Fig. 4. The activation energy for the thermally activated hopping process was obtained by fitting the DC conductivity data with Arrhenius equation:

$$\sigma_b T = A\exp\left(\frac{-E_\alpha}{kT}\right) \quad (3)$$

Table 1
Lattice parameter of the $Li_4Sn_{0.02}Si_{0.98}O_4$ and Li_4SiO_4.

Samples	$a \pm 0.107$	$b \pm 0.006$	$c \pm 0.101$	$\beta \pm 0.06$	V (Å^3)
$x = 0.00$	5.147	6.094	5.293	90.33	166.01
$x = 0.02$	5.298	6.102	5.150	90.25	166.49

Please cite this article as: S.B.R.S. Adnan, N.S. Mohamed, Solid State Ion. (2013), http://dx.doi.org/10.1016/j.ssi.2013.07.008

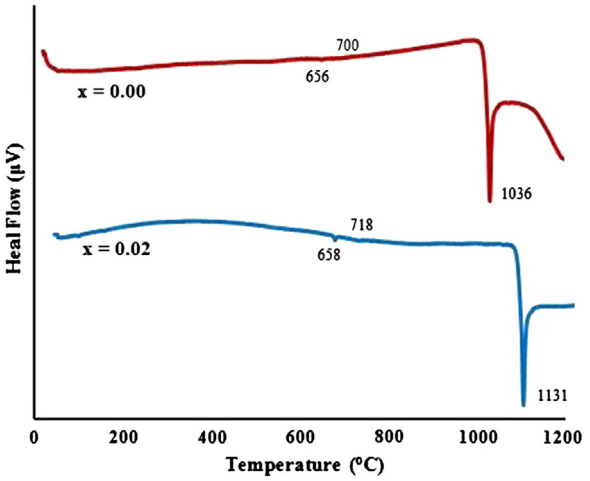

Fig. 2. DSC pattern of samples $Li_4Sn_xSi_{1-x}O_4$.

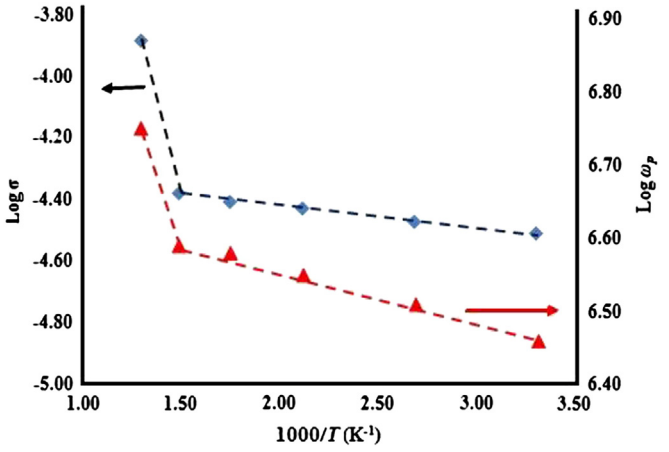

Fig. 4. Arrhenius plot of $Li_4Sn_{0.02}Si_{0.98}O_4$.

where A is the pre-exponential factor, E_α is the activation energy for conduction and k is the Boltzman constant. The conductivity of the samples increases with temperature. The compound gives a conductivity value of 3.07×10^{-5} S cm^{-1} at ambient temperature and 1.30×10^{-4} S cm^{-1} at 500 °C. The conductivity value at ambient temperature is an order of magnitude higher compared to that of the Li_4SiO_4 obtained in the author's previous work [2]. The σ-1000/T plots show a discontinuity at ~400 °C ($1000/T = 1.29$ K^{-1}), which is higher than the parents compound Li_4SiO_4 in the author's previous work who reported a discontinuity at 300 °C [12]. The change in slope of σ-1000/T plots could be due to an order–disorder transition of Si^{4+} and Sn^{4+} ions since there is no experimental evidence for a phase transition occurring in the sample upon heating at room temperature until 500 °C as shown in Fig. 2. In other words, the conductivity may be influenced at even slightest change in structure arrangement [13]. The activation energy of the sample for ($T < 400$ °C) was extracted from the slope of the Arrhenius graph is found to be 0.0930 eV. The low value of activation energy indicates high mobility of ions in the sample.

3.4. Frequency dependence conductivity

Fig. 5 depicts the frequency dependence conductivity spectra for $Li_4Sn_{0.02}Si_{0.98}O_4$, which display a low-frequency DC plateau and a high-frequency dispersion regions. The DC conductivity value determined by extrapolating the plateau on the y- axis is found to be in good agreement with the value obtained using Eq. (2). The transition from the DC to AC conductivity dispersion shifts towards higher frequency range when temperature increases. The higher frequency dispersion is due to random hopping of mobile ions.

The general formulation of the real part of the complex electrical conductivity is given by

$$\sigma'(\omega) = \sigma(0) + A\omega^{\alpha} \tag{4}$$

where $\sigma(0)$ is the DC conductivity of the sample, A is a temperature dependant parameter and α is the power law exponent, which represents the degree of interaction between the mobile ion and is less than 1. At high frequencies, the conductance spectra at different temperatures converge. This indicates that the AC conductivity is dominant in high-frequency region [11,14].

Using Almond and co-works formalism, the ionic hopping ω_p can be directly obtained from AC conductivity data since it corresponds to $\sigma(\omega) = 2\sigma(0)$ [14]. Ion hopping rates have been found to be thermally activated an can be described by

$$\omega_p = \omega_e \exp\left(\frac{-H_m}{kT}\right) \tag{5}$$

where ω_e is an effective attempt frequency that includes the entropy

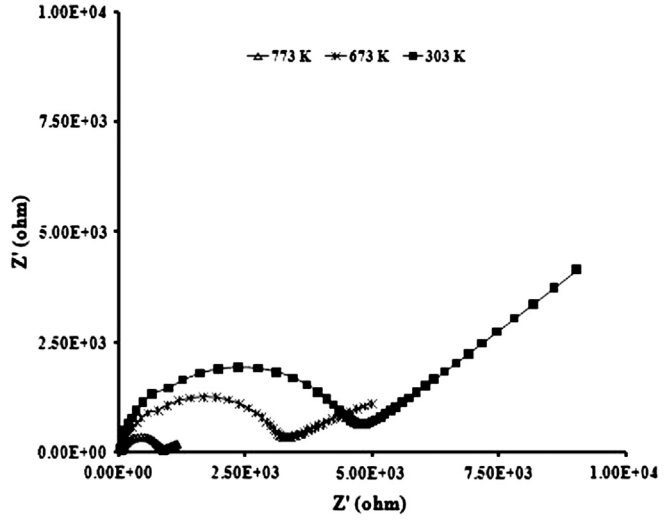

Fig. 3. Cole–cole plot of $Li_4Sn_{0.02}Si_{0.98}O_4$ at different temperatures.

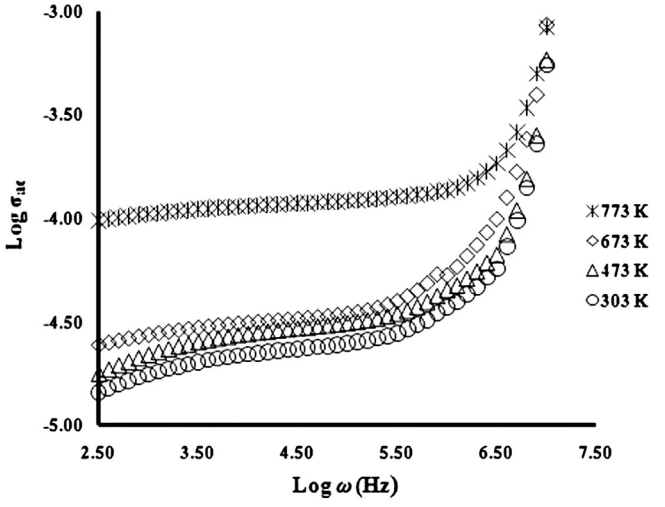

Fig. 5. Conductivity spectra of $Li_4Sn_{0.02}Si_{0.98}O_4$.

Table 2
Parameters of σ, ω_p, K, n and μ at various temperatures for $Li_4Sn_{0.02}Si_{0.98}O_4$ sample sintered at 800 °C.

T (k)	σ (S cm^{-1})	ω_p (MHz)	K (S cm^{-1} K Hz^{-1})	$n \times 10^{25}$ (cm^{-3})	μ (cm^2 V^{-1} s^{-1})
303	3.07×10^{-5}	2.31	4.03×10^{-9}	2.26	8.44×10^{-12}
473	3.70×10^{-5}	4.38	4.00×10^{-9}	2.24	1.03×10^{-11}
673	4.15×10^{-5}	6.91	4.04×10^{-9}	2.27	1.14×10^{-11}

term and H_m is the activation enthalpy for hopping or migration of ions. The character of log ω_p with temperature is demonstrated in Fig. 4. The value of H_m can be deduced from the slope of the straight line for ($T < 400$ °C) and is found to be 0.0925 eV. This value is very close to the activation energy determined above from DC conductivity measurements. The magnitude of the charge carrier concentration can be obtained using the equation [14]:

$$K = \frac{\sigma T}{\omega_p} \text{ where } K = ne^2a^2\gamma k^{-1} \tag{6}$$

Here e is the electron charge, γ is the correlation factor that is set equal to 1 and a is the jump distance between two adjacent sites for the ions to hope, which is assumed to be 3 Å for all materials [14]. n is the density of mobile ions (charge carrier), which can be calculated using Eq. (11), and k is the Boltzmann constant. Meanwhile, the ionic mobility, μ, can be calculated using equation:

$$\mu = \frac{\sigma_{DC}}{ne} \tag{7}$$

The values of σ, ω_p, K, n and μ at various temperature are tabulated in Table 2. From the table, the density of mobile ion, n, and mobile ion concentration, K, are found to be constant over the temperature range studied. This reveals that all the ions, which are responsible for the conductivity are in a mobile state, thus can be best represented by the strong electrolyte model [15]. Hence, the conduction mechanism in the investigated $Li_4Sn_{0.02}Si_{0.98}O_4$ is attributed to the hopping of charge carriers. Meanwhile, from the table the mobility of ions, μ increases with increasing temperature. As the temperature increases, the ion gains sufficient energy, and thus the number of ions that hop from one site to another increases. As such, the increase in conductivity in the samples can be attributed to the increase in ionic mobility since the density of mobile ions is constant over temperature range studied [15].

3.5. Linear sweep voltammetry

The electrochemical stability window is another important parameter of the ceramic electrolyte. The stability was evaluated by linear sweep voltammetry. Fig. 6 show the linear sweep voltammogram of the $Li_4Sn_{0.02}Si_{0.98}O_4$ ceramic electrolyte. From the figure, the anodic and cathodic limit potential was at −5.3 V and 5.3 V vs. Li/Li$^+$ respectively. This suggests a voltage stability window in the voltage range of −5.3 V to 5.3 V in the $Li_4Sn_{0.02}Si_{0.98}O_4$ electrolyte at ambient temperature.

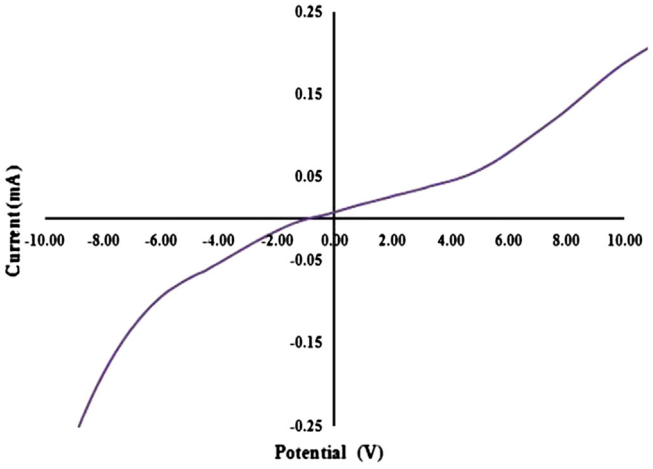

Fig. 6. Linear sweep voltammogram of the $Li_4Sn_{0.02}Si_{0.98}O_4$ at a sweep rate of 1 mV s^{-1}.

4. Conclusions

The effect of Sn doping on Li_4SiO_4 was studied by XRD, DSC and EIS. The XRD result shows that Sn^{4+} is successfully inserted into the Li_4SiO_4 structure. Meanwhile, the DSC result reveals that doping with Sn increases thermal stability of the compound. The conductivity–temperature study illustrates that the compound obeys the Arrhenius law and the activation energy of $Li_4Sn_{0.02}Si_{0.98}O_4$ sample is 0.0930 eV. The conductivity parameters such as hopping frequencies, charge carrier concentrations and mobile ion concentration prove that increase in conductivity with temperature is due to increase in ion mobility. The $Li_4Sn_{0.02}Si_{0.98}O_4$ sample shows a stable voltage window in the voltage range of −5.3 V to 5.3 V vs. Li/Li$^+$.

Acknowledgments

Financial support from the University of Malaya (research grant PV027/2012) is gratefully acknowledged.

References

[1] B. Scrosati, Electrochim. Acta 45 (2000) 2461.
[2] S.B.R.S. Adnan, N.S. Mohamed, Mater. Res. Innov. 16 (2012) 281.
[3] M. Wakihara, T. Uchida, T. Gohara, Solid State Ionics 31 (1988) 17.
[4] A.R. West, Appl. Electrochem. 3 (1973) 327.
[5] H. Taek Chung, J.G. Kim, H.G. Kim, Solid State Ionics 107 (1998) 153.
[6] T. Savitha, G. Hirankumar, M.S. Bhuvaneswari, S. Selvasekarapandian, C.S. Ramya, R. Baskaran, P.C. Angelo, J. Power Sources 157 (2006) 553.
[7] E.I. Burmakin, G.Sh. Shekhtman, Short Commun. (2009) 243.
[8] H. Yamamura, S. Takeda, K. Kakinuma, J. Chem. Soc. Jpn. 115 (2007) 264.
[9] H. Kleykamp, Thermochim. Acta 287 (1996) 191.
[10] G.W. Hollenberg, J. Nucl. Mater. 103 (1981) 591.
[11] S. Claus, H. Klaykamp, W. Smykatz-Kloss, J. Nucl. Mater. 230 (1996) 8.
[12] S.B.R.S. Adnan, N.S. Mohamed, Int. J. Electrochem. Sci. 8 (2013) 6055.
[13] M. Wakihara, T. Uchida, T. Gohara, Solid State Ionics 31 (1988) 17.
[14] L.P. Teo, M.H. Buraidah, A.F.M. Nor, S.R. Majid, Ionics 18 (2012) 655.
[15] D.P. Almond, A.R. West, Solid State Ionics 9–10 (1983) 277.

Available online at www.sciencedirect.com

ScienceDirect

Ceramics International 40 (2014) 6373–6379

CERAMICS INTERNATIONAL

www.elsevier.com/locate/ceramint

Short communication

Characterization of novel $Li_4Zr_{0.06}Si_{0.94}O_4$ and $Li_{3.94}Cr_{0.02}Zr_{0.06}Si_{0.94}O_4$ ceramic electrolytes for lithium cells

S.B.R.S. Adnan[a], N.S. Mohamed[b,*]

[a]Institute of Graduate Studies, University of Malaya, 50603 Kuala Lumpur, Malaysia
[b]Centre for Foundation Studies in Science, University of Malaya, 50603 Kuala Lumpur, Malaysia

Received 1 October 2013; received in revised form 6 November 2013; accepted 6 November 2013
Available online 28 November 2013

Abstract

Two ceramic electrolytes, $Li_4Zr_{0.06}Si_{0.94}O_4$ and $Li_{3.94}Cr_{0.02}Zr_{0.06}Si_{0.94}O_4$, were prepared by a citrate sol–gel method. The structure, morphology, particle size, conductivity and electrochemical property were investigated. Both electrolyte materials had quite similar lattice parameters. The $Li_{3.94}Cr_{0.02}Zr_{0.06}Si_{0.94}O_4$ exhibited higher total conductivity value of 1.83×10^{-4} S cm^{-1} at an ambient temperature and 1.13×10^{-3} S cm^{-1} at 500 °C which are an order of magnitude higher than those of $Li_4Zr_{0.06}Si_{0.94}O_4$. Ionic transference number corresponding to Li^+ ion transport was 0.92 for $Li_4Zr_{0.06}Si_{0.94}O_4$ and increased to 0.97 for $Li_{3.94}Cr_{0.02}Zr_{0.06}Si_{0.94}O_4$. The $Li_{3.94}Cr_{0.02}Zr_{0.06}Si_{0.94}O_4$ sample showed a maximum discharge capacity of 103 mAh g^{-1} at the rate of 0.05 C in a potential range of 3.0–4.2 V.

Keywords: Arrhenius; Ceramic electrolyte; Conductivity; Lithium orthosilicate; Solid electrolyte

1. Introduction

In the rapid development of science and technology, the demands for lithium ion secondary batteries in laptops, mobile phones, digital cameras and electric vehicles, are increasing. The question of safety is the most important issue for the development of those appliances. Traditional liquid electrolyte with high conductivity has many disadvantages, such as leakage and spillage, lack of mechanical integrity and narrow range of operating temperatures [1]. Therefore many efforts have been dedicated to the development of all solid-state lithium ion secondary battery comprising solid electrolyte lithium ion. Inorganic solid electrolytes are considered to be effective in improving the safety of lithium ion batteries. Among solid electrolytes, ceramic electrolyte forms an important class of materials due to large electrochemical stability window, good thermal stability, important safety asset, absence of leakage, high resistance to shock and vibrations, superior incombustibility and high energy density [2].

In search of new solid lithium-based electrolyte, Li_4SiO_4 is one of the promising members in Lisicon (Lithium Super Ionic Conductor) group. The basic structure of Li_4SiO_4 is monoclinic and composed of hexagonal close packed oxygen ion arrays which is iso-structural with γ-Li_3PO_4. One-eighth of the tetrahedral vacancies in this packing are occupied by silicon cations and three-eighth of the vacancies are occupied by the lithium. This means that half of the tetrahedral sites are occupied by the cations. Silicon is tetrahedrally co-ordinated to oxygen, SiO_4 and is isolated but connected by sharing edges. The SiO_4 and LiO_4 tetrahedrals share oxygen vertices to form a loose three-dimensional framework favorable for ion transport. The lithium ion diffusion is expected to occur through tetrahedral site and interstitial octahedral site pathway [3–7]. Partial substitution causes a distortion of the hexagonal close packed (hcp) sub lattice generating 'tetrahedral packed (tp)' array and is a mechanism which allows additional cations to be accommodated on tetrahedral co-ordinated sites. Half of the tetrahedral and octahedral sites within the hcp sublattice remain undistorted but the remainder are replaced by a larger number of sites with irregular octahedrally and tetrahedrally co-ordinated environments. This is especially advantageous for Li^+ which, owing to its small size, can be readily

*Corresponding author.
E-mail addresses: syed_bahari@yahoo.com (S.B.R.S. Adnan), nsabirin@um.edu.my (N.S. Mohamed).

0272-8842/$ - see front matter © 2013 Elsevier Ltd and Techna Group S.r.l. All rights reserved.
http://dx.doi.org/10.1016/j.ceramint.2013.11.031

accommodated in the distorted tetrahedrally and octahedrally co-ordinated. Thus, the lithium ion distribution between tetrahedral site and interstitial octahedral site is an important factor that affects their ionic conduction [8].

The partial substitutions of silicon ion by larger sized cation (Sn^{4+}) has already been proven and can enhance the conductivity of the Li_4SiO_4 compound by one order of magnitude [9]. The size of Sn^{4+} is larger than Si^{4+}. This increases the size of Li^+ migration channel which leads to an increase in ion mobility. However, study on Zr^{4+} (0.080 nm) doped into Li_4SiO_4 has never been reported in the literature. Apart of the larger size than Sn^{4+} (0.069 nm), lower electronegativity in Zr^{4+} (1.72) compared to Sn^{4+} (1.96) is expected to increase the average free path migration of lithium ions due to its lower attraction to lithium ion [10]. Meanwhile, the partial substitution of Cr^{3+} into Li_4SiO_4 structure has also been proven to be able to enhance the conductivity of the Li_4SiO_4 compound by an order of magnitude. The substitution of Cr^{3+} by $3Li^+$ in tetrahedral site creates two vacancy sites in the crystal and any lithium ion in the immediate vicinity can jump to the vacant sites. This leaves the previous site of the ion vacant and available to host another ion. This results in the transport of ions across the solid giving rise to conductivity [11].

In this work, a simple citrate sol–gel method was employed to synthesize partial substituted Li_4SiO_4 using Zr^{4+} ion and double partial substituted Li_4SiO_4 using Cr^{3+} and Zr^{4+} ions. The effects of Zr^{4+} which can enlarge the migration channel and Cr^{3+} which is able to create vacancy sites are expected to increase the conductivity of the parent compound. The properties of the synthesized $Li_4Zr_{0.06}Si_{0.94}O_4$ and $Li_{3.94}Cr_{0.02}Zr_{0.06}Si_{0.94}O_4$ were investigated using X-ray diffraction (XRD), Scanning electron microscope (SEM), energy dispersive X-ray (EDX), particle size analysis, impedance spectroscopy and lithium transference number measurement. Charge–discharge of the cell fabricated using selected compound was also done to study the potential of the compound to be used as electrolyte in all solid state cells.

2. Experimental procedure

2.1. Synthesis of $Li_{3.94}Cr_{0.02}Zr_{0.06}Si_{0.94}O_4$ and $Li_4Zr_{0.06}Si_{0.94}O_4$

For this study, the $Li_{3.94}Cr_{0.02}Zr_{0.06}Si_{0.94}O_4$ and $Li_4Zr_{0.06}Si_{0.94}O_4$ compounds were prepared via the citrate sol–gel method. For preparation of $Li_{3.94}Cr_{0.02}Zr_{0.06}Si_{0.94}O_4$ sample, stoichiometrics of lithium acetate, zirconium (IV) acetate hydroxide and chromium (III) acetate were first dissolved in distilled water with molar ratio of Li:Cr:Zr:Si fixed according to formula $Li_{4-3x}Cr_xZr_ySi_{1-y}O_4$ with $x=0.02$ and $y=0.06$. In the case of $Li_4Zr_{0.06}Si_{0.94}O_4$, lithium acetate and zirconium (IV) acetate hydroxide were employed. Solution of citric acid was mixed together to the previously prepared solutions under magnetic stirring. The solutions were transferred into reflux systems and continuously stirred until homogeneous solutions were formed. Solution of tetraethyl orthosilicate was later added to these homogeneous solutions. After stirring for 12 h, the solutions were taken out and then vaporized for about 2 h under magnetic stirring at 75 °C. The resulting sticky wet gels formed were dried in an oven at 150 °C for 24 h. The obtained powders were ball milled for 24 h using a Fritsch Pulverisettle-7 ball mill operated at 500 rpm. The powders were sintered at temperature 800 °C for 12 h and later pressed using a Specac pellet press to form pellets with diameter and thickness of 13 mm and 2.0 mm respectively.

2.2. Characterization techniques

X-ray diffraction (XRD) was done in order to elucidate structural information of the sample. The sintered ceramic powders were characterized using a Bruker AXS D8 Advance X-ray Diffraction spectrometer with Cu-K^{α} radiation of wavelength of 1.5406 Å. The patterns were recorded in the 2θ range between 10° and 45° at the rate of 0.016° in step width. The lattice parameters of the compound were calculated using the formulae [12]

$$\frac{1}{d^2}=\frac{h^2}{a^2}+\frac{k^2}{b^2}+\frac{l^2}{c^2} \text{ and } d=\frac{\lambda}{2\ \sin\ \theta} \quad (1)$$

where d is the distance between crystal planes of (hkl), λ is the X-ray wavelength, θ is the diffraction angle of crystal plane (hkl), hkl is the crystal index, and a, b and c are the lattice parameters. The morphologies of the sample powders were analyzed by SEM and EDX which were carried out using Scanning electron microscope spectrometer (Zeiss-Evo MA10). The particle size information was obtained using FRITSCH-Analysette 22 NanoTec laser particle sizer. The ceramic electrical properties were determined by ac impedance spectroscopy using Solatron 1260 impedance analyzer over a frequency range from 1 to 10^6 Hz. An applied voltage was fixed at 200 mV. The total conductivity, σ_t (bulk conductivity, σ_b+grain boundary conductivity, σ_{gb}) which represent the direct current (d.c) conductivity in the ceramic sample was calculated using equation [13]:

$$\frac{1}{\sigma_t}=\frac{1}{\sigma_b}+\frac{1}{\sigma_{gb}} \quad (2)$$

where

$$\sigma_b=\frac{d}{AR_b} \text{ and } \sigma_{gb}=\frac{d}{AR_{gb}}$$

In these equations, d is the sample thickness, A is the cross-sectional area of sample, R_b is the bulk resistance and R_{gb} is the grain boundary resistance. Lithium transference number measurement was carried out using the Bruce and Vincent method [14,15] in order to determine the actual type of charge carriers. The samples were sandwiched between lithium metal electrodes which served as non-blocking electrodes that only allowed Li^+ ions to transfer. The lithium transference number (τ_{Li}^{+}) was calculated using the equation:

$$\tau_{Li^+}=\frac{I_{ss}(\Delta V-I_oR_o)}{I_o(\Delta V-I_{ss}R_{ss})} \quad (3)$$

In Eq. (3), I_o is the initial current ($t=0$), I_{ss} is the steady state current, R_o and R_{ss} are the initial resistances of the passive layer, before polarization and after polarization respectively. ΔV is the applied voltage bias ($\Delta V=0.5$ V).

Electrochemical cells were constructed to investigate the cell performances using the $Li_{3.94}Cr_{0.02}Zr_{0.06}Si_{0.94}O_4$ solid electrolyte. The positive electrode (cathode) material was a mixture of $LiCoO_2$ as active material, acetylene black as conducting agent and polytetrafluoroethylene as a binder with the ratio of 80:10:10. The electrolyte powder was pressed into a two layer pellet together with the electrode of a diameter of 13 mm and thickness of 1 mm. The cell was assembled in a high purity argon-filled glove box using lithium foil as anode. The charge–discharge study was done using Wonatech ZIVE MP2 multichannel electrochemical workstation. The charge–discharge rate was performed in between 3.0 V and 4.2 V versus Li/Li^+. To compare its charge–discharge rate capability of the cell, the cell was cycled under different current intensities at 0.05 C (5 mA g^{-1}), 0.1 C (7 mA g^{-1}) and 0.2 C (10 mA g^{-1}) charge–discharge rates. Five cycles were performed for every rate.

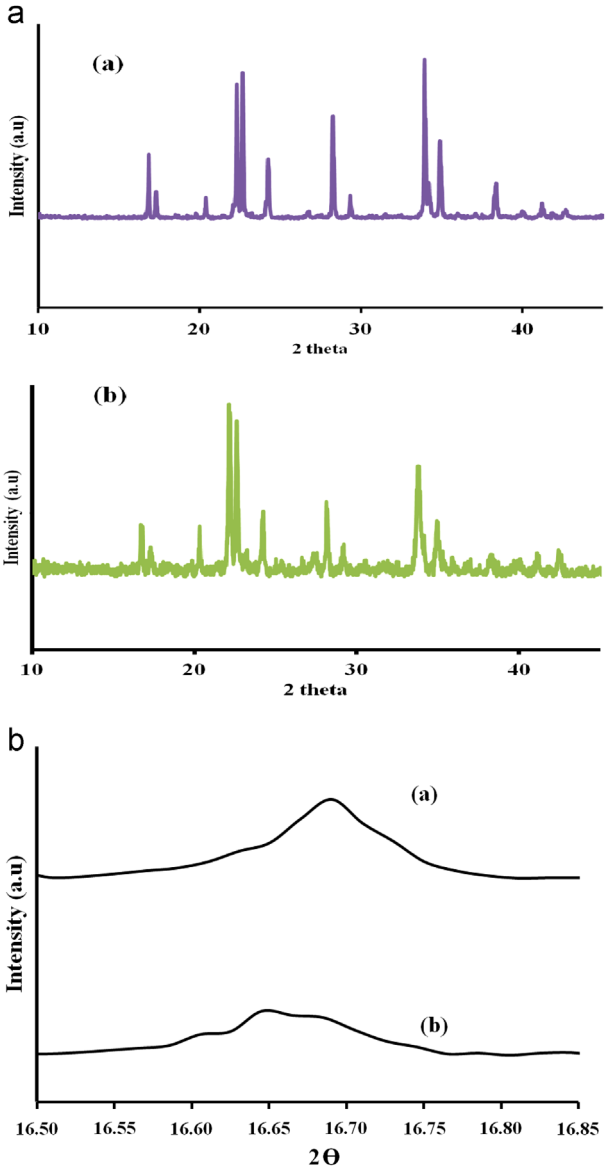

Fig. 1. (a): XRD pattern of the prepared (a) $Li_4Zr_{0.06}Si_{0.94}O_4$ and (b) $Li_{3.94}Cr_{0.02}Zr_{0.06}Si_{0.94}O_4$ samples. (b): XRD pattern of the prepared (a) $Li_4Zr_{0.06}Si_{0.94}O_4$ and (b) $Li_{3.94}Cr_{0.02}Zr_{0.06}Si_{0.94}O_4$ samples in 2Θ range from 16.50° to 16.85°.

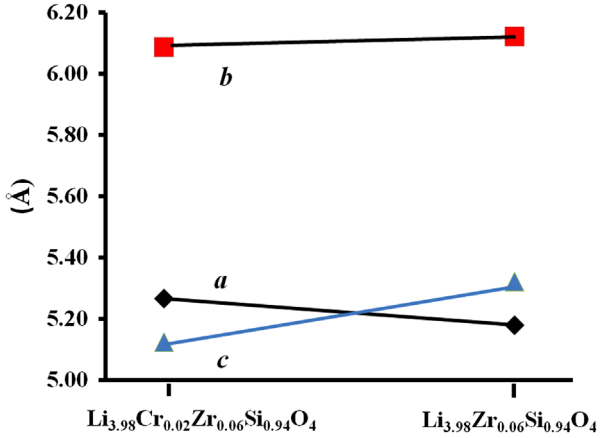

Fig. 2. Lattice parameters of $Li_4Zr_{0.06}Si_{0.94}O_4$ and $Li_{3.94}Cr_{0.02}Zr_{0.06}Si_{0.94}O_4$ samples.

3. Result and discussion

3.1. Phase identifications

The XRD patterns of the prepared $Li_{3.94}Cr_{0.02}Zr_{0.06}Si_{0.94}O_4$ and $Li_4Zr_{0.06}Si_{0.94}O_4$ are shown in Fig. 1(a). Both samples can be indexed to monoclinic unit cell in space group $P2_{1/m}$ which is iso-structural with γ-Li_3PO_4. The doping does not destroy the lattice structure of Li_4SiO_4 because of the low doping concentration. Both XRD main peaks at 2Θ range 16.50–16.85° (Fig.1(b)) shift to the lower diffraction angle compared to undoped Li_4SiO_4 in [11] indicating that Cr^{3+} and Zr^{4+} ions are in the Li4SiO4 structure rather than forming impurities. However, $Li_{3.94}Cr_{0.02}Zr_{0.06}Si_{0.94}O_4$ exhibits broader peaks than $Li_4Zr_{0.06}Si_{0.94}O_4$ indicating that it has of smaller size.

The lattice parameters (a, b and c) and unit cell volume, V of both samples were calculated using Eq. (1) and the results are shown in Fig. 2. Both samples have quite similar lattice parameters which are consistent with the parent compound, Li_4SiO_4. The value of V for $Li_4Zr_{0.06}Si_{0.94}O_4$ increases from 1.27 $Å^3$ to 167.28 $Å^3$ compared to that of the parent compound (166.01 $Å^3$) [3,9,11]. The increase in the unit cell volume is mostly related to the Zr^{4+} insertion into Li_4SiO_4 structure which can be attributed to the larger atomic size of Zr^{4+} than that of Si^{4+}. Meanwhile the value of V for $Li_{3.94}Cr_{0.02}Zr_{0.06}Si_{0.94}O_4$ decreases from 1.82 $Å^3$ to 164.19 $Å^3$ compared to that of the parent compound. This shows that the increase in the volume due to substitution of Si^{4+} with Zr^{4+} is smaller than the volume decrease due to substitution of $3Li^+$ with Cr^{3+}. So, the lattice change in $Li_{3.94}Cr_{0.02}Zr_{0.06}Si_{0.94}O_4$ could be mainly caused by the Cr^{+3}doping.

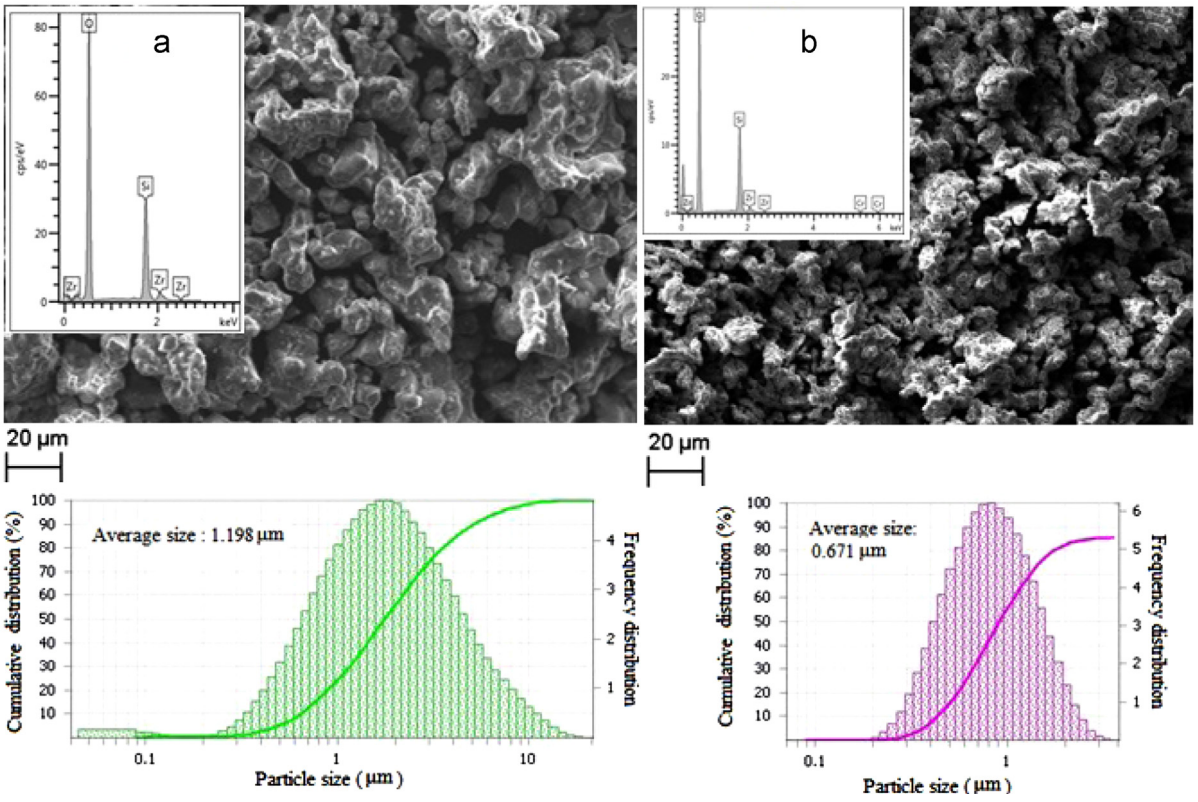

Fig. 3. SEM micrograph, EDX analysis and particle size distribution of (a) $Li_4Zr_{0.06}Si_{0.94}O_4$ (b) $Li_{3.94}Cr_{0.02}Zr_{0.06}Si_{0.94}O_4$ samples.

3.2. SEM, EDX and particle size distribution

The morphology of the $Li_{3.94}Cr_{0.02}Zr_{0.06}Si_{0.94}O_4$ and $Li_4Zr_{0.06}Si_{0.94}O_4$ samples was observed by SEM while their particle size was analyzed using laser particle sizer. The SEM images are shown in Fig. 3. From the figure, it is clear that the particles in both samples are smaller compared to those observed in the parent compound [11]. The average particle size for $Li_4Zr_{0.06}Si_{0.94}O_4$ and $Li_{3.94}Cr_{0.02}Zr_{0.06}Si_{0.94}O_4$ are 1.198 μm and 0.671 μm respectively while the average particle size in the Li_4SiO_4 parent compound is 11.8 μm. EDX analysis was also conducted to examine the elemental composition of both samples and the results are shown as insets in Fig. 3(a) and (b). The atomic ratios of Cr: Zr:Si:O and Zr:Si:O are determined to be 0.018:0.055:0.945:4.000 and 0.063:0.93 5:4.003 respectively. As such, the chemical compositions of the prepared $Li_{3.94}Cr_{0.02}Zr_{0.06}Si_{0.94}O_4$ and $Li_4Zr_{0.06}Si_{0.94}O_4$ samples can be identified as $Li_{3.98}Cr_{0.018}Zr_{0.055}Si_{0.945}O_4$ and $Li_4Zr_{0.063}Si_{0.935}O_{4.003}$, which are very close to the designed compositions. The EDX could not detected the presence of lithium because of its light weight.

3.3. Impedance measurement

Complex impedance plots obtained for $Li_4Zr_{0.06}Si_{0.94}O_4$ and $Li_{3.94}Cr_{0.02}Zr_{0.06}Si_{0.94}O_4$ at room temperature and 500 °C are displayed in Fig. 4. As can be seen from the figure, the Cole–Cole plots of the $Li_4Zr_{0.06}Si_{0.94}O_4$ sample reveal overlapped semicircles which are due to bulk resistance, R_b and grain boundary resistance, R_{gb} respectively. However, for the $Li_{3.94}Cr_{0.02}Zr_{0.06}Si_{0.94}O_4$ sample, the R_{gb} value is approximate to 0. This is because of the high ion mobility in the sample which minimizes the resistance from grain boundary. The total conductivity, σ_T which represents the DC conductivity was calculated using Eq. (2). As the temperature increases, the total resistance, $R_t = (R_b + R_{gb})$ value shifts towards lower values indicating increase in conductivity.

The plots of temperature dependence of conductivity for both $Li_4Zr_{0.06}Si_{0.94}O_4$ and $Li_{3.94}Cr_{0.02}Zr_{0.06}Si_{0.94}O_4$ samples are shown in Fig. 5. The activation energy for thermally activated hopping process was obtained by fitting the dc conductivity data with Arrhenius equation:

$$\sigma_t T = A \exp\left(\frac{-E_\alpha}{kT}\right) \quad (4)$$

where A is the pre-exponential factor, E_α is the activation energy for conduction and k is the Boltzman constant. The conductivity of both samples increases with increase in temperature. The $Li_{3.94}Cr_{0.02}Zr_{0.06}Si_{0.94}O_4$ compound exhibits total conductivity value of 1.83×10^{-4} S cm^{-1} at ambient temperature and 1.13×10^{-3} S cm^{-1} at 500 °C. Meanwhile, the $Li_4Zr_{0.06}Si_{0.94}O_4$ compound shows total conductivity value of 3.41×10^{-5} S cm^{-1} at ambient temperature and 1.83×10^{-4} S cm^{-1} at 500 °C. Both σ-1000/T plots show a discontinuity at ~400 °C (1000/T = 1.29 K^{-1}) which is higher than that observed for the parents compound Li_4SiO_4

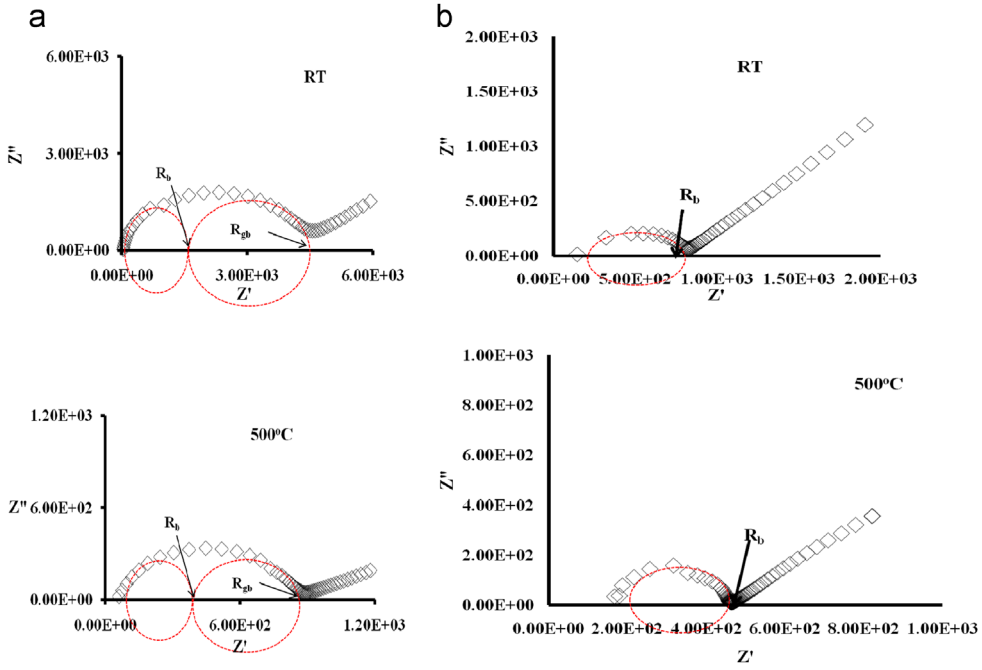

Fig. 4. Impedance spectra of (a) $Li_4Zr_{0.06}Si_{0.94}O_4$ and (b) $Li_{3.94}Cr_{0.02}Zr_{0.06}Si_{0.94}O_4$ samples at room temperature and 500 °C.

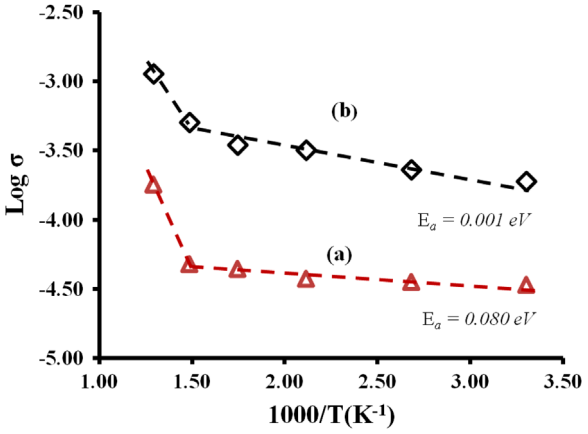

Fig. 5. Temperature dependence of d.c. conductivity for (a) $Li_4Zr_{0.06}Si_{0.94}O_4$ and (b) $Li_{3.94}Cr_{0.02}Zr_{0.06}Si_{0.94}O_4$ sample.

(~300 °C) [11] but in agreement with the result obtained for $Li_4Sn_{0.02}Si_{0.98}O_4$ compound reported earlier by the authors [9]. The change in the slope of σ-1000/T plots could be due to the change from extrinsic to intrinsic regime [3,7] which change the structure arrangement during the order-disorder process of transition between Si^{4+} with Zr^{4+} and Li^+ with Cr^{3+}. This is based on the authors' previous work which indicated no phase transition occurring in the sample upon heating up to 500 °C [9,16]. It is also noted that the activation energy values of the sample for $T < 400$ °C, extracted from the slope of the Arrhenius graph, are lower compared to that of the parent compound reported in [16]. The lower values of activation energy indicates higher mobility of ions in the samples. This could be due to the increase of Li^+ migration channel size and amount of vacancy site.

3.4. Lithium transference number

Depicted in Fig. 6 are the current versus time plots of both $Li/Li_4Zr_{0.06}Si_{0.94}O_4/Li$ and $Li/Li_{3.94}Cr_{0.02}Zr_{0.06}Si_{0.94}O_4/Li$ cells. The initial and final steady currents in $Li/Li_4Zr_{0.06}Si_{0.94}O_4/Li$ cell are $I_o = 1.78$ μA and $I_{ss} = 1.64$ μA respectively. The initial and final steady currents in $Li/Li_{3.94}Cr_{0.02}Zr_{0.06}Si_{0.94}O_4/Li$ cell are $I_o = 1.61$ μA and $I_{ss} = 1.545$ μA respectively. The impedance responses prior and after polarization for the $Li/Li_4Zr_{0.06}Si_{0.94}O_4/Li$ cell are $R_o = 17646\ \Omega$ and $R_{ss} = 17778\ \Omega$ respectively. Meanwhile for the $Li/Li_{3.94}Cr_{0.02}Zr_{0.06}Si_{0.94}O_4/Li$ cell, the impedance responses prior and after polarization are $R_o = 870\ \Omega$ and $R_{ss} = 1177\ \Omega$ respectively.

Calculation of Li^+ transference number using Eq. (3) gives lithium transference number value of 0.92 for the $Li_4Zr_{0.06}Si_{0.94}O_4$ compound and 0.97 for the $Li_{3.94}Cr_{0.02}Zr_{0.06}Si_{0.94}O_4$ compound. These values show that double substitutions lead greater Li^+ ions transport number more than substitutions using single ion.

3.5. Electrochemical cell test

Fig. 7 illustrates charge–discharge voltage profile for the cell fabricated using $Li_{3.94}Cr_{0.02}Zr_{0.06}Si_{0.94}O_4$ samples at the charge–discharge rate of 0.05 C in a potential range of 3.0–4.2 V. The charge plateau of the samples is about 4.15 V. Meanwhile the discharge plateau of the cell is about 4.0 V. The difference between the charge and discharge plateau potentials is related to the polarization of the cell system. The smaller the difference, the less the polarization [17]. Therefore, the polarization of the $Li_{3.94}Cr_{0.02}Zr_{0.06}Si_{0.94}O_4$ based cell is small

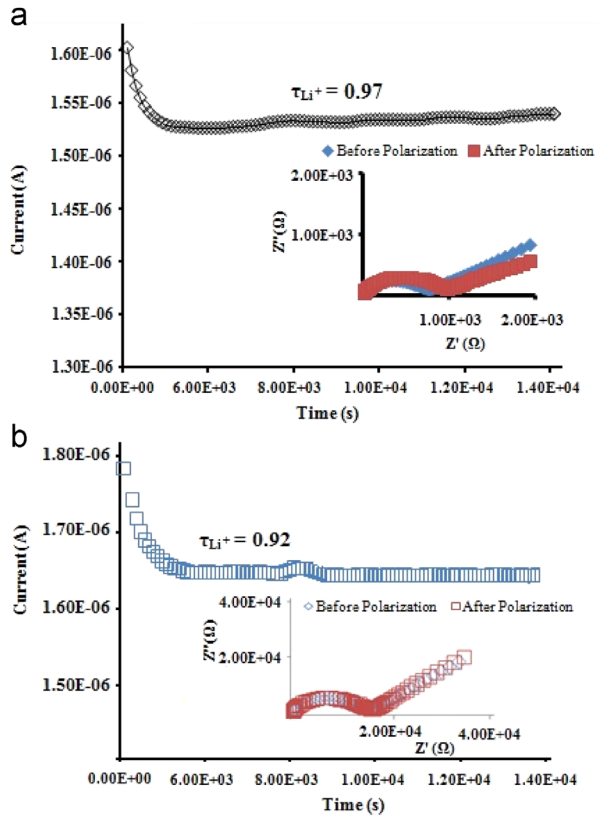

Fig. 6. Current versus time plots for (a) $Li_{3.94}Cr_{0.02}Zr_{0.06}Si_{0.94}O_4$ sample and (b) $Li_4Zr_{0.06}Si_{0.94}O_4$ sample. Both impedance responses of the sample before and after polarization are shown in insets.

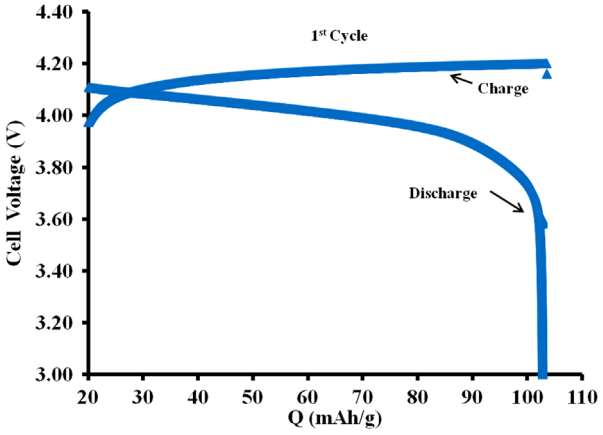

Fig. 7. Charge and discharge curves of the prepared $Li_{3.94}Cr_{0.02}Zr_{0.06}Si_{0.94}O_4$ sample.

since only small difference between charge and discharge plateau is observed. Cyclic charge–discharge performance profiles of the cell at 0.05 C, 0.1 C and 0.2 C are shown in Fig. 8. The charge–discharge capacity of the cell decreases with increase in C rate. This indicates that the cycling performance of the cell depends on the current intensity used in the electrochemical tests. The maximum discharge capacity measured at the rate of 0.05 C, 0.1 C and 0.2 C are 103 mAh g^{-1}, 85 mAh g^{-1} and 53 mAh g^{-1} respectively.

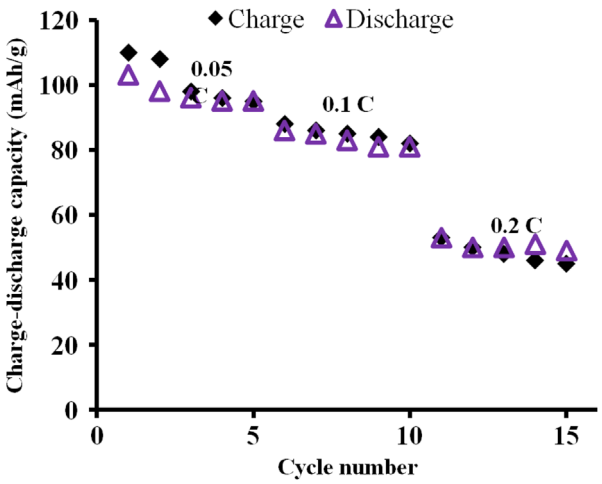

Fig. 8. Cyclic performance of the cell prepared using $Li_{3.94}Cr_{0.02}Zr_{0.06}Si_{0.94}O_4$ sample.

4. Conclusions

The $Li_4Zr_{0.06}Si_{0.94}O_4$ and $Li_{3.94}Cr_{0.02}Zr_{0.06}Si_{0.94}O_4$ ceramic electrolytes were successfully synthesized via the citrate sol–gel method. The conductivity–temperature study illustrated that both compounds obey the Arrhenius law. The conductivity of $Li_4Zr_{0.06}Si_{0.94}O_4$ compound was an order of magnitude higher than that of the Li_4SiO_4 parent compound while the $Li_{3.94}Cr_{0.02}Zr_{0.06}Si_{0.94}O_4$ compound exhibited conductivity value of two orders of magnitude higher than the conductivity of parent compound. Both samples showed high value of lithium transference number which is 0.92 for $Li_4Zr_{0.06}Si_{0.94}O_4$ compound and 0.97 for $Li_{3.94}Cr_{0.02}Zr_{0.06}Si_{0.94}O_4$ compound. This demonstrated that the majority charge carrier in the samples was Li^+ ion. The $Li_{3.94}Cr_{0.02}Zr_{0.06}Si_{0.94}O_4$ ceramic sample has been proven to be applicable as an electrolyte in electrochemical cell.

Acknowledgment

Financial support from the University of Malaya (research grant PV027/2012) is gratefully acknowledged.

References

[1] P. Ferloni, A. Magistris, New materials for solid state electrochemistry, J.Phys. IV 4 (1994) C1.3–C1.15.
[2] B. Scrosati, Recent advances in lithium ion battery materials, Electrochim. Acta 45 (2000) 2461–2466.
[3] S.B.R.S Adnan, N.S. Mohamed, Citrate sol–gel synthesised Li_4SiO_4: conductivity and dielectric behaviour, Mater. Res. Innovations 16 (2012) 281–285.
[4] J.G. Kamphorst, E.E. Hellstrom, Fast Li ionic conduction in solid solutions of the system Li_4GeO_4–Li_2ZnGeO_4–Li_3PO_4, Solid State Ionic 1 (1980) 187–197.
[5] D. Tranqui, R.D. Shannon, H.-Y. Chen, Crystal structure of ordered Li_4SiO_4, Acta Cryst. B 35 (1979) 2479–2487.
[6] R.D. Shannon, B.E. Taylor, A.D. English, T. Berzins, New Li solid electrolytes, Electrochem. Acta 22 (1977) 783–796.

[7] A.R. West, Ionic conductivity of oxide based on Li_4SiO_4, J. Appl. Electrochem. 3 (1973) 325–335.
[8] Stephan Hull, Superionics: crystal structure and conduction progress, Rep. Prog. Phys. 67 (2004) 1233–1314.
[9] S.B.R.S Adnan, N.S. Mohamed, Effect of Sn substitution on the properties of Li_4SiO_4 ceramic electrolyte, Solid State Ionics (2013)http://dx.doi.org/10.1016/j.ssi.2013.07.008.
[10] E.I. Burmakin, G.Sh. Shekhtman, Lithium-conducting solid electrolyte of Li_4GeO_4–Li_3PO_4 system with addition of zirconium ions, Russion J. Electrochem. 46 (2010) 234–246.
[11] S.B.R.S Adnan, N.S. Mohamed, The properties of novel $Li_{4-3x}Cr_xSiO_4$ ceramic electrolyte, Ceram. Int. (2013)http://dx.doi.org/10.1016/j.ceramint..2013.08.136.
[12] A.R. West, Solid State Chemistry and its Application, John Wiley and Son Ltd., New York, 1984, p. 478.
[13] Shiqiang (Rob) Hui, Justin Roller, Sing Yick, Xinge Zhang, Cyrille Decès-Petit, Yongsong Xie, Radenka Maric, Dave Ghosh, A brief review of the ionic conductivity enhancement for selected oxide electrolytes, J. Power Sources 172 (2007) 493–502.
[14] P.G. Bruce, J. Evans, C.A. Vincent, Conductivity and transference number measurements on polymer electrolytes, Solid State Ionics 28–30 (1998) 918–922.
[15] M. Riley, S. Peter, Fedkiw, S.A. Khan, Transport properties of lithium hectorite-based composite electrolytes, Electrochem. Soc. 149 (2002) A667–A674.
[16] S.B.R.S Adnan, N.S. Mohamed, Structural, thermal and electrical properties of Li_{4-2x} Zn_xSiO_4 ceramic electrolyte prepared by citrate sol gel technique, Int. J. Electrochem. Sci. 8 (2013) 6055–6067.
[17] Xiaobing Huang, Xing Li, Haiyan Wang, Zhonglai Pan, Meizhen Qu, Zuolong Yu, Synthesis and electrochemical performance of Li_2FeSiO_4/C as cathode material for lithium batteries, Solid State Ionics 181 (2010) 1451–1455.

Available online at www.sciencedirect.com

ScienceDirect

Ceramics International ▮ (▮▮▮▮) ▮▮▮–▮▮▮

CERAMICS INTERNATIONAL

www.elsevier.com/locate/ceramint

Short communication

AC conductivity and dielectric studies of modified Li_4SiO_4 ceramic electrolytes

S.B.R.S. Adnan[a], N.S. Mohamed[b,*]

[a]*Institute of Graduate Studies, University of Malaya, 50603 Kuala Lumpur, Malaysia*
[b]*Centre for Foundation Studies in Science, University of Malaya, 50603 Kuala Lumpur, Malaysia*

Received 20 February 2014; received in revised form 26 March 2014; accepted 26 March 2014

Abstract

AC conductivity of modified Li_4SiO_4 ($Li_{3.94}Cr_{0.02}SiO_4$, $Li_4Zr_{0.06}Si_{0.94}O_4$ and $Li_{3.94}Cr_{0.02}Zr_{0.06}Si_{0.94}O_4$) was measured as a function of frequency in the range between 1 Hz to 1000 Hz and in temperature range between 303 K to 773 K. The frequency dependence of conductivity for these ceramic electrolytes followed the universal power law variation, $\sigma_{AC}(\omega)=\sigma_o+A\omega^s$. The plots of pre-exponent s versus temperature of all systems suggested that the conduction mechanism in all systems can be described using correlated barrier hopping model. Meanwhile, the charge carrier concentration and mobile ion concentration in all samples was found to be constant over the temperature range of this study while mobility of ion increased with temperature implying that the increase in conductivity with temperature was due to the increase in ion mobility. The experimental results also revealed that the dielectric constant and dielectric loss decreased with frequency. The double substituted sample, $Li_{3.94}Cr_{0.02}Zr_{0.06}Si_{0.94}O_4$ showed the highest dielectric constant and dielectric loss at low frequencies. The increase in temperature also increased the dielectric constant and dielectric loss values in all samples.

Keywords: AC conductivity; Ceramic electrolyte; Lithium Orthosilicate; Solid electrolyte

1. Introduction

Lisicon-type lithium orthosilicate, Li_4SiO_4 offers several advantages over other types of Li^+ ion conductors. This compound can be easily synthesized, less expensive to produce, safe, stable in air, no reaction with lithium metal, low self-discharge, and maintains its conductivity (constant conductivity) with time [1]. This compound also shows favorable characteristics for practical application due to its superior incombustibility, high energy density and wide electrochemical stability window[2]. Stoichiometric Li_4SiO_4, which is a poor conductor ($\sigma_{100\,^\circ C}=10^{-6}$ S cm^{-1}) has been modified in order to enhance its conductivity. The modification was done by partial substitution using isovalent or aliovalent cation. The partial substitution of Si^{4+} with Zr^{4+} ($Li_4Zr_{0.06}Si_{0.94}O_4$) can enlarge the Li^+ migration channel while the substitution of $3Li^+$ with Cr^{3+} ($Li_{3.94}Cr_{0.02}SiO_4$) is able to create vacancy sites in Li_4SiO_4 structure. The studies on these partial substitutions have been recently reported by the authors [3,4]. In fact, the double partial substituted Li_4SiO_4 using both Cr^{3+} and Zr^{4+} ions ($Li_{3.94}Cr_{0.02}Zr_{0.06}Si_{0.94}O_4$) has also been reported [4]. However, the reports focus only on the structural and direct current (DC) conductivity of the compounds.

In this article, the AC conductivity and dielectric behaviour of the modified Li_4SiO_4 ($Li_{3.94}Cr_{0.02}SiO_4$, $Li_4Zr_{0.06}Si_{0.94}O_4$ and $Li_{3.94}Cr_{0.02}Zr_{0.06}Si_{0.94}O_4$) are presented. Based on Jonscher's universal power law, the conduction mechanism in all samples was analyzed. Meanwhile, the Almond and West formalism was used to investigate the contribution of the charge carrier concentration and charge carrier mobility on the partially substituted Li_4SiO_4.

*Corresponding author.
E-mail addresses: syed_bahari@yahoo.com (S.B.R.S. Adnan), nsabirin@um.edu.my (N.S. Mohamed).

http://dx.doi.org/10.1016/j.ceramint.2014.03.149
0272-8842/

Please cite this article as: S.B.R.S. Adnan, N.S. Mohamed, AC conductivity and dielectric studies of modified Li_4SiO_4 ceramic electrolytes, Ceramics International (2014), http://dx.doi.org/10.1016/j.ceramint.2014.03.149

2. Experimental procedure

2.1. Synthesis of $Li_{3.94}Cr_{0.02}Zr_{0.06}Si_{0.94}O_4$, $Li_{3.94}Cr_{0.02}SiO_4$ and $Li_4Zr_{0.06}Si_{0.94}O_4$

All of the compounds investigated in this work were prepared via citrate sol gel method. For preparation of $Li_{3.94}Cr_{0.02}Zr_{0.06}Si_{0.94}O_4$ sample, appropriate amounts of lithium acetate, zirconium(IV) acetate hydroxide and chromium(III) acetate were first dissolved in distilled water. In the case of $Li_{3.94}Cr_{0.02}SiO_4$ and $Li_4Zr_{0.06}Si_{0.94}O_4$, lithium acetate and chromium(III) acetate and lithium acetate and zirconium(IV) acetate hydroxide were employed, respectively. Solution of citric acid was mixed together to the previously prepared solutions under magnetic stirring. The solutions were later transferred into reflux systems and continuously stirred until homogeneous solutions were formed. Solutions of tetraethyl orthosilicate was then added to these homogeneous solutions. After stirring for 12 h, the solutions were taken out and vaporized for about 2 h under magnetic stirring at 75 °C. The resulting sticky wet gels formed were dried in an oven at 150 °C for 24 h. The obtained powders were ball milled for 24 h using a Fritsch Pulverisette-7 ball mill operated at 500 rpm. The powders were sintered at temperature of 800 °C for 12 h and later pressed using a Specac pellet press to form pellets with diameter and thickness of 13 mm and 2.0 mm.

2.2. Characterization techniques

AC conductivity has been evaluated from dielectric data in accordance with the relation:

$$\sigma_{AC} = \omega\varepsilon_o\varepsilon'' \tan\ \delta \quad (1)$$

where ε_o=is the permittivity of the free space (8.854×10^{-14} F cm^{-1}), tan δ is the loss tangent factor, ε'' is the dielectric loss. The real and imaginary parts of permittivity and modulus are calculated from the relation [5,6]:

$$\varepsilon^* = \varepsilon' - j\varepsilon'' \quad (2)$$

where;

$$\varepsilon' = \frac{Z''}{\omega C_o(Z'^2 + Z''^2)}$$

and

$$\varepsilon'' = \frac{Z'}{\omega C_o(Z''^2 + Z'^2)}$$

In the above equations, Z' and Z'' are the real and imaginary impedances obtained from impedance measurements. The currents (I) can be separated into charging current ($i\omega\varepsilon'$) C_oV and loss current ($\omega\varepsilon''$) C_oV as given by the following equation,

$$I = (i\omega\varepsilon' + \omega\varepsilon'')C_oV \quad (3)$$

By using the relation $C_o = \varepsilon_o A/d$ (ε_o: permittivity in vacuum, A: area of electrode and d: distance between electrode), the current density (J) can be related to the complex admittance (Y^*) as follows,

$$J = (i\omega\varepsilon' + \omega\varepsilon'')E = (i\sigma'' + \sigma')E = Y^*E \quad (4)$$

Therefore,

$$\sigma' = \omega\varepsilon_o\varepsilon'' \text{ and } \sigma'' = \omega\varepsilon_o\varepsilon', \quad (5)$$

where σ' is loss current conductivity (conductance), also known as AC conductivity σ_{AC} in the present study, and σ'' is the conductivity due to charging current (susceptance). On the other hand, complex admittance (Y^*) is the inverse of Z^* [5,7].

3. Result and discussion

3.1. Phase identification

Fig. 1 shows the XRD patterns of the prepared $Li_{3.94}Cr_{0.02}SiO_4$, $Li_4Zr_{0.06}Si_{0.94}O_4$ and $Li_{3.94}Cr_{0.02}Zr_{0.06}Si_{0.94}O_4$. All compounds were successfully indexed according to monoclinic unit cell in space group $P2_{1/m}$ which has been explained by the authors previously in [3] and [4]. Fig. 2 shows the magnified XRD patterns in 2Θ range 16.50°–17.00° in order to confirm that the Cr^{3+} and Zr^{4+} ions is in the Li_4SiO_4 lattice structure.

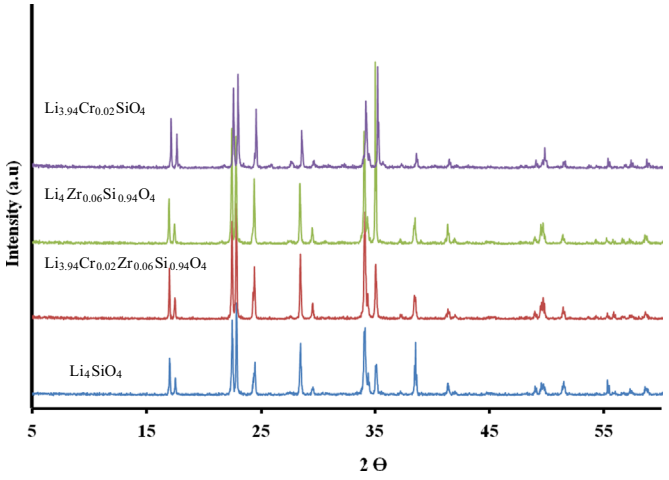

Fig. 1. XRD patterns of different compounds.

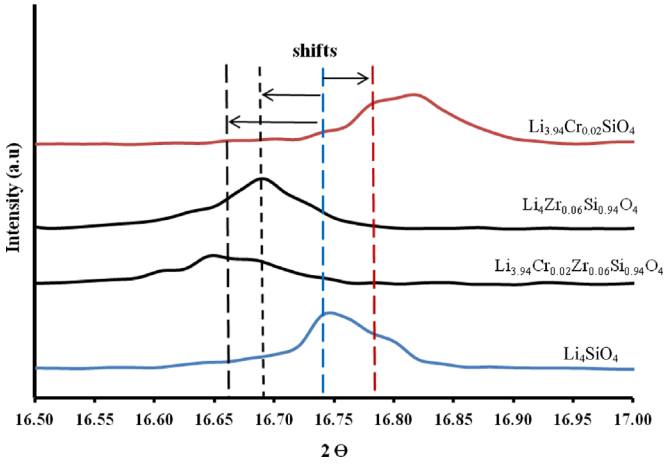

Fig. 2. XRD patterns of different compounds in 2Θ range from 16.50° to 17.00°.

Please cite this article as: S.B.R.S. Adnan, N.S. Mohamed, AC conductivity and dielectric studies of modified Li_4SiO_4 ceramic electrolytes, Ceramics International (2014), http://dx.doi.org/10.1016/j.ceramint.2014.03.149

Table 1
Lattice parameters and unit cells volume for different compounds.

Compounds	$a \pm 0.048$ (Å)	$b \pm 0.009$ (Å)	$c \pm 0.064$ (Å)	$\beta \pm 0.03$	V (Å)^3
Li_4SiO_4 [4]	5.147	6.094	5.293	90.33	166.01
$Li_{3.94}Cr_{0.02}SiO_4$ [4]	5.249	6.079	5.100	90.25	162.74
$Li_4Zr_{0.06}Si_{0.94}O_4$ [3]	5.308	6.114	5.155	90.25	167.28
$Li_{3.94}Cr_{0.02}Zr_{0.06}Si_{0.94}O_4$ [3]	5.271	6.090	5.114	90.25	164.19

As seen in this figure, the peak from the $Li_{3.94}Cr_{0.02}SiO_4$ sample shifts to higher diffraction angle meanwhile the peaks from $Li_4Zr_{0.06}Si_{0.94}O_4$ and $Li_{3.94}Cr_{0.02}Zr_{0.06}Si_{0.94}O_4$ samples shift to lower diffraction angle compared to the peak from undoped Li_4SiO_4. This indicates that the Cr^{3+} and Zr^{4+} ions are in the Li_4SiO_4 lattice structure rather than forming impurities [3,4]. Table 1 shows the lattice parameters of all compound. The value of V in $Li_4Zr_{0.06}Si_{0.94}O_4$ increases by 1.27 Å^3 compared to parent compound. Meanwhile the value of V in the $Li_{3.94}Cr_{0.02}SiO_4$ and $Li_{3.94}Cr_{0.02}Zr_{0.06}Si_{0.94}O_4$ decreases by 3.27 Å^3 and 1.82 Å^3, respectively. The increase and decrease of V are attributed to large atomic size of Zr^{4+} than that of Si^{4+} and the creation of two vacancies site due to substitution of $3Li^+$ with Cr^{3+}, respectively.

3.2. AC conductivity

The log σ_{AC} vs log ω plots of $Li_{3.94}Cr_{0.02}SiO_4$, $Li_4Zr_{0.06}Si_{0.94}O_4$ and $Li_{3.94}Cr_{0.02}Zr_{0.06}Si_{0.94}O_4$ samples for different temperatures are illustrated in Fig. 3. Each plot consists of a spike in low frequency region, a plateau in intermediate frequency region and high frequency dispersion. At low frequencies, dispersion is observed. This is due to electrode polarization effects. Meanwhile, the intermediate frequency plateau is due to frequency independence of conductivity corresponding to DC conductivity. The highest conductivity is exhibited by the in $Li_{3.94}Cr_{0.02}Zr_{0.06}Si_{0.94}O_4$ samples. The transition from the DC plateau to AC conductivity dispersion region shifts towards higher frequency range when temperature increases. At high frequencies, the conductance spectra at different temperatures converge. This indicates that AC conductivity is independent of temperature at high frequencies. In addition, the observed dispersion of conductivity with frequency is in general agreement with the prediction of the jump relaxation model [5,8,9].

According to the jump relaxation model, which takes into account the Coulomb interaction between mobile ions, the exponent of the power law in Eq. (6) is expressed as [5,8]:

$$s = \frac{\text{backhop rate}}{\text{site relaxation rate}} \quad (6)$$

The backhop is the backward motion of a hopping ion to its initial site, which is caused by the Coulombic repulsive interaction between mobile ions. The site relaxation is the shift of a site potential minimum to the position of the hopping ion, which is caused by a rearrangement of neighboring ions. The decrease in s in all modified Li_4SiO_4 samples (Fig. 4) may be due to the formation of vacant sites and the movement

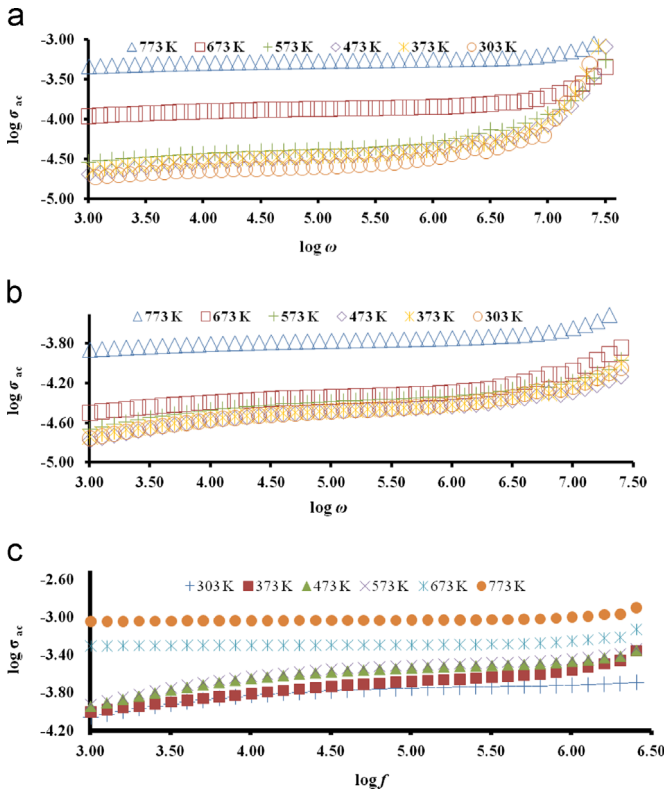

Fig. 3. Conductivity spectra for (a) $Li_{3.94}Cr_{0.02}SiO_4$ (b) $Li_4Zr_{0.06}Si_{0.94}O_4$ and (c) $Li_{3.94}Cr_{0.02}Zr_{0.06}Si_{0.94}O_4$.

of Li^+ from one site to another, which in turn reduces the backhop rate and hence decreases s.

The conductivity behavior in all samples obeyed the universal power law, $\sigma_{AC}(\omega) = \sigma_o + A\omega^s$, where σ_o is the DC conductivity, A is the pre-exponential factor and s is the power law exponent which represents the degree of interaction between the mobile ion and is less than 1. The value of s shown in Fig. 4 were extracted from the slope of log σ_{AC} (ω) versus log ω in Fig. 3. The parameter of s obtained for $Li_{3.94}Cr_{0.02}Zr_{0.06}Si_{0.94}O_4$ compound is 0.64 at room temperature and decreases to 0.12 at 773 K. Meanwhile the parameter of s obtained for $Li_{3.94}Cr_{0.02}SiO_4$ and $Li_4Zr_{0.06}Si_{0.94}O_4$ compounds are 0.61 at room temperature and 0.38 at 773 K and 0.61 at room temperature and 0.22 at 773 K, respectively. This indicates that the frequency dependence of σ_{AC} can be explained in terms of correlated barrier hopping (CBH) model. The plots in Fig. 4 can also be fitted to the equations $s = -0.0011\,T + 1.0628$, $s = -0.0006\,T + 1.0902$ and $s = -0.0008\,T + 1.1505$ for $Li_{3.98}Cr_{0.02}SiO_4$, $Li_4Zr_{0.06}Si_{0.94}O_4$ and $Li_{3.94}Cr_{0.02}Zr_{0.06}Si_{0.94}O_4$

Please cite this article as: S.B.R.S. Adnan, N.S. Mohamed, AC conductivity and dielectric studies of modified Li_4SiO_4 ceramic electrolytes, Ceramics International (2014), http://dx.doi.org/10.1016/j.ceramint.2014.03.149

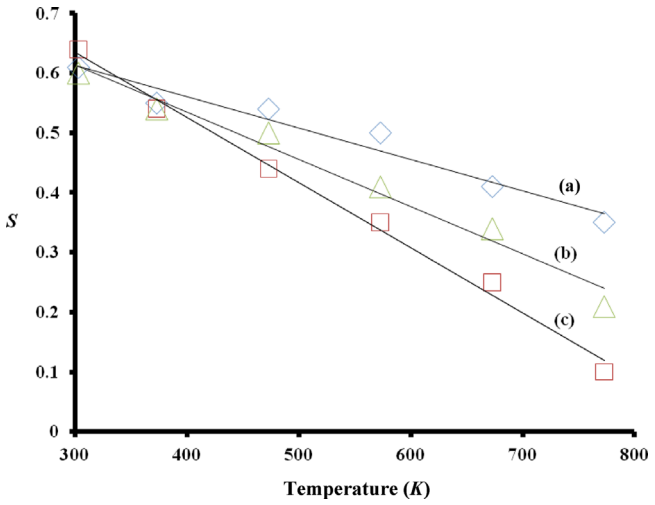

Fig. 4. Value of s for (a) $Li_{3.94}Cr_{0.02}SiO_4$ (b) $Li_4Zr_{0.06}Si_{0.94}O_4$ and (c) $Li_{3.94}Cr_{0.02}Zr_{0.06}Si_{0.94}O_4$ at different temperatures.

sample, respectively. These equations suggests that $s \rightarrow 1$ when $T \rightarrow 0$ in all samples.

The frequency exponent s in the CBH model is in the range from 0.7 to 1 at room temperature and decreases with increasing temperature and can be evaluated as follows [5,10–14]:

$$s = 1 - \frac{6kT}{W_M} \tag{7}$$

where k is Boltzmann constant, T is temperature, W_M is maximum barrier height [12–14]. From Eq. (7), it can be deduced that $s \rightarrow 1$ if $T \rightarrow 0$. The trend of s with T is consistent with that observed for the modified Li_4SiO_4 samples. This confirms that the conduction mechanism in the $Li_{3.94}Cr_{0.02}SiO_4$, $Li_4Zr_{0.06}Si_{0.94}O_4$ and $Li_{3.94}Cr_{0.02}Zr_{0.06}Si_{0.94}O_4$ systems studied in this work can be described using CBH model. In the correlated barrier hopping model, ions or charge carriers are assumed to be surrounded by several potentials such as the Coulombic repulsive potential between the ions and a potential well in which the ions reside. Superposition of the potentials yields a single-ion potential that is actually felt by the ions. When the ion gain sufficient energy, they hop from one site to another. When temperature increases, the rate of ion hopping from one site to another increases resulting in an enhancement in conductivity with temperature as observed in Fig. 3 [10–14].

The ionic hopping rate, ω_p can be determined directly from AC conductivity data since it corresponds to $\sigma(\omega) = 2\sigma(0)$ [8,15,16]. The charge carrier concentration, K can be calculated from the definition of DC conductivity of the ion conducting material which is given by [8,9,15–17]:

$$K = \frac{\sigma_{dc} T}{\omega_p} \tag{8}$$

where

$$K = ne^2a^2\gamma k^{-1} \tag{9}$$

Here e is electron charge, γ is the correlation factor which is set equal to 1, and a is the jump distance between two adjacent sites for the ions to hope which is assumed to be 3 Å for all materials. n is the concentration of mobile ions which can be calculated using Eq. 9 and k is the Boltzmann constant. The ionic mobility, μ can be calculated using equation:

$$\mu = \frac{\sigma_{dc}}{ne} \tag{10}$$

The values of ω_p, K, n and μ for $Li_{3.94}Cr_{0.02}SiO_4$, $Li_4Zr_{0.06}Si_{0.94}O_4$ and $Li_{3.94}Cr_{0.02}Zr_{0.06}Si_{0.94}O_4$ samples at various temperatures are listed in Table 2. The table reveals that the charge carrier concentration, K and mobile ion concentration, n are constant over the temperature range studied. This implies that all the lithium ions which are responsible for the conductivity are in mobile state thus can be best represented by the strong electrolyte model [8,9,15,18]. The higher conductivity observed for $Li_{3.94}Cr_{0.02}Zr_{0.06}Si_{0.94}O_4$ is due to high mobile ion concentration ($\sim 10^{26}$) compared to that ($\sim 10^{25}$) observed for both $Li_{3.94}Cr_{0.02}SiO_4$ and $Li_4Zr_{0.06}Si_{0.94}O_4$ samples.

Meanwhile, the mobility of ions, μ increases with increase in temperature in all samples. This proves that the increase in conductivity with increasing temperature in the samples can be attributed to the increase in ionic mobility or hopping rate since the density of mobile ions is constant over the temperature range chosen for this study [8,9,17].

3.3. Frequency dependence of dielectric constant

Fig. 5 illustrates the variation of the dielectric constant, ε' with composition at different frequencies for all samples at room temperature. From the figure, it is clear that the dielectric constant decreases with increase in frequency. The double substituted compound, $Li_{3.94}Cr_{0.02}Zr_{0.06}Si_{0.94}O_4$ exhibits the highest ε' compared to other compounds at all frequencies except 1000 Hz. At low frequencies, the large amount of charge carriers in this compound gives high contribution of charge carrier accumulation at the interface of electrode and hence increases the value of ε'. When frequency increases, due to high periodic reversal of the field, the contribution of charge carriers towards dielectric constant decreases and reaches a value which is about the same to the value of $Li_{3.94}Cr_{0.02}SiO_4$ and $Li_4Zr_{0.06}Si_{0.94}O_4$ compounds at 1000 Hz [5,13,14,19–21].

Meanwhile, the dielectric constant in all samples increases with temperature (Fig. 6). The increase of ε' with temperature can be attributed to the fact that at low temperature, most of the charge carriers cannot orient themselves with respect to the direction of the applied field giving a weak contribution to the polarization and ε'. When temperature increases, the charge carriers acquire sufficient excitation thermal energy and are able to rotate more easily to obey the change in external field. This in turn increases their contribution to the polarization leading to an increase in ε' [5,13,14,19–21].

3.4. Frequency dependence of dielectric loss

The variation of the dielectric loss, ε'' with composition at different frequencies for all samples at room temperature is shown in Fig. 7. As seen in this figure, the ε'' decreases with increase in frequency. At low frequencies (1 Hz and 10 Hz),

Please cite this article as: S.B.R.S. Adnan, N.S. Mohamed, AC conductivity and dielectric studies of modified Li_4SiO_4 ceramic electrolytes, Ceramics International (2014), http://dx.doi.org/10.1016/j.ceramint.2014.03.149

Table 2
The values of ω_p, K, n and μ for $Li_{3.94}Cr_{0.02}SiO_4$, $Li_4Zr_{0.06}Si_{0.94}O_4$ and $Li_{3.94}Cr_{0.02}Zr_{0.06}Si_{0.94}O_4$ samples at various temperatures.

Samples	T (K)	ω_p (MHz)	K (S cm^{-1} K Hz^{-1})	n (cm^{-3})	μ (cm^2 V^{-1} s^{-1})
$Li_4Zr_{0.06}Si_{0.94}O_4$	303	1.531	6.72×10^{-9}	4.02×10^{25}	5.27×10^{-12}
	373	1.970	6.72×10^{-9}	4.02×10^{25}	5.52×10^{-12}
	473	2.630	6.74×10^{-9}	4.03×10^{25}	6.85×10^{-12}
	573	3.755	6.74×10^{-9}	4.03×10^{25}	6.84×10^{-12}
	673	4.799	6.71×10^{-9}	4.01×10^{25}	7.15×10^{-12}
	773	20.607	6.74×10^{-9}	4.03×10^{25}	2.78×10^{-11}
$Li_{3.940}Cr_{0.020}SiO_4$	303	0.548	1.38×10^{-8}	8.30×10^{25}	1.89×10^{-12}
	373	0.820	1.38×10^{-8}	8.32×10^{25}	2.30×10^{-12}
	473	1.120	1.38×10^{-8}	8.30×10^{25}	3.00×10^{-12}
	573	1.645	1.38×10^{-8}	8.31×10^{25}	3.00×10^{-12}
	673	6.903	1.39×10^{-8}	8.28×10^{25}	1.07×10^{-11}
	773	31.662	1.38×10^{-8}	8.30×10^{25}	4.28×10^{-11}
$Li_{3.94}Cr_{0.02}Zr_{0.06}Si_{0.94}O_4$	303	0.548	1.04×10^{-7}	6.22×10^{26}	1.89×10^{-12}
	373	0.820	1.04×10^{-7}	6.22×10^{26}	2.30×10^{-12}
	473	1.420	1.05×10^{-7}	6.30×10^{26}	3.41×10^{-12}
	573	1.845	1.07×10^{-7}	6.40×10^{26}	3.36×10^{-12}
	673	3.103	1.08×10^{-7}	6.51×10^{26}	1.82×10^{-11}
	773	7.962	1.09×10^{-7}	6.56×10^{26}	4.08×10^{-11}

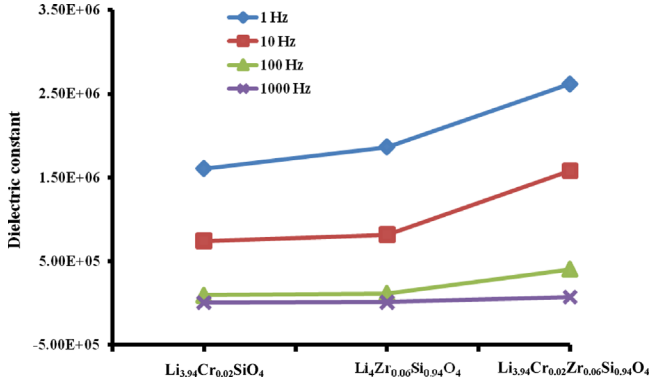

Fig. 5. Variation of the dielectric constant, ε' with composition at different frequencies.

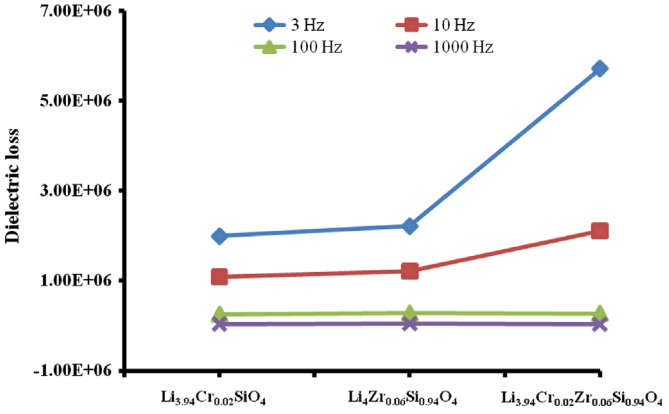

Fig. 7. Variation of the dielectric loss, ε'' with composition at different frequencies.

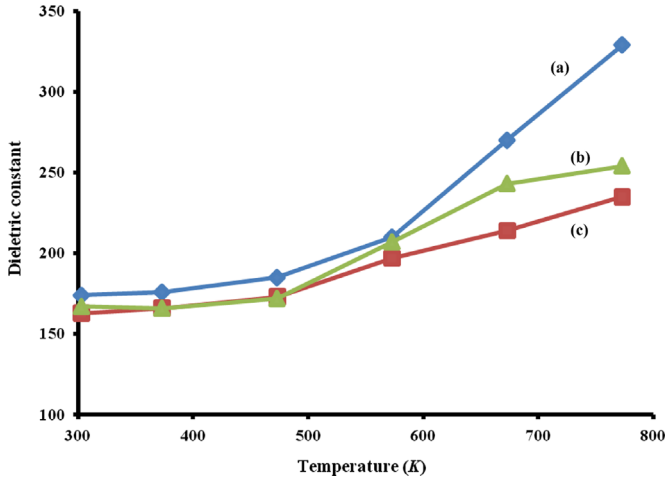

Fig. 6. Variation of the dielectric constant, ε' with temperature at frequency of 1 MHz for (a) $Li_{3.94}Cr_{0.02}Zr_{0.06}Si_{0.94}O_4$ (b) $Li_{3.94}Cr_{0.02}SiO_4$ (c) $Li_4Zr_{0.06}Si_{0.94}O_4$.

the higher migration rate causes greater loss of energy to the lattice as heat and is reflected by higher value of ε''. Meanwhile, at high frequencies (100 Hz and 1000 Hz), all sample show the same value of ε''. This is because at these frequencies, ion vibration may be the only source of dielectric loss and as a consequence the values of ε'' are more or less the same for all samples [22,23]. However, ε'' increases with temperature as shown in Fig. 8. The increase in dielectric loss with temperature is attributed to an increase of ion migration rate. This is due to increase mobility of ions as shown in Table 2.

4. Conclusions

The AC conductivity of the compound studied in this work obeyed the universal power law and can be described using the CBH model. The conductivity parameters such as hopping frequency, charge carrier concentration and mobile ion

Please cite this article as: S.B.R.S. Adnan, N.S. Mohamed, AC conductivity and dielectric studies of modified Li_4SiO_4 ceramic electrolytes, Ceramics International (2014), http://dx.doi.org/10.1016/j.ceramint.2014.03.149

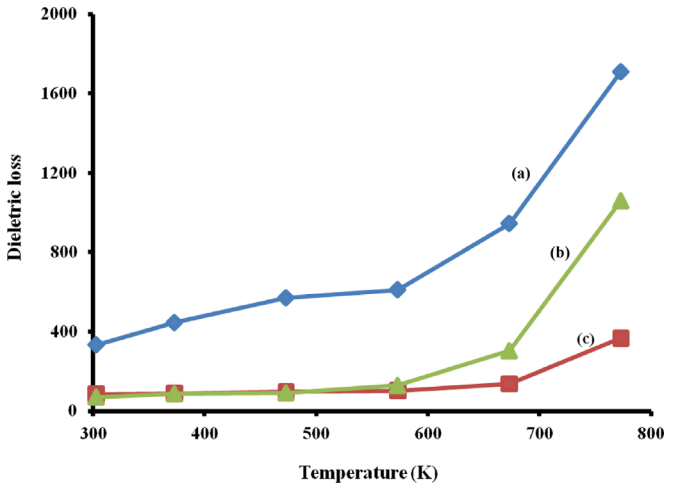

Fig. 8. Variation of the dielectric loss, ε'' with temperature at frequency of 1 MHz for (a) $Li_{3.94}Cr_{0.02}Zr_{0.06}Si_{0.94}O_4$ (b) $Li_{3.94}Cr_{0.02}SiO_4$ (c) $Li_4Zr_{0.06}Si_{0.94}O_4$.

concentration have been calculated by fitting the conductance spectra to the power law variation. $Li_{3.94}Cr_{0.02}Zr_{0.06}Si_{0.94}O_4$ showed the highest dielectric constant and dielectric loss compared to $Li_{3.94}Cr_{0.02}SiO_4$ and $Li_4Zr_{0.06}Si_{0.94}O_4$ compounds at low frequencies. Dielectric constant and dielectric loss of all samples decreased with increase in frequency but increase as temperature increase. The increase of dielectric constant with temperature was due easier orientation of charge carrier to obey change in external field. Meanwhile, the increases of dielectric loss with temperature was attributed to an increase of ion migration rate.

Acknowledgments

Financial support from the University of Malaya (research grant PV027/2012A) is gratefully acknowledged.

References

[1] T. Ying, Y. Danqin, L. Jie, Electrochemical formation of crystalline Li_3VO_4/Li_4SiO_4 solid solutions film, Solid State Ionics 179 (2008) 2396–2398.
[2] B. Scrosati, Recent advances in lithium ion battery materials, Electrochim. Acta 45 (2000) 2461–2466.
[3] S.B.R.S Adnan, N.S Mohamed, Characterization of novel $Li_4Zr_{0.06}Si_{0.94}O_4$ and $Li_{3.94}Cr_{0.02}Zr_{0.06}Si_{0.94}O_4$ ceramic electrolytes for lithium cells, Ceram. Int. 40 (2014) 6373–6379.
[4] S.B.R.S Adnan, N.S. Mohamed, Properties of novel Li_4–3xCr$x$$SiO_4$ ceramic electrolyte, Ceram. Int. 40 (2014) 5033–5038.
[5] S.B.R.S Adnan, N.S Mohamed, Citrate sol–gel synthesized Li_4SiO_4: conductivity and dielectric behavior, Mater. Res. Innovations 16 (2012) 281–285.
[6] Dillip K. Pradhan, R.N.P. Choudhary, B.K. Samantaray, Studies of dielectric relaxation and AC conductivity behavior of plasticized polymer nanocomposite electrolytes, Int. J. Electrochem. Sci. 3 (2008) 597–608.
[7] Hanako Nishino Hirosyi Yamamura, Katsuyoshi Kakinuma, Relationship between oxide-ion conductivity and dielectric constant in Ce0.9Sm0.102-δ, J. Ceram. Soc. Jpn. 115 (2007) 23–27.
[8] S.B.R.S Adnan, N.S. Mohamed, Structural, thermal and electrical properties of Li_{4-2x} Zn_xSiO_4 ceramic electrolyte prepared by citrate sol gel technique, Int. J. Electrochem. Sci. 8 (2013) 6055–6067.
[9] S.B.R.S Adnan, N.S Mohamed, Effects of Sn substitution on the properties of Li4SiO4 ceramic electrolyte, Solid State Ionics 07 (2013) 008, http://dx.doi.org/10.1016/j.ssi.
[10] M.A. Afifi, M M El-Nahass, A.E Bekheet, I.T Zedan, S.R Elliott, DC and ac electrical conductivity of bulk CdSexTe1-x ($0 < x < 0.4$), Phys. Rev. B: Condens. Matter 400 (2007) 248.
[11] F. Yakuphanoglu, Y. Aydogdu, U. Schatzschneider, E. Rentschler, DC and AC conductivity and dielectric properties of the metal-radical compound: aqua[bis(2-dimethylaminomethyl-4-NIT-phenolato)]copper (II), Solid State Commun. 128 (2003) 63–67.
[12] N. Mehta, D. Kumar, S. Kumar, A. Kumar, Applicability of CBH model in the AC conduction study of glassy Se100–xInx alloys, Chalcogenide Lett. 2 (2005) 103–107.
[13] M.H. Buraidah, L.P Teo, S.R Majid, A.K Arof, Ionic conductivity by correlated barrier hopping in NH_4I doped chitosan solid electrolyte, Phys. Rev. B: Condens. Matter 404 (2009) 1373–1379.
[14] A.A. Hendi, AC conductivity and dielectric measurements of bulk tertracyanoquinodimethane, Aust. J. Basic Appl. Sci. 5 (2007) 380–386.
[15] D.P. Almond, A.R West, Mobile ion concentrations in solid electrolytes from an analysis of AC conductivity, Solid State Ionics 9 and 10 (1983) 277–282.
[16] D.P. Almond, A.R West, The activation entropy for transport in ionic conductors, Solid State Ionics 23 (1987) 27–35.
[17] L.P. Teo, M.H. Buraidah, A.F.M. Nor, S.R. Majid, Conductivity and dielectric studies of Li_2SnO_3, Ionics 18 (2012) 655–665.
[18] M. Vijayakumar, G. Hirankumar, M.S. Bhuvaneswari, S. Selvasekarapandian, Influence of B_2O_3 doping on conductivity of $LiTiO_2$ electrode material, J. Power Sources 117 (2003) 143–147.
[19] A.M. Abo El Ata, S M Atia, T M Meaz, AC conductivity and dielectric behavior of $CoAl_xFe_{2-x}O_4$, Solid State Sci. 6 (2004) 61–69.
[20] C.R. Mariappan, G Govindaraj, AC conductivity, dielectric studies and conductivity scaling of NASICON materials, Mater. Sci. Eng. B 94 (2002) 82–88.
[21] E.G. El-Metwally, M. Fadel, A.M Shakra, M.A Afifi, AC conductivity and dielectric properties of Se70Ge30-xMx {x=0 and 5 and M=Ag,Cd or Pb} amorphous films, J. Optoelectron. Adv. Mater. 10 (2008) 1320–1327.
[22] N.A. Hegab, A.E Bekheet, M.A Afifi, L.A Wahaba, H.A Shehata, Effect of Cd addition on the AC conductivity and dielectric properties of Ge70Te30 films, J. Ovonic Res. 3 (2007) 71–82.
[23] Dev K. Mahato, Alo Dutta, T.P. Sinha, Dielectric relaxation and AC conductivity of double perovskite oxide HO_2ZnZrO_6, Phys. Rev. B: Condens. Matter 406 (2011) 2703–2708.

Please cite this article as: S.B.R.S. Adnan, N.S. Mohamed, AC conductivity and dielectric studies of modified Li_4SiO_4 ceramic electrolytes, Ceramics International (2014), http://dx.doi.org/10.1016/j.ceramint.2014.03.149

CHAPTER 4

CONCLUSIONS AND RECOMMENDATIONS FOR FUTURE WORKS

4.1 Conclusions

The LISICON-type member, Li_4SiO_4 ceramic electrolyte was successfully obtained by employing sol gel method for the first time. So, it is proven that the sol gel method can produce pure ceramic electrolyte without the presence of impurities. This research also successful in developing new LISICON structured ceramic electrolytes by partial substitutions of aliovalent and isovalent ions into the Li_4SiO_4 structure. The partial substitutions of aliovalent ions using Zn^{2+} and Cr^{3+} improve the ionic conductivity to an order of magnitude higher compared to that of parent compound at ambient temperature. The bulk, grain boundary and total conductivities of Li_4SiO_4 compound were 3.36×10^{-6}, 1.58×10^{-6} and 1.51×10^{-6} S cm^{-1} respectively increased to 3.20×10^{-5}, 2.79×10^{-5} and 1.51×10^{-5} S cm^{-1} respectively for the $Li_{3.88}Zn_{0.06}SiO_4$ compound and 7.93×10^{-5}, 3.68×10^{-5} and 2.51×10^{-5} respectively for the $Li_{3.94}Cr_{0.02}SiO_4$ compound. In addition, the AC conductivity studies showed that the mobile ion concentration also increased from 10^{24} cm^{-3} in Li_4SiO_4 to 10^{25} cm^{-3} in $Li_{3.88}Zn_{0.06}SiO_4$ and $Li_{3.94}Cr_{0.02}SiO_4$ compounds.

Meanwhile, the substitution of aliovalent ions using Sn^{4+} and Zr^{4+} also increased the bulk, grain boundary and total conductivities to 1.00×10^{-4}, 4.42×10^{-5} and 3.07×10^{-5} S cm^{-1}

respectively for $Li_4Sn_{0.02}Si_{0.98}O_4$ compound and 1.19×10^{-4} , 4.75×10^{-5} and 3.41×10^{-5} S cm^{-1} respectively in $Li_4Zr_{0.06}Si_{0.94}O_4$ compound. The value of mobile ion concentration from AC conductivity studies were 10^{25} cm^{-3} in both $Li_4Sn_{0.02}Si_{0.98}O_4$ and $Li_4Zr_{0.06}Si_{0.94}O_4$ compounds which is higher than that of Li_4SiO_4. The most significant enhancement of ionic conductivity was two orders of magnitude higher than parent compound occurred when double partial substitution using Cr^{3+} and Zr^{4+} was employed. The total conductivity at ambient temperature raised 1.83×10^{-4} S cm^{-1} in $Li_{3.94}Cr_{0.02}Zr_{0.06}Si_{0.94}O_4$ compound. The mobile ion concentration value also increased to 10^{26} cm^{-3} in $Li_{3.94}Cr_{0.02}Zr_{0.06}Si_{0.94}O_4$ compound.

The conductivity–temperature study showed that all compounds obey the Arrhenius behavior. The ionic conductivities of all compounds increased with temperature. The highest conducting compound ($Li_{3.94}Cr_{0.02}Zr_{0.06}Si_{0.94}O_4$) possessed the lowest E_a of 0.001 eV (< 400^oC) and its lithium transference number was 0.97.

The fabrication of lithium ion rechargeable all-solid-state electrochemical cells was done by using the highest ionic conducting sample, $Li_{3.94}Cr_{0.02}Zr_{0.06}Si_{0.94}O_4$. The cells showed a maximum discharge capacity of 103 $mAhg^{-1}$ under 10 mA constant current in a potential range of 3.0 – 4.2 V. This cell performance is better than that of the cell fabricated using thio-LISICON ceramic electrolyte type, $Li_{3.4}Si_{0.4}P_{0.6}S_4$ which exhibited maximum capacity of 60 $mAhg^{-1}$ under a much lower current density of 13 μA cm^{-2} (16.55 μA) at the same potential range (Murayama *et al*, 2002). This shows that the $Li_{3.94}Cr_{0.02}Zr_{0.06}Si_{0.94}O_4$ ceramic electrolyte can be used in electrochemical cells.

4.2 Recommendations for future works

In Li_4SiO_4 parent compound, a tunnel size is too small for Li^+ ions to migrate because of the small size of silicon atom. So, a larger tunnel size is necessary for smoother Li^+ migration. The suitable tunnel size for Li^+ migration is expected to be obtained by substituting the silicon (Si) in the Li_4SiO_4 with zirconium (Zr) to form Li_4ZrO_4 parent compound. The size of Zr, which is larger than Si is expected to enlarge the lattice size of the structure. Meanwhile the low electronegativity of Zr compared to that of Si is expected to increase the average free path migration of lithium ions due to its lower attraction to the ions.

The interstitial ion and vacant site can also be obtained by aliovalent substitution of the Li_4ZrO_4 parent compound. The partial substitution of divalent ions will introduce two interstitial ions and a vacant site in the structure of Li_4ZrO_4 with the formulae of $Li_{4+2x}D_xZr_{1-x}O$ (interstitial ion) and $Li_{4-2x}D_xZrO_4$ (vacant ion). Besides, the partial substitution of trivalent ions will introduce an interstitial ion and two vacant sites with the formulae of $Li_{4+x}T_xZr_{1-x}O_4$ (interstitial ion) and $Li_{4-3x}T_xZrO_4$ (vacant ion).

The replacement of Li^+ with Mg^{2+} in Li_4SiO_4 structure to form stoichiometric Mg_2SiO_4 can be considered. The replacement of Li^+ ions with Mg^{2+} ions process is expected to be successful since the ion radius difference between Li^+ (0.69 Å) and Mg^{2+} ion (0.65 Å) is below 15% which does not exceed the solubility limit for atomic radii differences in solid solution (Liu, 2008). In addition, the magnesium is easier to handle, cheap, environment friendly and safer than lithium.

REFERENCES

Agrawal, R. C. & Gupta, R. K. (1999). Review superionic solids: Composite electrolyte phase-an overview. *Journal of Materials Science,34,* 1131 – 1162.

Aono. H , Imanaka. N, Adachi, G. (1994). High Li^+ Conducting Ceramics. *Account of Chemical Research,, 27,* 265–270.

Aotani, N., Iwamoto, K., Takada, K. & Kondo, S. (1994). Synthesis and electrochemical properties of lithium ion conductive glass, Li_3PO_4 - Li_2S - SiS_2. *Solid State Ionics, 68,* 35 – 39.

Awaka, J, Kijima N, Hayakawa H, Akimoto J. (2009). Synthesis and structure analysis of tetragonal $Li_7La_3Zr_2O_{12}$ with the garnet-related type structure. *Journal of Solid State Chemistry,* 182, 2046–2052.

Bruce P.G. (1984). Ion trapping and its effect on the conductivity of LISICON and other solid electrolyte. *Journal of Solid State Chemistry,* 53, 430-434.

Bruce, P.G, West, A.R (1980). Phase diagram of the LISICON, solid electrolyte system Li_4GeO_4-Zn_2GeO_4, *Mat.Res Bulletin,* 15, 379-385.

Chavarria J.B, Quintana P, Huanosta A,(1996). Electrical properties of the solid solution $Li_{4-3x}In_xSiO_4$. *Solid State Ionics,*83, 245-248.

Dissanayake M.A.K.L, Gunawardane R.P, West A.R (1993). Lithium ion conducting $Li_{4-2x}Ge_{1-x}S_xO4$ solid electrolytes. *Solid State Ionics,* 62, 217-223.

Fergus J.W (2006). Electrolytes for solid oxide fuel cells. *Journal of Power Sources,* 1*62,*30-40.

Fergus J.W (2010). Ceramic and polymeric solid electrolytes for lithium-ion batteries . *Journal of Power Sources,* 1*95,*4554-4569.

Ferloni P, A. Magistris (1994). New materials for solid state electrochemistry, Journal de physique IV. 4, C1.3-C1.15.

Goodenough J.B, Hong H.Y.P, Kafalas J.A (1976). Fast Na^+-ion transport in skeleton structures . *Materials Research Bulletin, 11,* 203-220.

Hirai, K., Tatsumisago, M. & Minami, T. (1995). Thermal and electrical properties of rapidly quenched glasses in the systems $(100 - x)\ (0.6Li_2S \cdot 0.4SiS_2) \cdot zLixMOy$ ($Li_xMO_y = Li_4SiO_4, Li_2SO_4$). *Solid State Ionics, 78,* 269 – 273.

Hong H.Y.P (1978). Crystal structure and ionic conductivity of $Li_{14}Zn(GeO_4)_4$ and other new Li^+ superionic conductors. *Materials Research Bulletin, 13,* 117-124.

Hull S, (2004) Superionics: crystal structure and conduction progress. *Reports on progress in Physics,* 67, 1233-1314.

Kamphorst J.G, Hellstrom E.E, (1980) . Fast Li ionic conduction in solid solutions of the system Li_4GeO_4-Li_2ZnGeO_4-Li_3PO_4. *Solid State Ionic,* 1, 187-197.

Kanno R, Hata T, Kawamoto Y, Irie M, (2000). Synthesis of new lithium ionic conductor thio-LISICON- lithium germanium sulfide system. *Solid state Ionics,* 130,97-104.

Kanno R, Murayama M, (2001). Lithium ionic conductor thio-LISICON- The Li2SGeS2P2S5. *Journal of electrochemical society*, 148,A742-A746.

Knauth. P (2009). Inorganic solid Li ion conductors: An overview. *Solid State Ionics,180,* 911-916.

Khorassani A, West A.R, (1984). Li^+ ion conductivity in the system Li_4SiO_4-Li_3VO_4. *Journal of Solid State Chemistry*, 53, 369-375.

Khorassani A, West A.R, (1982). New Li^+ ion conducting in the system Li_4SiO_4-Li_3AsO_4. *Journal of Solid State Chemistry*, 53, 369-375.

Kumar P.P, Yashonath S, (2006). Ionic conduction in the solid state. *Journal of Chemical Sciences,* 118, 135-154.

Kuwano J, Rodger A.R, West A.R (1985). Li^+ ion conducting γ solid solutions in the systems Li_4XO_4-Li_3YO_4: X=Si, Ge, Ti; Y=P, As, V; Li_4XO_4-$LiZO_2$: Z=Al, Ga, Cr and Li_4GeO_4-Li_2CaGeO_4. *Solid State Ionics*, *15,* 185-198.

Landerosa J.O, Martínez-dlCruz L, Gómez-Yá˜nez C, Pfeiffer H, (2011). Towards understanding the thermoanalysis of water sorption on lithium orthosilicate (Li_4SiO_4). *Thermochimica Acta,* 515,73-78.

Liu Z, Huang F, Yang J, Wang B, Sun J, (2008). New lithium ion conductor, thio-LISICON lithium zirconium sulphide system. *Solid state Ionics*, 179, 1714-1716.

Maier, J. (1995). Ionic conduction in space charge regions. *Progress in Solid State Chemistry, 23*, 171 – 263.

Maier, J. (2003). Defect chemistry and ion transport in nanostructured materials: Part II. Aspects of nanoionics. *Solid State Ionics, 157*, 327 – 334.

Masquelier C, Tabuchi M, Takeuchi T, Soizumi W, Kageyama H, Nakamura O, (1995). Influence of the preparation process on the cation transport properties of $Li_{4+x}M_xSi_{1-x}O_4$ (M = B, Al) solid electrolytes, *Solid State Ionics*, 79, 98-105.

Menetrier, M., Estournes, C., Levasseur, A. & Rao, K. J. (1992). Ionic conduction in B_2S_3-Li_2S-LiI glasses. *Solid State Ionics, 53 – 56*, 1208 – 1213.

Murayama M, Kanno R, Irie M, Ito T, Hata T, Sonoyama N, Kawaoto Y. (2002). Synthesis of new lithium ionic conductor Thio-LISICON- Lithium Sulfides System *Solid State Chemistry ,168,* 140-148.

Nancy J. D (1989). Solid State Division. *Annual review of materials science* , 19 , 103-120)

Ooura Y, Machida N,Naito M, Shigematsu T (2012). Electrochemical properties of the amorphous solid electrolytes in the system $Li_2S–Al_2S_3–P_2S_5$. *Solid State Ionics,225,* 350-353.

Park. M, Zhang. X, Chung. M, Gregory B. Less, Sastr. A.M (2010). A review of conduction phenomena in Li-ion batteries. *Journal of Power Sources*, *195*, 7904-7929.

Robertson A.D, West A.R, Ritchie A.G (1997). Review of crystalline lithium-ion conductors suitable for high temperature battery applications. *Solid state Ionics, 104*, 1-11.

Robertson A.D, West A.R (1992). Phase equilibria crystal chemistry and ionic conductivity in the LISICON system Li_4GeO_4-$Li_2Ga_{0.5}GeO_4$. *Solid State Ionics*, 58, 351-358.

Rotimi, E (2010). Synthesis of Ceramic Perovskites and Fabrication of Ceramic Proton Conducting Button Cell Electrolyte (PCC's) for Solid Oxide Fuel cells (SOFC). *Thesis*, Howard University.

Santos A.M. D, Fernando M. B. Marques, Luís D. Carlos and João Rocha (2006). Photoluminescence of lanthanide NASICONs: $Na_5LnSi_4O_{12}$, Ln = Eu, Tb. *J. Mater***.** Chem**.**, ,16, 3139-3144.

Sarıboga. V, Özdemir. H, M.A. Faruk Öksüzömer (2013). Cellulose templating method for the preparation of $La_{0.8}Sr_{0.2}Ga_{0.83}Mg_{0.17}O_{2.815}$ (LSGM) solid oxide electrolyte. *Journal of the European Ceramic Society*, *33*, 1435-1446.

Scrosati. B (2000). Recent advances in lithium ion battery materials. *Electrochimica Acta, 45*, 2461 -2466.

Scrosati, B. and Vincent, C.A. (2000) Polymer electrolytes: the key to lithium polymer batteries, *Material Research Bulletin*, 25, 28-30.

Shannon R.D, Taylor B.E, English A.D, T. Berzins, New Li Solid electrolytes, Electrochemica Acta, 22 (1977) 783-796.

Shi. J, Guo L. (2012). ABO_3-based photocatalysts for water splitting. *Progress in Natural Science: Materials International*, 22 592-615.

Sumathipala H.H, Disanayake M.A.K.L, West A.R, (1996). Novel LISICON mixed conductors, $Li_{4-2x}Co_xGeO_4$. *Solid State Ionics*, 86-88, 719-724.

Shannon R.D, Taylor B.E, English A.D, Berzins T,(1977). New Li Solid electrolytes. *Electrochemica Acta*, 22,783-796.

Takada K, Inada. T, Kajiyama. A, Kouguchi. M, Sasaki.H, Kondo.S, Michiue. Y, Nakano. S, Tabuchi. M, Watanabe. M (2004). Solid State batteries with sulfide-based solid electrolytes, *Solid State Ionics*, 172, 25-30.

Tao Ying, Yi Danqin, Li Jie (2008). Electrochemical formation of crystalline Li_3VO_4/Li_4SiO_4 solid solution film, *Solid State Ionic*s, 179, 2396-2398.

Tatsumisago, M., Hayashi, A. (2008). Preparation of lithium ion conducting glasses and glass–ceramics for all-solid-state batteries. *Journal of Non-Crystalline Solids, 354*, 1411 – 1417.

Tatsumisago, M., Minami, T. (1987). Lithium ion conducting glasses prepared by rapid quenching. *Materials Chemistry and Physics, 18,* 1 – 17.

Thangadurai V, Weppner W, (2002). Solid state lithium ion conductor: Design considerations by thermodynamic approach. *Ionics* 8, 281-291.

Thangadurai V, Weppner W, (2006). Recent progress in solid oxide and lithium ion conducting electrolytes research. *Ionics* 12, 81-92.

Thangadurai V, Weppner W, (2005). $Li_6ALa_2Nb_2O_{12}$ (A = Ca, Sr, Ba): A New Class of Fast Lithium Ion Conductors with Garnet-Like Structure. *J. Am. Ceram. Soc.,* 88, 411- 418.

Tranqui D, Shannon R.D, Chen H.Y, (1979). Crystal structure of ordered Li_4SiO_4, *Acta Cryst*. B35, 2479-2487.

Wakihara M, Uchida T, Gohara T, (1988). Ionic conductivity of $Li_{4-2x}Mg_xSiO_4$. *Solid State Ionics* ,31, 17-20.

West A.R (1984). Solid state chemistry and its application. *New York, John Wiley and Son Ltd* , 478.

West A.R (1973). Ionic conductivity of oxides based on Li_4SiO_4. *Journal of Applied Electrochemistry*. 3, 327-335.

West A.R, Hodge I, Ingram M.D (1976). Ionic conductivity of Li_4SiO_4, Li_4GeO_4 and their solid solution. *American Ceramic Soc.,* 59, 360-366.

Yamashita, M., Yamanaka, H. & Wakabayashi, H. (1996). Thin-film preparation of the Li_2S-GeS_2-Ga_2S_3 glass system by sputtering. *Solid State Ionics*, *89*, 299 – 304.

Zhang B, Nieuwoudt M, Easteal A.J (2008). Sol gel route to nanocrystalline lithium metasilicate particles. *Journal of the American Ceramic Society*, 91, 1927-1932.